

R760887

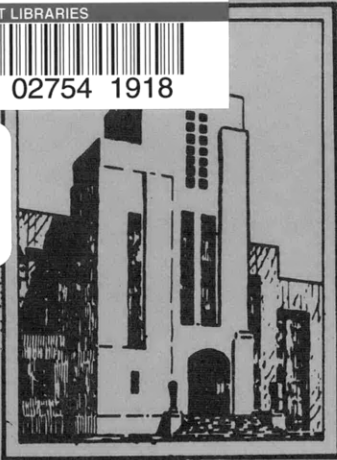
Report 949

MIT LIBRARIES



3 9080 02754 1918

V393
.R46



DEPARTMENT OF THE NAVY
DAVID TAYLOR MODEL BASIN

HYDROMECHANICS

○

AERODYNAMICS

○

STRUCTURAL
MECHANICS

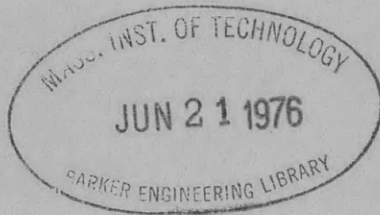
○

APPLIED
MATHEMATICS

STRUCTURAL TESTS OF FLIGHT DECK ON USS HANCOCK
(CVA 19) UNDER SIMULATED A3D-1 AND F2H-3
AIRCRAFT LANDING LOADS

by

Ralph B. Allnutt



STRUCTURAL MECHANICS LABORATORY
RESEARCH AND DEVELOPMENT REPORT

April 1959

Report 949



DEPARTMENT OF THE NAVY
DAVID TAYLOR MODEL BASIN
WASHINGTON 7, D. C.

IN REPLY REFER TO
S11
A9/1
(710:MCC:kc)
Ser 7-111
21 May 1959

From: Commanding Officer and Director
To: Chief, Bureau of Ships (312) (in duplicate)
Subj: NS731-040; Structural tests of flight deck on
USS HANCOCK (CVA 19); forwarding of report on
Ref: (a) BUSHIPS CONFIDENTIAL 1tr C-CVA 19
Class/S83(442) Ser 442-019 of 2 Sep 1953
Encl: (1) DTMB Report 949 entitled, "Structural Tests
of Flight Deck on USS HANCOCK (CVA 19) under
Simulated A3D-1 and F2H-3 Aircraft Landing
Loads" 15 copies

1. By reference (a) the David Taylor Model Basin was requested to conduct extensive static and dynamic tests on the flight deck of USS HANCOCK (CVA 19), the first ESSEX-Class aircraft carrier authorized for Project 27-C conversion. The purposes of these tests were to obtain data on dynamic response factor and to evaluate existing design procedures in which only static loads are used to simulate the landing reactions of aircraft.
2. Static and dynamic strains and deflections measured in transverse beams, longitudinals, and flight-deck planking at various critical locations in the landing area are reported in enclosure (1). A specially designed loading apparatus was used for simulating wheel loadings of A3D-1 and F2H-3 aircraft.
3. From the results of these tests, it is concluded that the present Bureau of Ships design method is accurate for calculating the stresses in the steel supporting structure for a wood-planked flight deck and that failure of the planking will not occur at loads less than those determined by the design calculations. Also the test results show that design



S11
A9/1
(710:MCC:kc)
Ser 7-111
21 May 1959

based on initial yielding of the steel supporting structure is conservative.


S. R. HELLER, JR.
By direction

Copy to:

BUSHIPS (106)
(420)
(440)
(442)
(443)
(522)
(633)

CHBUAER (with 2 copies of encl (1)).
CNO (with 2 copies of encl (1)).
CHONR (with 2 copies of encl (1)).
DIR, USNRL (with 2 copies of encl (1)).
NAVSHIPYD NORVA (with 2 copies of encl (1)).
NAVSHIPYD PUG (with 2 copies of encl (1)).
NAVSHIPYD NYK (with 2 copies of encl (1)).
NAVSHIPYD SFRAN (with 2 copies of encl (1)).
NAVSHIPYD BSN (with 2 copies of encl (1)).
NAVSHIPYD LBEACH (with 2 copies of encl (1)).
NAVSHIPYD PEARL (with 2 copies of encl (1)).
NAVSHIPYD PHILA (with 2 copies of encl (1)).
CDR, NATC (ET) (with 1 copy of encl (1)).
CDR, NADC, Johnsville, Pa. (with 1 copy of encl (1)).
CDR, NAMC, Philadelphia, Pa. (with 1 copy of encl (1)).
Asst Sec of Defense (R and D) (with 1 copy of encl (1)).
COMOPDEVFORLANT (with 1 copy of encl (1)).
NRF, San Diego, California (with 2 copies of encl (1)).
SRF, Subic Bay, P. I. (with 2 copies of encl (1)).
SRF, Yokosuka, Japan (with 2 copies of encl (1)).
Supt, USN Postgrad School, Monterey, Calif. (with 1 copy of encl (1)).
CO, NAVADMINUNIT, MIT, Cambridge, Mass. (with 1 copy of encl (1)).
OinC Postgrad School, Webb Inst of Naval Arch, Glen Cove, N. Y. (with 1 copy of encl (1)).



S11
A9/1
(710:MCC:kc)
Ser 7-111
21 May 1959

Copy to:

SUPSHIPINSORD, NYSB Corp, Camden, N. J. (with 1 copy of
encl (1)).

NYSB Corp, Camden, N. J. (with 1 copy of encl (1)).

SUPSHIPINSORD, NNSB and DD Co., Newport News, Va., (with
1 copy of encl (1)).

SUPSHIPINSORD, Quincy, Mass. (with 1 copy of encl (1)).

Bethlehem Steel Corp, Quincy, Mass. (with 1 copy of encl (1)).

NNSB and DD Co., Newport News, Va. (with 1 copy of encl (1)).

**STRUCTURAL TESTS OF FLIGHT DECK ON USS HANCOCK
(CVA 19) UNDER SIMULATED A3D-1 AND F2H-3
AIRCRAFT LANDING LOADS**

by

Ralph B. Allnutt

April 1959

**Report 949
NS 731-040**

TABLE OF CONTENTS

	Page
ABSTRACT	1
INTRODUCTION	1
DESCRIPTION OF FLIGHT-DECK STRUCTURE	2
INSTRUMENTATION	2
LOADING APPARATUS	8
TEST PROCEDURE	15
TEST RESULTS AND DISCUSSION	16
Positions 1, 9, and 14 (A 3 D-1)	39
Position 2 (A 3 D-1)	43
Position 3 (A 3 D-1)	44
Positions 4 and 6 (A 3 D-1)	44
Position 7 (A 3 D-1)	44
Positions 5, 8, and 15 (A 3 D-1)	44
Positions 10, 11, 12, and 13 (F 2 H-3)	46
COMPARISON OF EXPERIMENT WITH THEORY	47
Bureau of Ships Design Procedure	47
Maxwell's Reciprocity Theorem	49
Dynamic Response	49
EVALUATION OF STRENGTH	52
SUMMARY AND CONCLUSIONS	54
ACKNOWLEDGMENTS	54
REFERENCES	55

LIST OF FIGURES

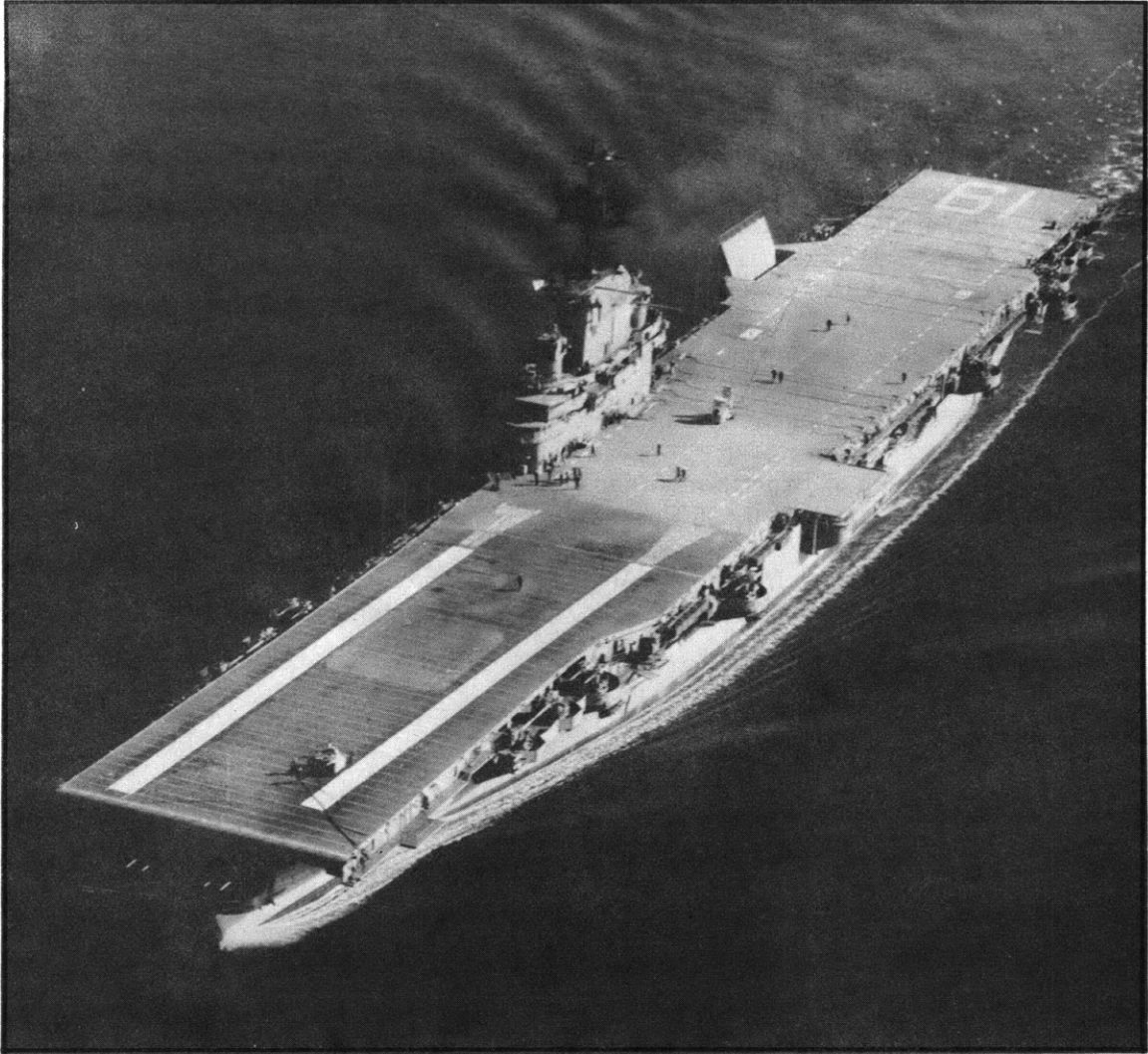
	Page
Figure 1 – Location of Test Positions	3
Figure 2 – Location of Strain Gages on Longitudinals and Transverse Beams	5
Figure 3 – Location of Strain Gages on Transverse Bent and Centerline Girder	6
Figure 4 – Location of Deflection Gages	7
Figure 5 – Deflection Gages Mounted below Transverse Beams	8
Figure 6 – Test Rig with A 3 D-1 Landing Gear Installed for Static Test	9
Figure 7 – Test Rig with A 3 D-1 Landing Gear Showing Quick-Release Device	9
Figure 8 – Peak Deck Reaction versus Drop Height for Test Rig with A 3 D-1 Landing Gear	11
Figure 9 – Peak Deck Reaction versus Sinking Speed for A 3 D-1	11
Figure 10 – Load-Time Curves for A 3 D-1 Test Rig Compared with Actual Airplane Landing.....	12
Figure 11 – Test Rig with F 2 H-3 Landing Gear Installed	13
Figure 12 – Peak Deck Reaction versus Drop Height for Test Rig with F 2 H-3 Landing Gear	14
Figure 13 – Peak Deck Reaction versus Sinking Speed for F 2 H-3	14
Figure 14 – Load-Time Curves for F 2 H-3 Test Rig Compared with Airplane Drop Tests under Simulated Landing Conditions	15
Figure 15 – Typical Plots of Load versus Static Strain and Peak Dynamic Strain	32
Figure 16 – Typical Oscillograph Record Obtained for an A 3 D-1 Deck Reaction of 138,200 Pounds at Position 14.....	33
Figure 17 – Load-Strain Plots for Gages on Wooden Planking, Test Positions 5 and 8 (A 3 D-1)	34
Figure 18 – Load-Strain Plots for Gages on Wooden Planking, Test Positions 10 and 11 (F 2 H-3)	35
Figure 19 – Load-Strain Plots for Gages on Wooden Planking, Test Positions 12 and 13 (F 2 H-3)	36
Figure 20 – Tire Imprints for Various Static Loads	40

	Page
Figure 21 – Tire Bottoming during Drop Tests	41
Figure 22 – Distribution of Static and Dynamic Strains in Lower Flanges of Grillage Members for an A 3 D-1 Loading of 138,200 Pounds at Test Position 1	42
Figure 23 – Deflections and Corresponding Bending Stresses in Longitudinal Member for Deck Reaction of 99,000 Pounds for Various A 3 D-1 Test Positions	43
Figure 24 – Portion of Flight-Deck Planking Removed from Test Position 1 after Tests with A 3 D-1 Landing Gear	45
Figure 25 – Portion of Flight-Deck Planking Removed from Test Position 9 after Deck Reaction of 138,200 Pounds with A 3 D-1 Landing Gear	45
Figure 26 – Portion of Flight-Deck Planking Removed from Test Position 5 after Deck Reaction of 138,200 Pounds with A 3 D-1 Landing Gear	45
Figure 27 – Portion of Flight-Deck Planking Removed from Test Position 10 after Deck Reaction of 66,000 Pounds with F 2 H-3 Landing Gear	47
Figure 28 – Effect of Damping on Amplification Spectra	51
Figure 29 – Ratio of Peak Response Time t_p to Peak Pulse Time t_m	51
Figure 30 – Comparison of Drop-Test Results with BuShips Design Calculations of Maximum Bending Stress in Longitudinal Member versus Deck Reaction	53

LIST OF TABLES

Table 1 – Stress Studied at Each Test Position	4
Table 2 – Characteristics of A 3 D-1 and F 2 H-3 Airplanes and Certified Flight-Deck Reactions	10
Table 3 – Strains and Deflections at Test Positions 1 A and 1 B for A 3 D-1	17
Table 4 – Strains and Deflections at Test Positions 1 C and 1 D for A 3 D-1	18
Table 5 – Strains and Deflections at Test Position 2 for A 3 D-1	19
Table 6 – Strains and Deflections at Test Position 3 for A 3 D-1	20
Table 7 – Strains and Deflections at Test Positions 4 and 6 for A 3 D-1	21
Table 8 – Strains and Deflections at Test Position 5 for A 3 D-1	22
Table 9 – Strains and Deflections at Test Position 7 for A 3 D-1	23

	Page
Table 10 – Strains and Deflections at Test Position 8 for A 3 D-1	24
Table 11 – Strains and Deflections at Test Position 9 for A 3 D-1	25
Table 12 – Peak Dynamic Strains and Deflections at Test Position 14 for A 3 D-1	26
Table 13 – Peak Dynamic Strains and Deflections at Test Position 15 for A 3 D-1	27
Table 14 – Strains and Deflections at Test Position 10 for F 2 H-3	28
Table 15 – Strains and Deflections at Test Position 11 for F 2 H-3	29
Table 16 – Strains and Deflections at Test Position 12 for F 2 H-3	30
Table 17 – Strains and Deflections at Test Position 13 for F 2 H-3	31
Table 18 – Shear Stresses Computed from Rosette Strains on Webs	37
Table 19 – Measured Permanent Sets or Zero Shifts of Strain Gages	38
Table 20 – Comparison of Experimental and Calculated Stresses for A 3 D-1 Deck Reaction of 90,000 Pounds	48
Table 21 – Experimental Verification of Maxwell’s Reciprocity Theorem for Longitudinals Located One, Two, and Three Spacings Apart.....	50



USS HANCOCK (CVA 19)

ABSTRACT

Static and dynamic strains and deflections were measured on the flight-deck structure of USS HANCOCK (CVA 19) after Project 27-C conversion. A specially designed loading apparatus was used for simulating wheel loadings of A 3 D-1 and F 2 H-3 aircraft. It is concluded that the present Bureau of Ships design method is accurate for calculating the stresses in the steel supporting structure for a wood-planked flight deck, and that failure of the planking will not occur at loads less than those determined by the design calculations. Also, the test results show that design based on initial yielding of the steel supporting structure is conservative.

INTRODUCTION

USS HANCOCK (CVA 19) was the first ESSEX-Class aircraft carrier authorized for Project 27-C conversion. During this conversion at the Puget Sound Naval Shipyard in 1954 many extensive changes were made, including stiffening of the flight deck, an increase in beam, installation of steam catapults and heavier arresting gear, an increased aircraft-fuel capacity, ordnance and electronic improvements, and installation of higher-capacity aircraft elevators.

The Bureau of Ships¹ requested the David Taylor Model Basin to conduct extensive static and dynamic tests on the strengthened flight deck of HANCOCK to obtain data regarding the dynamic response factor and to evaluate existing design procedures. This information was required because of the increase in weight and landing loads for new jet aircraft. It is current practice to design carrier flight decks by using only static loads to simulate the landing reactions of aircraft. The validity of this assumption and the accuracy of the design method required experimental verification. During these tests strains and deflections were read in transverse beams, longitudinals, and flight-deck planking at various critical locations in the landing area. Originally, tests were to have been conducted with a Douglas A 3 D-1 landing-gear assembly attached to a loading apparatus to simulate landing of an A 3 D-1 aircraft, but the tests were later expanded to include a McDonnell F 2 H-3 landing gear.

This report describes the structure under study, the instrumentation and gage locations, the loading device, and the sequence of events during the test. Results of the static and dynamic tests are given, and the experimental results are compared with those obtained from BuShips design calculations.^{2,3} A brief discussion of the dynamic response of the structure is included. The strength of the flight deck is evaluated.

¹References are listed on page 55.

DESCRIPTION OF FLIGHT-DECK STRUCTURE

The portion of the flight deck selected for these tests was the area between Frames 173 and 178 port of the ship's centerline; see Figure 1. This specific area was chosen for the following reasons:

1. The 20-ft span between bents is one of the largest in the landing area.
2. The uninterrupted athwartship span is the largest in the landing area.
3. No reinforcing gallery deck is installed in this area.
4. Deflection gages could be supported directly from the hangar deck, thereby providing a firm base from which deflections could be accurately determined independent of adjacent structure.
5. Tests could be conducted with a minimum of interference in the normal functioning of the shipyard and ship's company.

The flight deck of HANCOCK is a composite wooden and steel structure. The standard flight-deck plating used throughout the landing area is 4.2-lb galvanized steel supported by longitudinals on 22.5-in. centers and transverse beams spaced 5 ft 6 in. and 4 ft 6 in. apart. Aft of Frame 149, longitudinals are 12-in. by 4-in. by 19-lb HTS I-beams. These longitudinals rest on transverse beams of identical scantlings. Flight-deck planking in the landing area is laminated Douglas fir and teak, the top 1-in. lamina being teak. Individual planks measure 3 in. deep by 6 in. wide and are secured to the deck plating by studs. In addition to the grillage of longitudinals and transverse beams, the flight deck is further supported by a system of heavy, deep transverse bents and longitudinal girders. Transverse bents are spaced on either 16-ft or 20-ft centers, and longitudinal girders are located on the ship's centerline and on both sides of the hangar space. The structure tested is shown in Figures 1, 2, and 3. The span of the flight deck is supported by this system of transverse bents, longitudinal girders, longitudinals, and transverse beams from Frame 42 to Frame 202½, a distance of 642 ft.

INSTRUMENTATION

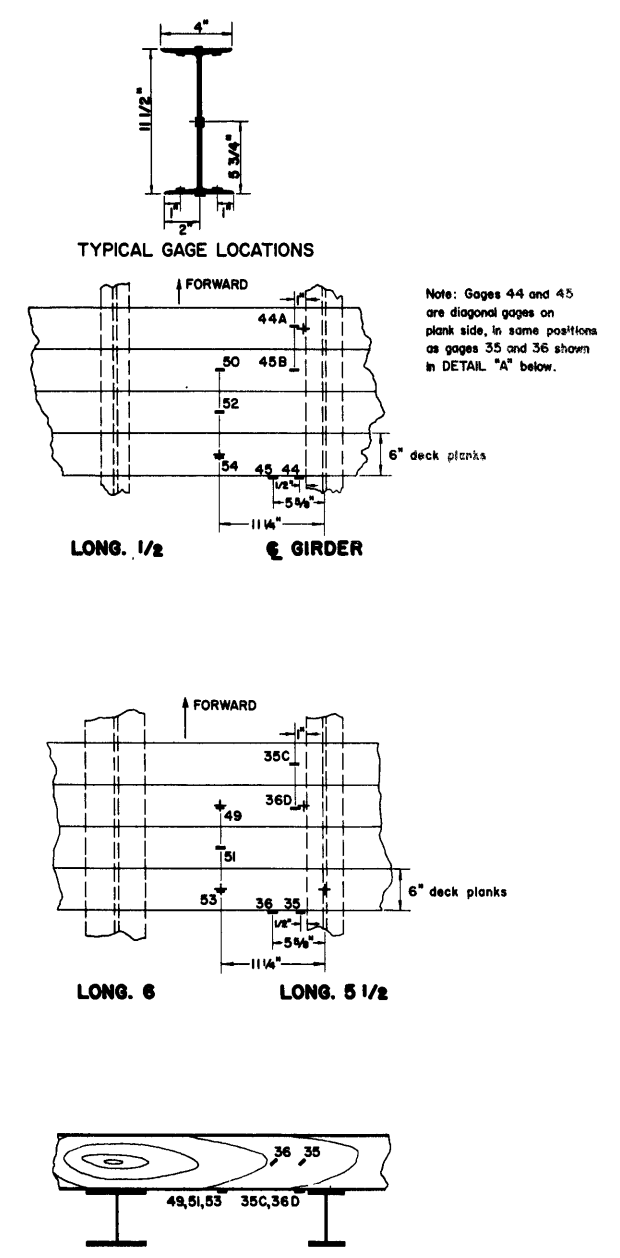
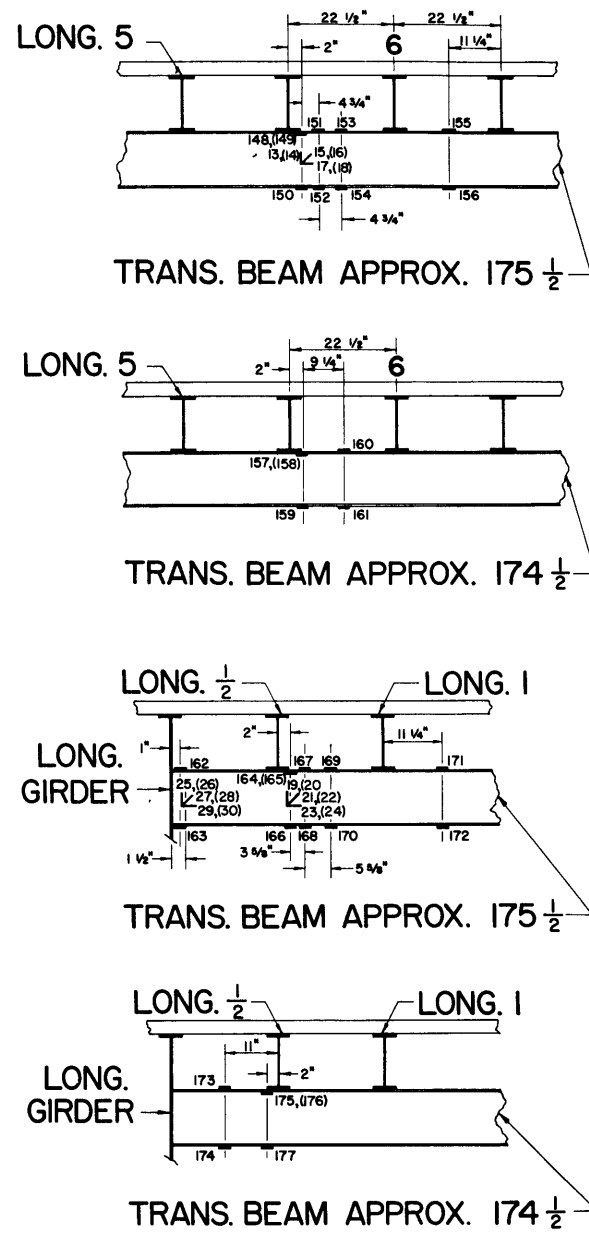
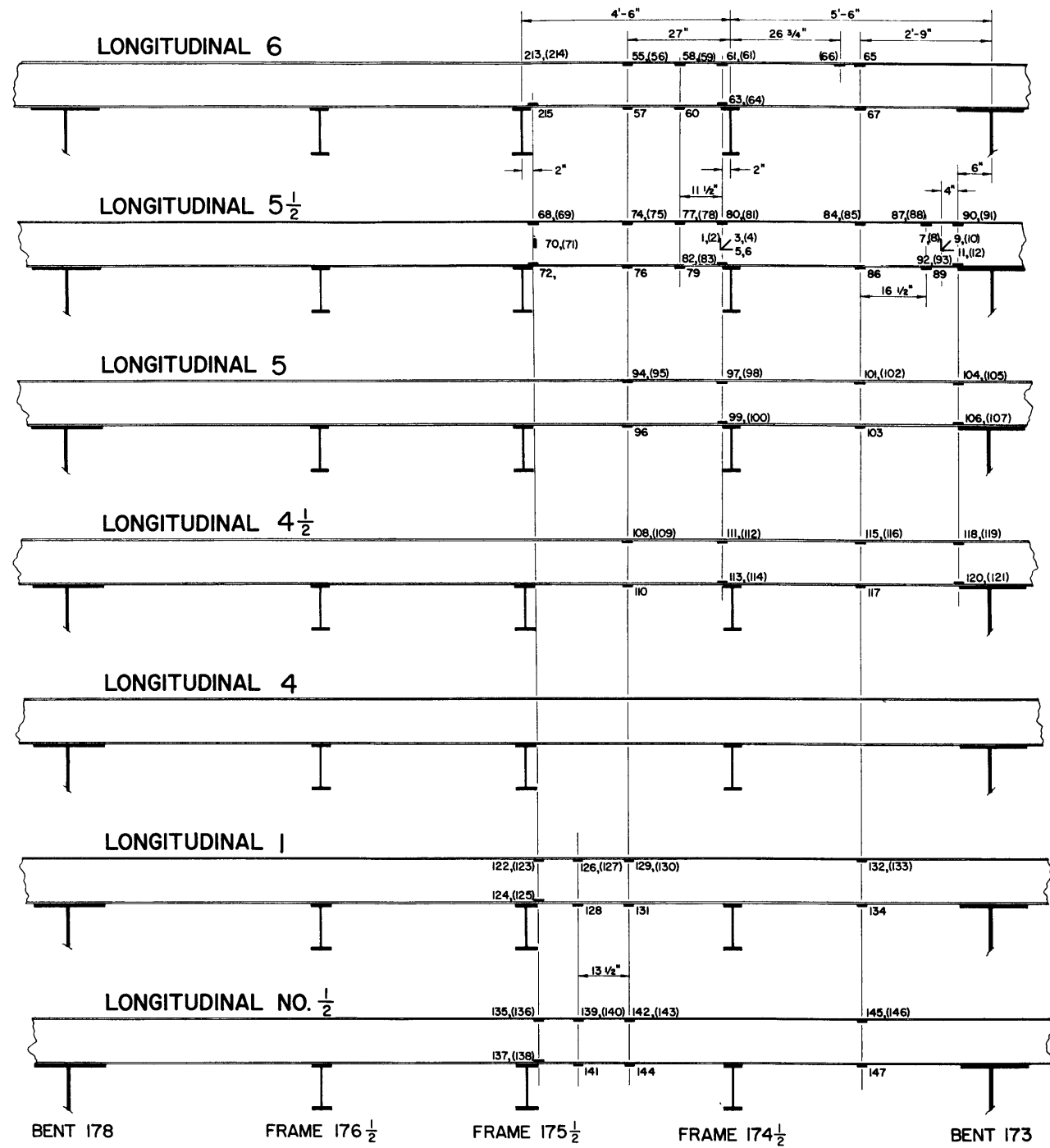
Fifteen test positions were selected in the test area, as shown in Figure 1. The location of each test position, the aircraft wheel assembly used for the test, and the critical structure under study are given in Table 1.

Figures 2 and 3 show the orientation of strain gages on the structure. Gages 1 through 30 were arranged as rosettes to measure shear in the web of the steel longitudinals and transverse beams. Gages 35, 36, 44, and 45 were single gages oriented diagonally at 45 deg on the side of the wooden planking to give a measure of the shear strain. Gages 37 through 43 and 46 through 54 were located on the bottom surface of the wooden planking to measure bending. Gages 55 through 147 and 213 through 215 were located on the flanges of longitudinals to measure bending strains. Gages 148 through 177 were located on the flanges of the transverse

TABLE 1

Stress Studied at Each Test Position

Test Position	Location	Landing Gear Used	Stress
1	Longitudinal 5½, midway between transverse beams, Frames 174½ and 175½	A 3 D-1	Bending and shear in longitudinals
2	Longitudinal 5½, midway between transverse beam, Frame 174½, and Bent 173	A 3 D-1	Bending and shear in longitudinals
3	Longitudinal 5½, at intersection with transverse beam, Frame 175½	A 3 D-1	Bending and Shear in transverse beam
4	Longitudinal 5½, 6 in. aft of Bent 173	A 3 D-1	Shear in longitudinals
5	Midway between Longitudinals 5½ and 6 between transverse beams	A 3 D-1	Bending and shear in flight-deck planking
6*	Longitudinal 5½ at Bent 173	A 3 D-1	Bending in transverse bent
7	Longitudinal ½ at intersection with transverse beam, Frame 175½	A 3 D-1	Bending and shear in transverse beams
8	Midway between Longitudinal ½ and centerline girder between transverse beams	A 3 D-1	Bending and Shear in transverse beams
9**	Longitudinal 4½, midway between transverse beams	A 3 D-1	Bending and shear in longitudinals
10	Midway between longitudinal girder and Longitudinal ½	F 2 H-3	Bending and shear in flight-deck planking
11	2 in. outboard of centerline longitudinal girder	F 2 H-3	Shear in flight-deck planking
12	2 in. outboard of Longitudinal 5½	F 2 H-3	Shear in flight-deck planking
13	Midway between Longitudinals 5½ and 6 between transverse beams	F 2 H-3	Shear in flight-deck planking
14	Longitudinal 6, midway between transverse beams	A 3 D-1	Check on Position 1
15	Midway between Longitudinals 5½ and 6. 10 in. aft of Pos. 5	A 3 D-1	Check on Position 5 (wood only)
<p>*Tests were not run at Position 6 because of its nearness to Position 4 where very low strains were recorded.</p> <p>**Test Position 9 was selected to obtain data to validate Maxwell's theorem.</p>			



DETAIL "A"
PLANKING INSTRUMENTATION

Figure 2 – Location of Strain Gages on Longitudinals and Transverse Beams

Gage numbers in parentheses indicate that the gage was either on the inboard side of a longitudinal or on the forward side of a transverse member.

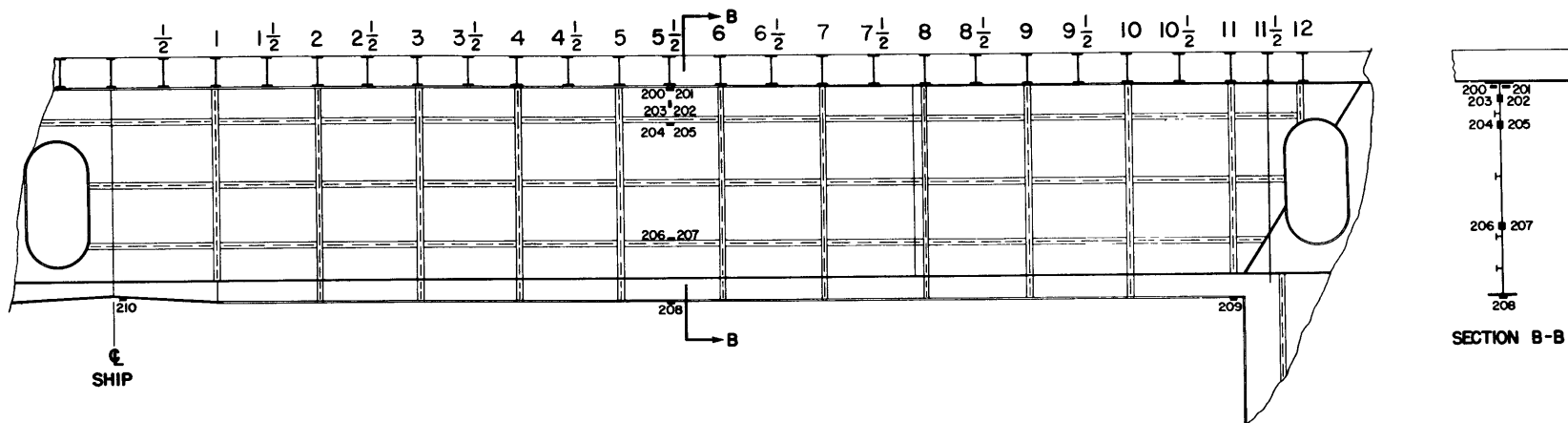


Figure 3a – Transverse Bent Frame 173, Looking Aft

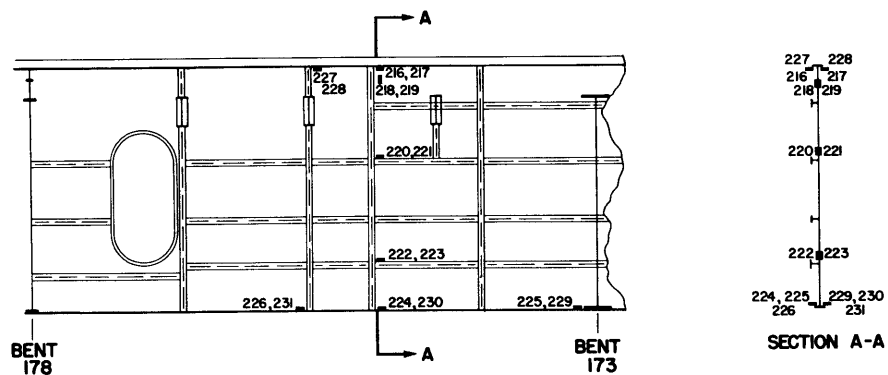


Figure 3b – Longitudinal Centerline Girder, Looking to Port

Figure 3 – Location of Strain Gages on Transverse Bent and Centerline Girder

beams to measure bending. Gages 200 through 210 were on the heavy transverse bent, and Gages 216 through 231 were on the heavy centerline girder.

All gages were moistureproofed by painting the gage and surrounding area with Ozite "B," a commercial bituminous compound. Before the gages on the wooden planking were installed, a prime coat of tygon, a plastic paint, was applied to the wood to prevent moisture in the wood from affecting the strain gages.

The same strain gages were used to measure both dynamic and static strains. Each active gage was connected to a dummy or temperature-compensating gage which was mounted on an adjacent unstrained steel block.

For the static phase the gages were run directly to 48-position strain-gage switching units, and the strains were read by means of Baldwin SR-4 strain-gage indicators.

The limited amount of dynamic recording equipment available for the test made it impossible to record the output of more than 36 gages at one time. A plugboard arrangement was used to provide a convenient means of quickly selecting the proper gages to be recorded for each test position. Dynamic strains were amplified by carrier-type amplifiers and recorded on electromagnetic oscillographs.

Deflections were measured for both static and dynamic loading at the positions shown in Figure 4. The deflections under static loading were measured by mounting dial gages at

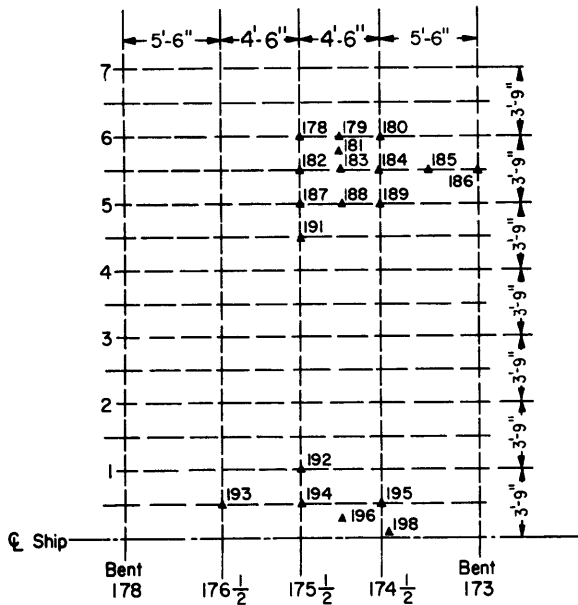


Figure 4 – Location of Deflection Gages

the selected stations and reading the deflections directly. The deflections under dynamic loading were determined by scratch gages. In this type of gage an aluminum plunger slides in a tubular base. The tube has an inner diameter slightly larger than the diameter of the plunger. The base is mounted directly under the plunger at a height which allows about half the plunger to enter the tubing. The plunger is attached to the deflecting structure; the base, to a stationary reference. As the structure moves up or down, the plunger moves relative to the tube, and a stylus fixed with respect to the base produces a vertical scratch on the plunger. The maximum deflection for each loading is given by the length of the scratch. By rotating the plunger a horizontal reference zero is produced. Both types of deflection gages are shown in Figure 5.

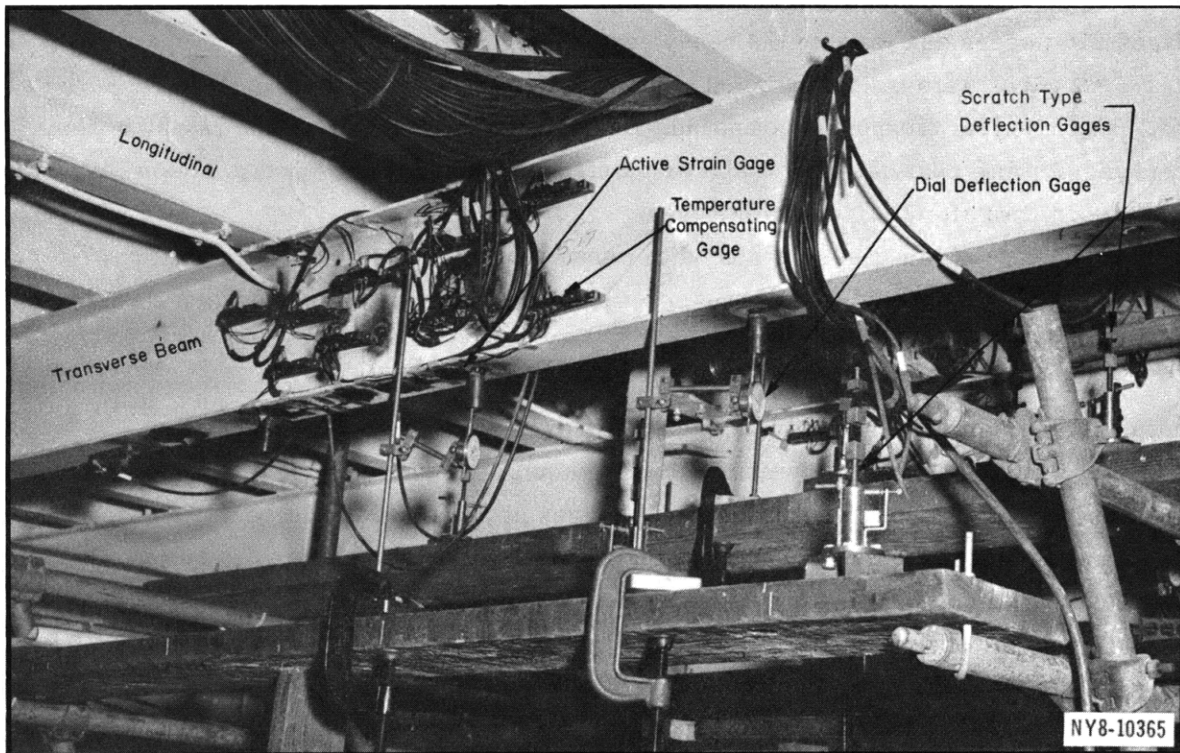


Figure 5 – Deflection Gages Mounted below Transverse Beams

LOADING APPARATUS

A loading apparatus or test rig was designed, built, and maintained during the test by Douglas Aircraft Company, El Segundo Division, under Bureau of Aeronautics Contract Noa(s) 10414. The test rig, Figure 6, was designed to accommodate a single landing gear complete with wheel, tire, and oleo strut mechanism as used on the A3D-1 and F2H-3 airplanes. One landing-gear assembly was sufficient since the airplane wheels are far enough apart that the interaction between the loads they impose on the flight-deck structure does not significantly affect the critical stresses. The rig consisted of a steel-truss structure that was pivoted at one end. The landing gear was secured at the other end.

As shown in Figure 6, the pivoted end of the loading apparatus was supported by channels welded to a flat plate. To prevent movement of the rig during tests, ballast weighing 6000 lb was placed on the flat plate. The plate and channel supports were located so that any hinge reaction would occur forward of the section of the flight deck being tested and would be distributed over a large deck area and over a bent. Thus the effects of the hinge reactions and hold-down weights on the portion of the structure under test were negligible.

For static loading, weights were piled on top of the rig directly over the wheel. For dynamic loading, circular weights were attached to the sides of the rig in line with the wheel to give a low center of gravity relative to the wheel, as shown in Figure 7. For the dynamic

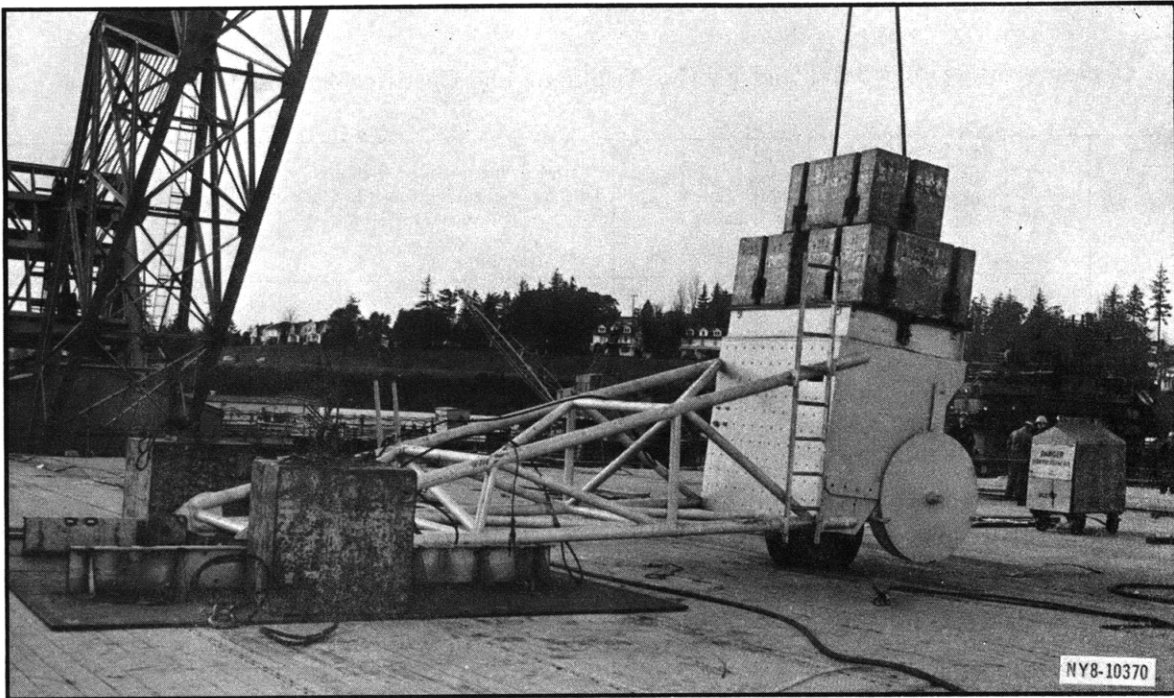


Figure 6 – Test Rig with A3D-1 Landing Gear Installed for Static Test

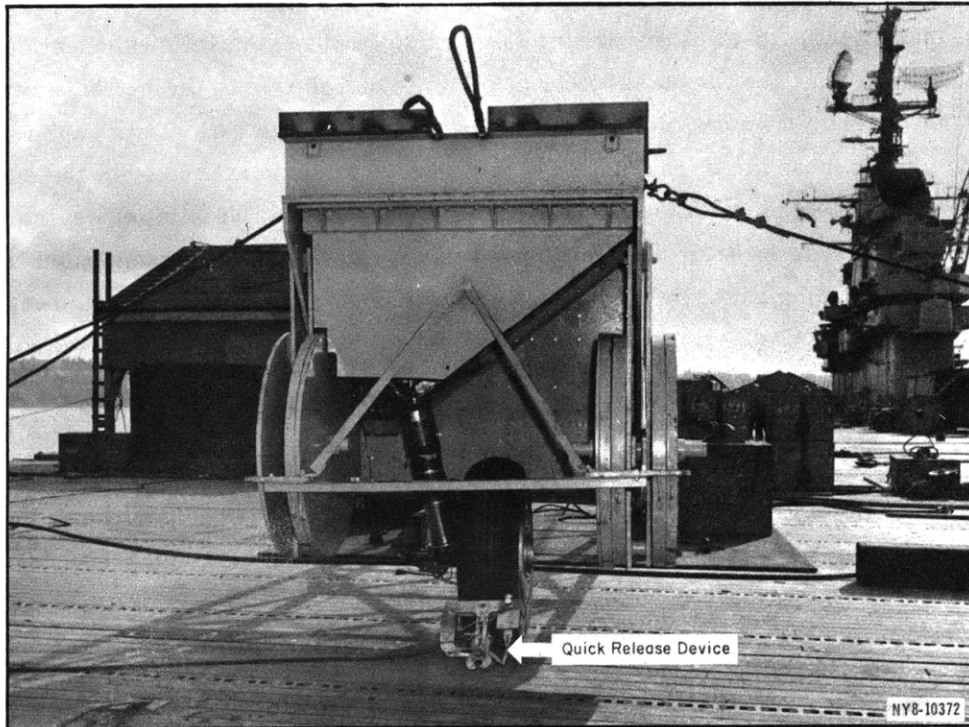


Figure 7 – Test Rig with A3D-1 Landing Gear Showing Quick-Release Device

TABLE 2

Characteristics of A3D-1 and F2H-3 Airplanes and Certified Flight-Deck Reactions

Airplane	Gross Landing Weight lb	Reaction on Landing Gear for Yield lb.	Tire Size		Ply Rating	Rated Load lb	Rated Inflation Pressure psi	Operating Inflation Pressure psi	Distance Center to Center of Rim in.	Rim Diameter in.	Oleo Strut Pressure psi	CVA 19 Certified Deck Reaction lb
			O.D. in.	Casing Depth in.								
A3D-1	45,900	119,000	44	× 13	26	35,000	200	190	12.00	23.750	470	90,000
F2H-3	16,700	59,500	26	× 6.6	14	10,000	210	245	5.69	16.00	170	46,650

(drop) tests the landing-gear end of the rig was raised by a crane to the desired height and dropped by means of an electrically operated quick-release mechanism.

No wheel "spin-up"* was provided nor was provision made for simulating the running loads that occur during actual landings. This latter effect is no more severe than the dynamic loads applied by the test rig.⁴

Extensive preliminary calibrations of the test rig were made to insure that the dynamic loads would adequately simulate airplane-landing reactions. To assist with the calibrations and to provide a measure of the dynamic forces during the shipboard tests, the wheel axles were instrumented with SR-4 strain gages for measuring the wheel or deck reaction. These gages were calibrated by dropping the test rig from various heights onto a calibrated platform. Additional instrumentation employed during the calibrations was as follows: A slide wire to indicate the position of the shock absorber or oleo piston relative to the barrel, a Statham pressure transducer to measure oleo pressure, links instrumented with strain gages at the pivots of the rig to measure pivot reactions, and a portable device to measure the sinking speed just prior to contact with the deck or calibration platform. This latter device employed an electronic counter to measure the time between pulses caused by a brush attached to the falling test rig sweeping past fixed contact points. These contacts were located 0.1 ft apart with the lowest contact actuating $\frac{1}{4}$ in. before the wheel hit the deck. Further details concerning this instrumentation can be found in Reference 5.

The oleo strut pressures and tire pressures are listed in Table 2, along with the general characteristics of A3D-1 and F2H-3 airplanes and the certified deck reactions.

It was originally intended to provide a peak wheel reaction of 90,000 lb at a sinking speed of 15 fps for the A3D-1. After considerable experimentation with different oleo metering pins and rig weights, a reaction of 90,000 lb at a sinking speed of 14 fps was selected as a practical compromise. This was justified on the basis that it was considered more important to obtain a good correlation of load versus time for the test rig and the airplane than to obtain

*The term "spin-up" refers to initial wheel rotation corresponding to the rotational acceleration of the wheel of an aircraft as it contacts the flight deck during landing.

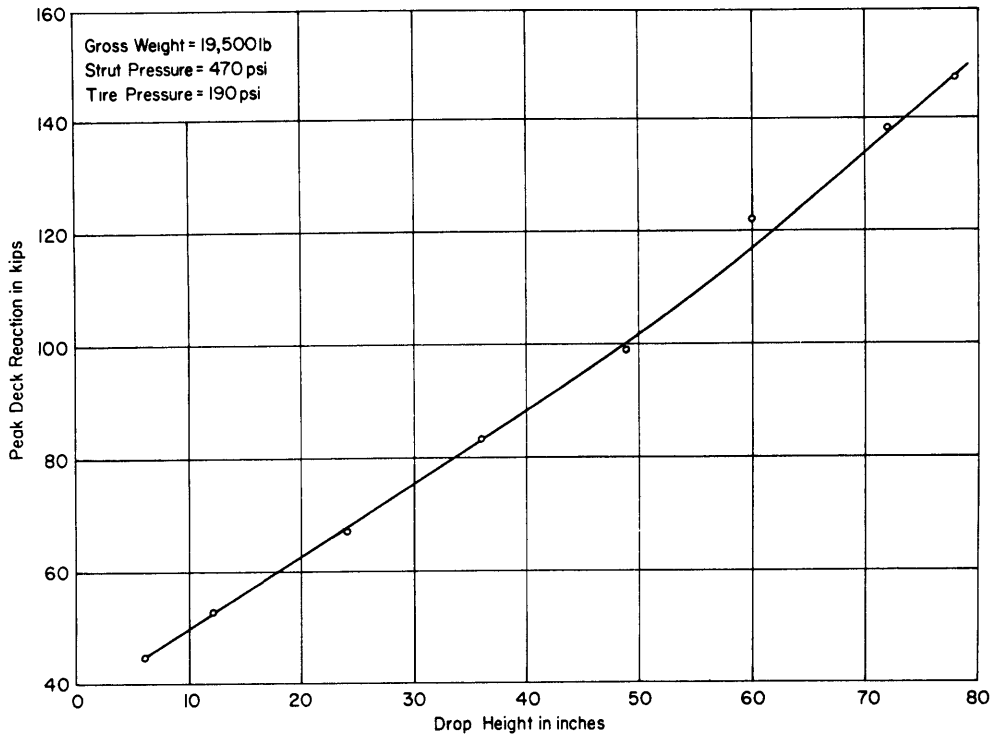


Figure 8 – Peak Deck Reaction versus Drop Height for Test Rig with A3D-1 Landing Gear

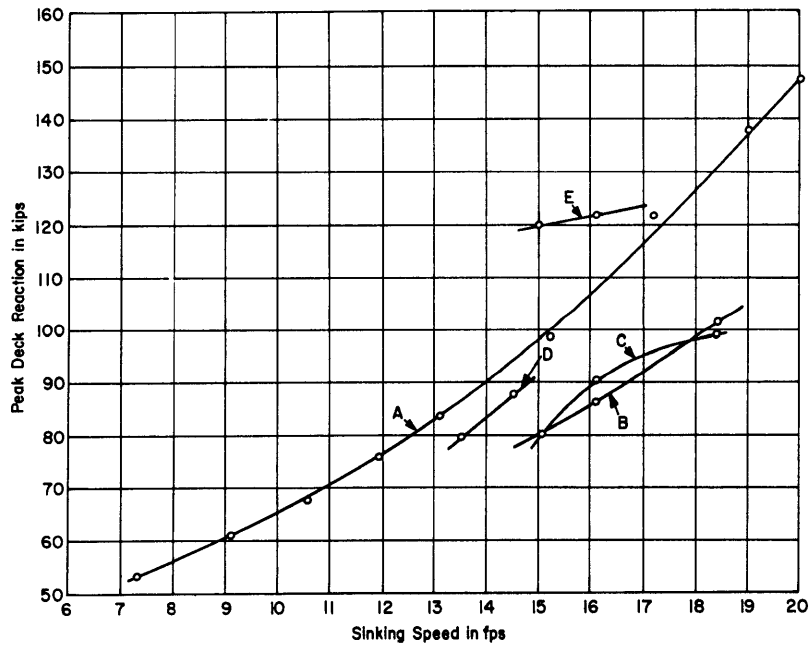


Figure 9 – Peak Deck Reaction versus Sinking Speed for A3D-1

Curve A is the calibration curve for the test rig. Curve B is for an airplane weight of 45,900 lb, 3-point level landing, and 125-knot spin-up. Curve C is for an airplane weight of 45,900 lb, 2-point level landing, and 125-knot spin-up. Curve D is for an airplane weight of 55,950 lb and 135-knot spin-up. Curve E is for an airplane weight of 45,900 lb, 5-deg roll, and 125-knot spin-up.

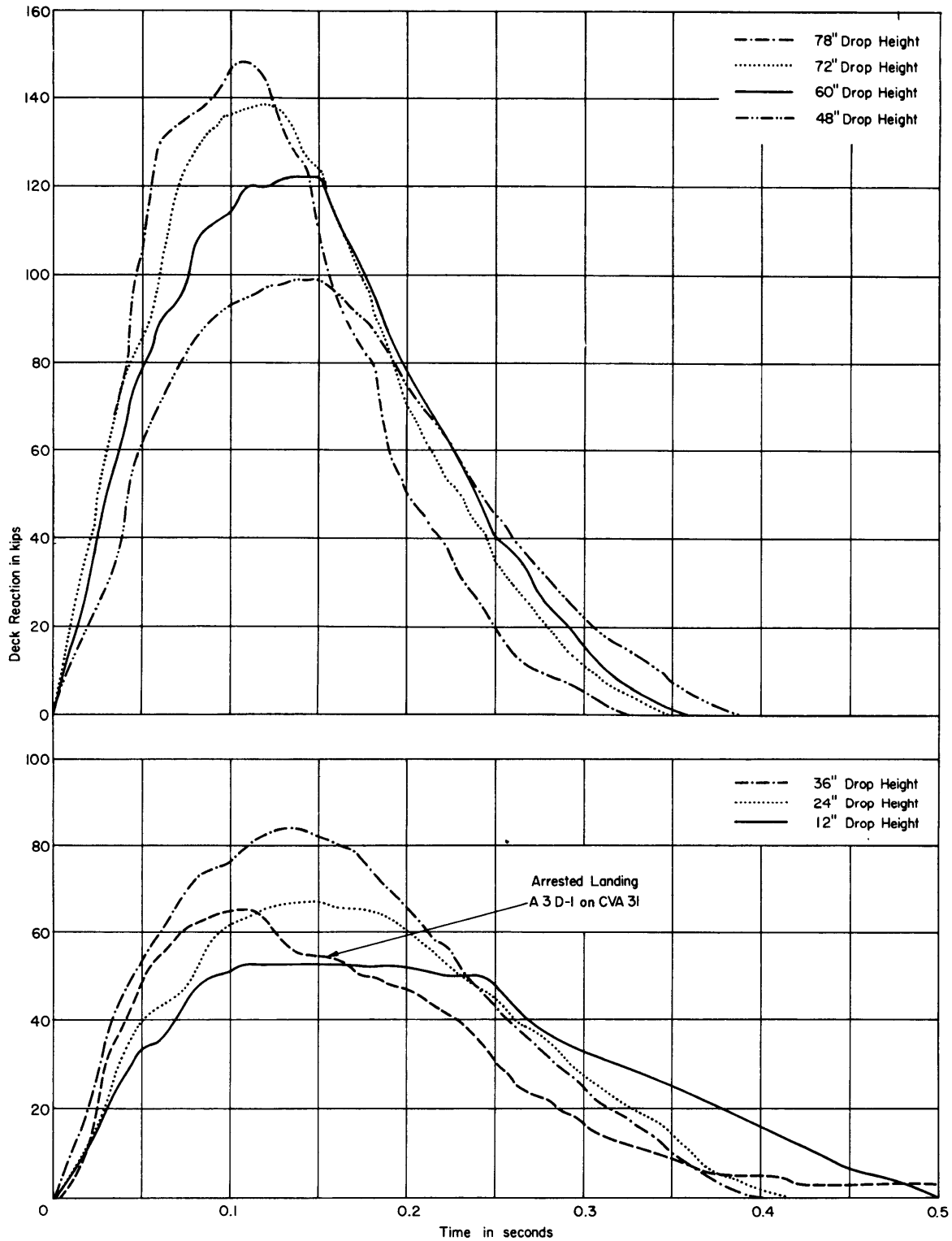


Figure 10 – Load-Time Curves for A 3 D-1 Test Rig Compared with Actual Airplane Landing

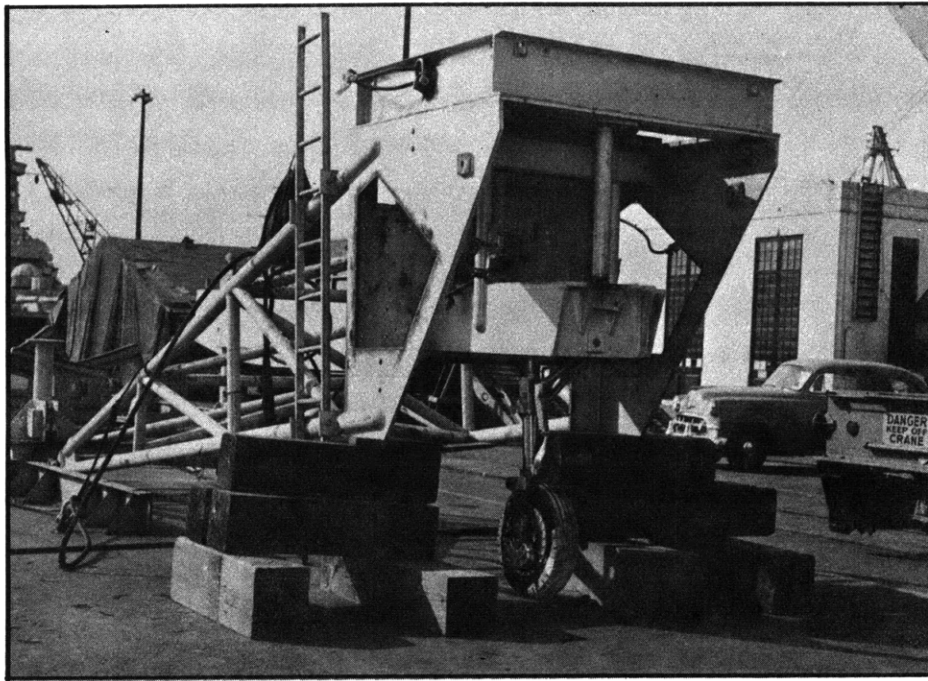


Figure 11 – Test Rig with F 2H-3 Landing Gear Installed

the exact relationship between deck reaction and sinking speed. The load-time relationship for the test rig was made to correlate with similar data obtained from drop tests conducted on the actual airplane at the manufacturer's plant. The final weight of the test rig and the A 3D-1 landing gear was 19,500 lb. Figure 8 shows the relationship between drop height and peak deck reaction for the test rig with the A 3D-1 assembly. In Figure 9 the relationship between peak deck reaction and sinking speed of the test rig is compared with results of the manufacturer's tests of the airplane under various simulated landing conditions. Figure 10 shows the load-time curves for the test rig for various drop heights. These curves show good correlation with the broken-line curve which was obtained later during actual landing tests of an A 3D-1 airplane on USS BON HOMME RICHARD (CVA 31).

Since the F 2H-3 was added to the program after the tests were under way, it was necessary to make these calibrations at dockside. Oscillograph records of deck reaction versus time for this airplane were not available at this time, and the criteria used in adjusting the weight of the test rig was to provide a sinking speed of 18 fps for a deck reaction of 67,000 lb. The weight of the test rig with the F 2H-3 landing gear installed was approximately 9000 lb. To obtain this weight it was necessary to cut away portions of the test rig, as shown in Figure 11. Figure 12 shows the relationship between drop height and peak deck reaction for the test rig with the F 2H-3 landing gear. In Figure 13 the relationship between deck reaction and sinking speed is compared with results of drop tests of the actual airplane obtained by the manufacturer under various simulated landing conditions. Figure 14 shows the load-time curves for the test rig for various drop heights. The broken-line curve shows the load-time relationship for the airplane from manufacturer's tests.

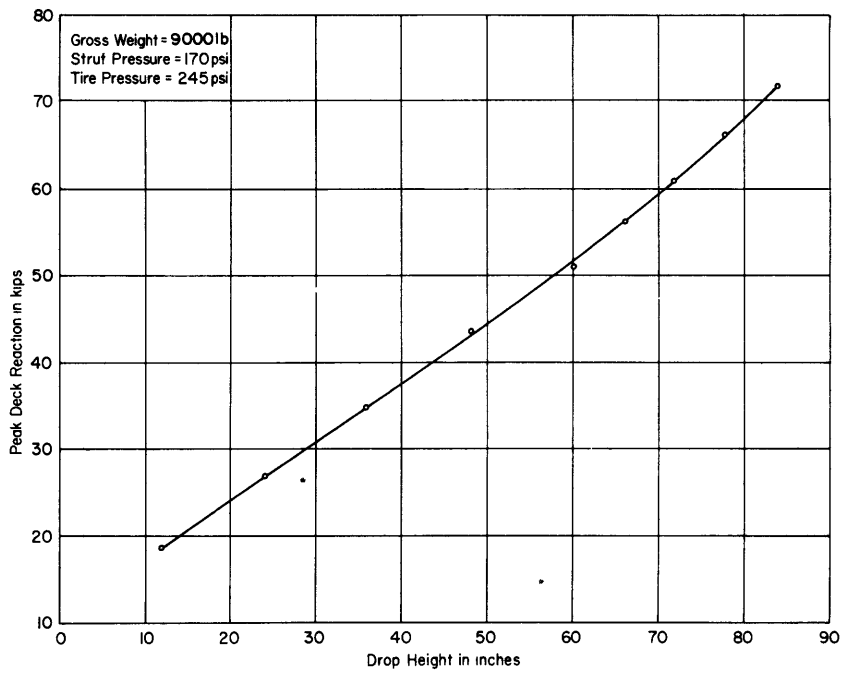


Figure 12 – Peak Deck Reaction versus Drop Height for Test Rig with F 2 H-3 Landing Gear

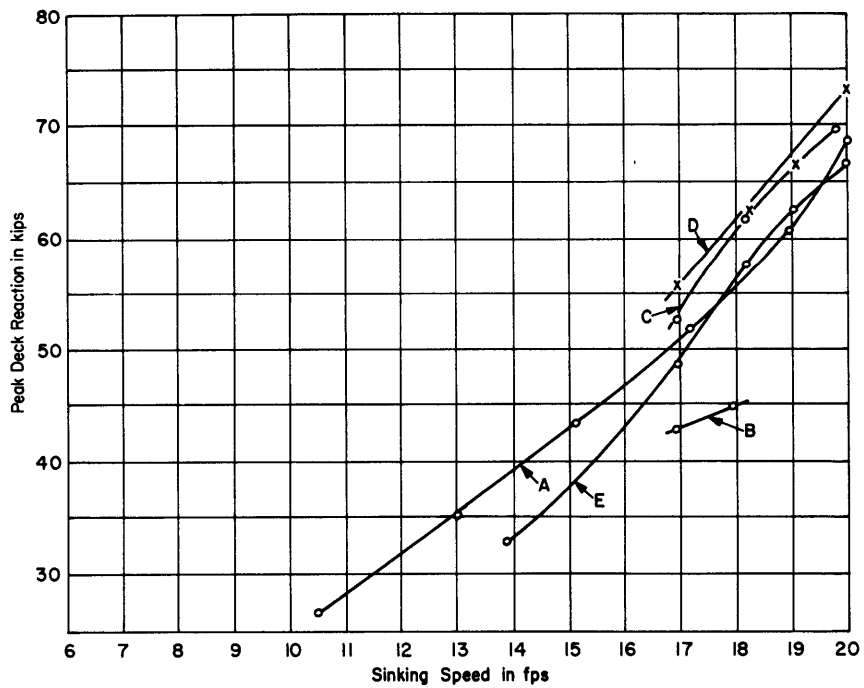


Figure 13 – Peak Deck Reaction versus Sinking Speed for F 2 H-3

Curve A is the calibration curve for the test rig. Curve B is for an airplane weight of 16,700 lb, 3-point level landing, and 104-knot spin-up. Curve C is for an airplane weight of 17,600 lb, 2-point level landing, and 104-knot spin-up. Curve D is for the right wheel of an F 2 H-3 airplane weighing 16,700 lb, landing with the tail 14 deg 18 min low. Curve E is for the left wheel of an F 2 H-3 airplane weighing 16,700 lb, landing with the tail 14 deg 18 min low.

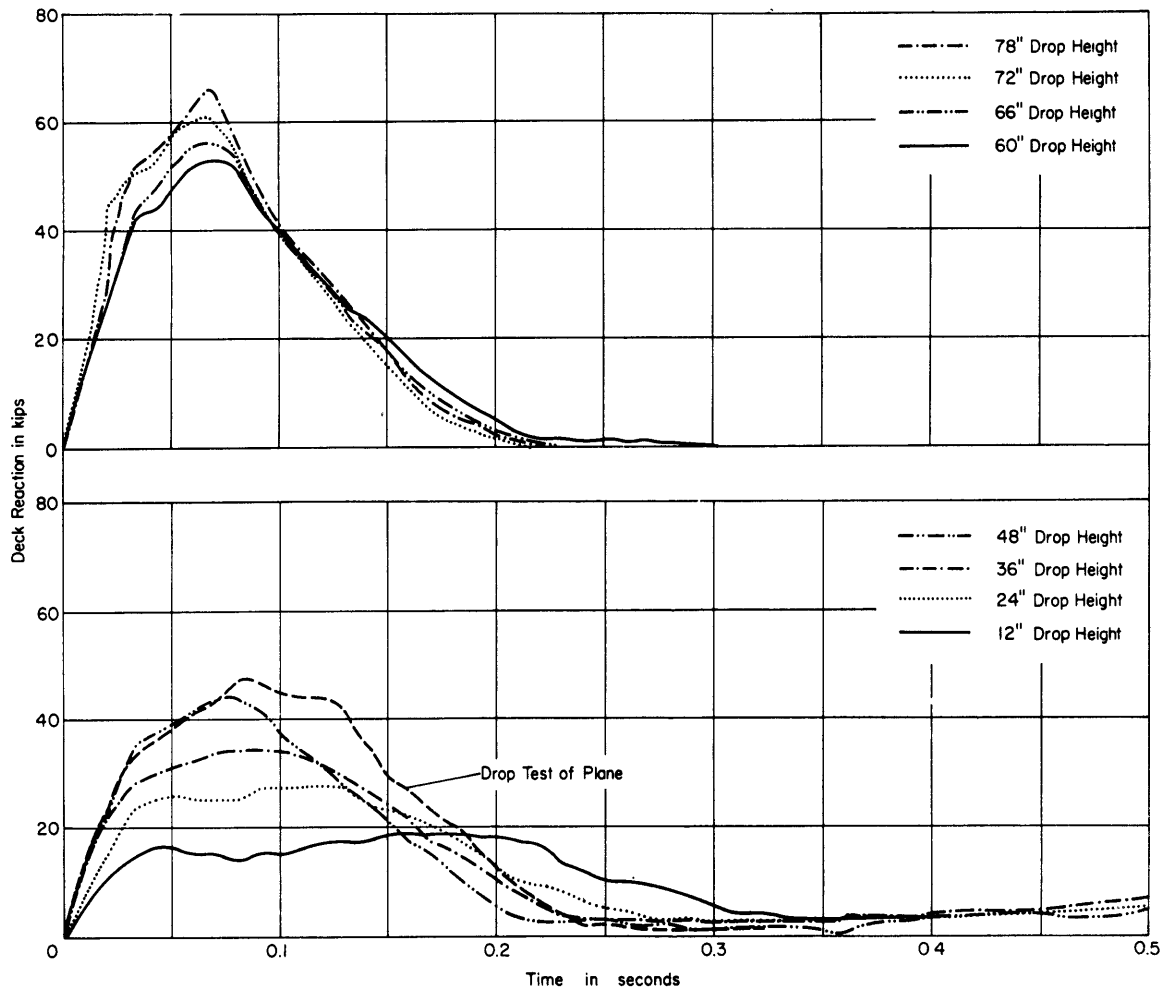


Figure 14 – Load-Time Curves for F2H-3 Test Rig Compared with Airplane Drop Tests under Simulated Landing Conditions

TEST PROCEDURE

For the static tests, the test rig was centered over the test position and secured in place by ballast weights and guy wires. Zero readings were taken on all strain and deflection gages with the landing gear lifted from the deck. The landing gear was then lowered, and static loads were applied by placing weights on the top of the test rig. The above procedure was reversed for unloading. Strain and deflection data were taken at each increment during the loading and unloading processes. Load increments were approximately 20,000 lb. A maximum static load of 98,000 lb was applied with the A3D-1 landing gear, and a maximum of 48,000 lb was applied with the F2H-3 landing gear. The loading sequence was repeated several times at each test position in order to relieve residual welding and fabricating stresses and thereby obtain reproducible data. During one of the static tests a series of tire imprints was obtained at various increments of load by placing a piece of white muslin under the tire.

For the dynamic tests, the rig was positioned as before and was lifted from the deck to a given height with the quick-release device attached to the rig and hung from a pendant secured

to a crane hook. With the landing gear suspended above the deck, the amplifier channels were balanced and calibrated. When the release mechanism was energized, the landing gear was dropped to the deck. The strains in the flight-deck members and the dynamic load were recorded by oscillographs. The peak deflections of the flight-deck structure were recorded simultaneously by the scratch gages. This procedure was repeated at each test position for various free-fall or drop heights. The height was measured from the deck to the bottom of the tire. For the A3D-1 landing gear the drop heights ranged from 6 in. to 78 in.; for the F2H-3 landing gear they ranged from 24 in. to 84 in.

Originally, 13 test positions were selected to cover areas of critical strength. These were expanded somewhat, as noted in Figure 1 and Table 1. Positions 1 through 9 and 14 and 15 were used in conjunction with the A3D-1 landing gear. Positions 10 through 13 were used with the F2H-3 gear and were located to provide critical loading to the wooden planking only.

Position 1 was considered the most important because high stresses were expected in the longitudinals when they were loaded at midspan. Because of the limited amount of recording equipment, the series of drops was repeated so that data could be recorded from all desired gages. These two similar series of drops were designated Tests 1A and 1B. During Test 1B it was observed that, because of a leak, tire pressure had dropped below specification, and the tire was bottoming at lower loads than would normally be expected. This bottoming action caused the upper flange of Longitudinal 5½ to be bent downward. After the tire and tube had been replaced, tests at Position 1 were rerun as Tests 1C and 1D with proper tire pressure but without repairing Longitudinal 5½.

To confirm results obtained from Tests 1C and 1D, an additional test was run at a similar location on Longitudinal 6, which was undamaged. This position was designated as Position 14.

Position 5 was selected to investigate the strength of the wooden planking when loaded by the A3D-1 landing gear. Unfortunately, there was a lightly reinforced transverse butt in the 4.2-lb deck plating at this location. Hence, after tests had been completed at Position 5, an additional test was run 10 in. aft of Position 5 (designated Position 15) to obtain data on the failure of deck planking in an area more typical of unreinforced deck.

Unless otherwise noted, damaged planking was replaced upon completion of a series of drops at a given position before any additional tests were run in the same area.

TEST RESULTS AND DISCUSSION

The results obtained from the strain and deflection data are condensed and summarized in Tables 3 through 17 for each test position. The strain-sensitivity factor m for each gage in microinches per inch per kip is the slope of the linear plot of strain versus static load. The dynamic-response factor for each drop is the ratio of the peak dynamic strain to the static strain for a load equivalent to the dynamic deck reaction for the particular drop. For this purpose, static strains at loads in excess of those actually applied are obtained by extending

(Text continued on page 32.)

Table 4 - Strains and Deflections at Test Positions 1C and 1D for A3D-1

Gage Function	Test Positions 1C and 1D (A3D-1)												Dynamic Strain at Maximum Deck Reaction $\mu\text{in/in.}$		
	Gage	Static Strain Strain-Sensitivity Coefficient m $\mu\text{in/in/kip}$	Drop Height, in. React., kip	Dynamic Response Factor											
				46	51	47	52	48	53	49	50	54		55	
				36	36	48	48	60	60	72	72	72		72	
				83.3	83.3	99.0	99.0	122.0	122.0	138.2	138.2	138.2	138.2		
Shear on Web of Long'l 5½	1	-2.50		0.83	-	0.92	-	1.02	-	0.96	0.98	-	-	-340	
	2	-1.55		0.92	-	1.00	-	1.02	-	1.09	1.07	-	-	-240	
	3	5.55		1.02	-	1.11	-	1.07	-	1.13	1.17	-	-	900	
	4	4.75		0.99	-	1.04	-	1.04	-	1.09	1.09	-	-	720	
	5	2.10		0.94	-	1.00	-	1.02	-	1.09	1.10	-	-	320	
	6	1.80		0.97	-	1.11	-	1.05	-	1.09	1.10	-	-	280	
	7	-0.10		-	-	-	-	-	-	-	-	-	-	-	
	8	0.20		-	-	-	-	-	-	-	-	-	-	-	
	9	1.70		1.00	-	1.06	-	1.02	-	1.09	0.98	-	-	255	
	10	1.40		1.04	-	1.11	-	1.09	-	1.10	1.08	-	-	220	
	11	-0.60		-	-	-	-	-	-	-	-	-	-	-	
	12	-0.45		-	-	-	-	-	-	-	-	-	-	-	
Bending of Long'l 6	55	-4.70		-	-	-	-	-	-	-	-	-	-	-	
	56	-4.30		-	-	-	-	-	-	-	-	-	-	-	
	57	8.75		0.97	-	1.00	-	0.99	-	1.04	1.02	-	-	1260	
	58	-3.35		-	-	-	-	-	-	-	-	-	-	-	
	59	-3.85		-	-	-	-	-	-	-	-	-	-	-	
	60	7.15		0.82	-	0.92	-	0.98	-	0.99	0.98	-	-	980	
	61	-2.40		-	-	-	-	-	-	-	-	-	-	-	
	62	-2.40		-	-	-	-	-	-	-	-	-	-	-	
	63	5.00		-	-	-	-	-	-	-	-	-	-	-	
	64	4.10		0.94	-	0.99	-	0.97	-	1.03	1.02	-	-	590	
	65	0.45		-	-	-	-	-	-	-	-	-	-	-	
	66	0.10		-	-	-	-	-	-	-	-	-	-	-	
67	0.35		-	-	-	-	-	-	-	-	-	-	-		
Bending of Long'l 5½	68	-2.30		0.84	-	0.96	-	1.07	-	0.97	0.94	-	-	-310	
	69	-1.70		0.86	-	0.88	-	0.90	-	0.89	0.83	-	-	-210	
	70	-3.65		0.88	-	0.94	-	0.94	-	1.04	0.99	-	-	-530	
	71	2.90		-	-	-	-	-	-	-	-	-	-	-	
	72	5.70		0.92	-	0.96	-	0.97	-	0.98	1.01	-	-	800	
	73	4.80		0.98	-	1.00	-	0.97	-	1.01	1.03	-	-	680	
	74	-5.75		1.44	-	1.53	-	1.51	-	1.56	-	-	-	-1240	
	75	-8.80		0.97	-	1.09	-	1.10	-	1.12	1.13	-	-	-1380	
	76	15.25		1.02	-	1.08	-	1.06	-	1.10	1.13	-	-	2380	
	77	-4.90		0.83	-	0.82	-	0.78	-	0.81	0.84	-	-	-570	
	78	-4.80		1.23	-	1.20	-	1.16	-	1.18	1.18	-	-	-780	
	79	11.20		1.07	-	1.09	-	1.09	-	1.09	1.14	-	-	1770	
	80	-2.05		1.03	-	1.07	-	1.02	-	0.98	0.98	-	-	-280	
	81	-1.55		-	-	-	-	-	-	-	-	-	-	-	
	82	3.25		1.06	-	1.20	-	1.11	-	1.12	1.14	-	-	510	
	83	4.00		1.09	-	1.20	-	1.11	-	1.14	1.15	-	-	640	
	84	1.05		0.94	-	0.95	-	1.00	-	1.10	1.06	-	-	160	
	85	0.95		-	-	-	-	-	-	-	-	-	-	-	
86	-1.60		0.93	-	0.97	-	0.97	-	0.98	1.00	-	-	-220		
87	1.90		0.95	-	1.00	-	0.98	-	1.10	1.12	-	-	300		
88	2.55		-	-	-	-	-	-	-	-	-	-	-		
89	-3.80		-	0.97	-	1.03	-	0.98	-	-	1.02	1.01	-	-540	
90	2.70		-	-	-	-	-	-	-	-	-	-	-		
91	2.70		0.93	-	0.98	-	0.97	-	0.99	1.01	-	-	380		
92	-3.95		-	1.02	-	1.05	-	1.02	-	-	1.04	1.07	-	-590	
93	-3.75		-	1.05	-	1.07	-	1.01	-	-	1.06	1.08	-	-560	
Bending of Long'l 5	94	-4.05		-	1.10	-	1.07	-	1.01	-	0.98	0.87	-	-550	
	95	-3.50		-	1.17	-	1.15	-	1.11	-	1.07	1.10	-	-530	
	96	7.25		1.14	-	1.17	-	1.12	-	1.12	1.14	-	-	1140	
	97	-2.60		-	-	-	-	-	-	-	-	-	-	-	
	98	-2.35		-	-	-	-	-	-	-	-	-	-	-	
	99	4.35		-	1.06	-	1.13	-	-	-	1.13	1.12	-	680	
	100	5.50		-	0.99	-	1.04	-	1.08	-	1.06	1.07	-	820	
	101	0.55		-	-	-	-	-	1.00	-	-	-	-	-	
	102	0.55		-	-	-	-	-	-	-	-	-	-	-	
	103	-0.25		-	-	-	-	-	-	-	-	-	-	-	
	104	2.60		-	-	-	-	-	-	-	-	-	-	-	
	105	2.55		-	-	-	-	-	-	-	-	-	-	-	
	106	-3.20		-	1.07	-	1.10	-	1.04	-	-	1.08	1.08	-	-480
	107	-1.95		-	1.13	-	1.13	-	1.06	-	-	1.13	1.13	-	-310
Bending of Long'l 4½	108	-2.05		-	0.76	-	0.83	-	0.88	-	0.88	0.91	-	-260	
	109	-2.20		-	1.05	-	1.02	-	1.09	-	1.11	1.14	-	-350	
	110	4.40		-	1.04	-	1.09	-	1.01	-	1.08	1.08	-	660	
	111	-2.15		-	-	-	-	-	-	-	-	-	-	-	
	112	-1.80		-	-	-	-	-	-	-	-	-	-	-	
	113	2.70		-	1.07	-	1.15	-	1.03	-	1.09	1.09	-	410	
	114	3.15		-	1.10	-	1.11	-	1.05	-	1.09	1.10	-	480	
	115	-0.05		-	-	-	-	-	-	-	-	-	-	-	
	116	-0.15		-	-	-	-	-	-	-	-	1.30	1.30	-	-70
	117	-0.35		-	-	-	-	-	-	-	-	-	-	-	-
	118	1.90		-	-	-	-	-	-	-	-	-	-	-	-
	119	1.55		-	-	-	-	-	-	-	-	-	-	-	-
120	-1.50		-	1.00	-	1.10	-	0.92	-	1.02	1.02	-	-	-210	
121	-2.30		-	1.11	-	1.09	-	1.04	-	1.17	1.16	-	-	-370	
Bending of Transv. Beam Fr 175½	148	-8.60		-	0.96	-	1.06	-	1.07	-	1.11	1.12	-	-1340	
	149	-10.30		-	-	-	-	-	-	-	1.14	1.17	-	-1670	
	150	9.90		-	0.99	-	1.05	-	-	-	1.05	1.05	-	1440	
	151	-8.15		0.92	-	1.04	-	0.98	1.01	1.08	1.05	-	-	-1180	
	152	9.00		-	0.97	-	0.99	-	0.98	-	-	1.02	1.07	-	1330
	153	-7.55		-	0.93	-	1.01	-	0.98	-	-	1.07	1.07	-	-1120
154	8.05		-	0.92	-	0.99	-	0.93	-	-	1.02	1.03	-	1150	
155	-2.80		-	1.28	-	1.02	-	0.95	-	-	1.10	1.17	-	-450	
156	3.25		-	0.87	-	0.94	-	0.90	-	-	1.01	1.00	-	450	
Bending of Transv. Beam Fr 174½	157	-7.10		-	0.88	-	0.99	-	0.99	-	1.06	1.08	-	-1060	
	158	-6.35		-	1.01	-	1.07	-	1.05	-	1.13	1.15	-	-1010	
	159	8.70		-	0.99	-	1.04	-	1.02	-	1.09	1.10	-	1320	
	160	-6.80		-	0.96	-	1.02	-	0.89	-	1.07	1.09	-	-1030	
	161	6.92		-	0.91	-	0.91	-	1.01	-	0.99	1.02	-	980	
Static Deflection															
Deflection-Sensitivity Coefficient Δ milli-in/kip	180	3.45		0.91	-	0.97	-	1.02	-	1.11	-	-	-	0.53	
	182	4.60		1.04	-	1.10	-	1.09	-	1.12	1.13	-	-	0.72	
	183	5.00		0.96	-	1.33	-	1.26	-	1.17	-	-	-	0.81	
	184	3.80		-	-	-	-	-	-	-	-	-	-	-	
	187	4.30		1.03	-	1.08	-	1.05	-	1.08	1.09	1.13	-	0.67	
	189	3.40		0.88	-	1.04	-	1.06	-	1.13	1.15	-	-	0.54	

Table 5 – Strains and Deflections at Test Position 2 for A 3 D-1

Gage Function	Test Position 2 (A 3 D-1)										Dynamic Strain at Maximum Deck Reaction $\mu\text{in}/\text{in.}$	
	Gage	Static Strain Strain-Sensitivity Coefficient m $\mu\text{in}/\text{in}/\text{kip}$	Dynamic Response Factor									
			Drop	63	64	65	66	67	68	69		
			Height, in.	24	36	48	60	72	72	78		
React., kip	67.2	83.3	99.0	122.0	138.2	138.2	147.8					
Shear on Web of Long'l 5½	1	- 1.90	-	-	-	-	-	-	-	-	-	-
	2	- 1.05	-	-	-	-	-	-	-	-	-	-
	3	- 1.70	0.95	1.07	1.12	1.07	1.09	1.11	1.10	-280	-	
	4	- 0.55	-	-	1.27	1.23	1.07	1.13	1.13	-90	-	
	5	1.30	-	-	-	-	-	-	-	-	-	
	6	1.55	-	-	-	-	-	-	-	-	-	
	7	0.50	-	-	-	-	-	-	-	-	-	
	8	0.80	-	-	-	-	-	-	-	-	-	
	9	6.70	0.93	0.93	1.05	1.01	1.01	1.02	0.99	980	-	
	10	5.95	0.97	1.02	1.05	1.02	1.01	1.04	1.01	890	-	
	11	- 0.80	-	-	-	-	-	-	-	-	-	
	12	0.00	-	-	-	-	-	-	-	-	-	
Bending of Long'l 6	55	- 1.00	-	-	-	-	-	-	-	-	-	-
	56	- 0.90	-	-	-	-	-	-	-	-	-	-
	57	2.05	1.12	1.16	1.28	1.17	1.18	1.20	1.19	360	-	
	58	1.30	-	-	-	-	-	-	-	-	-	-
	59	1.30	-	-	-	-	-	-	-	-	-	-
	60	2.65	1.12	1.24	1.30	1.21	1.24	1.28	1.24	490	-	
	61	- 1.45	-	-	-	-	-	-	-	-	-	-
	62	- 1.85	-	-	-	-	-	-	-	-	-	-
	63	- 3.35	-	-	-	-	-	-	-	-	-	-
	64	2.60	0.97	1.02	1.12	1.10	1.14	1.15	1.12	430	-	
	65	- 3.00	-	-	-	-	-	-	-	-	-	-
	66	- 3.35	0.80	0.82	0.89	0.87	0.95	0.98	0.96	-480	-	
	67	4.45	0.83	0.86	0.93	0.96	1.00	1.10	1.03	680	-	
	Bending of Long'l 5½	74	- 0.55	-	-	-	-	-	-	-	-	-
75		- 0.60	-	-	-	-	-	-	-	-	-	-
76		1.00	1.00	1.06	1.10	1.00	1.27	1.00	1.00	150	-	
77		- 0.50	-	-	-	-	-	-	-	-	-	-
78		- 0.55	-	-	-	-	-	-	-	-	-	-
79		1.00	-	-	-	-	-	-	-	-	-	-
80		0.50	-	-	-	-	-	-	-	-	-	-
81		0.10	-	-	-	-	-	-	-	-	-	-
82		0.95	-	-	-	-	-	-	-	-	-	-
83		1.10	-	-	-	-	-	-	-	-	-	-
84		- 6.05	1.01	1.01	0.99	0.87	0.66	0.73	0.77	-690	-	
85		- 6.40	0.95	0.96	1.01	1.10	1.34	1.49	1.55	-1470	-	
86		11.10	0.98	1.07	1.08	1.04	1.12	1.16	1.13	1850	-	
87		- 1.15	6.66	0.79	0.91	1.00	0.88	1.00	0.97	-170	-	
88		- 2.15	1.24	1.47	1.58	1.54	1.55	1.57	1.56	-500	-	
89		2.30	0.52	0.71	0.78	0.84	0.83	0.86	0.84	290	-	
90		1.50	-	-	-	-	-	-	-	-	-	
91		2.60	-	-	-	-	-	-	-	-	-	
92		- 3.95	1.04	1.05	1.12	1.10	1.11	1.17	1.10	-650	-	
93	- 3.00	1.00	1.02	1.11	1.06	1.12	1.19	1.19	-530	-		
Bending of Long'l 5	94	- 1.05	-	-	-	-	-	-	-	-	-	-
	95	- 0.75	-	-	-	-	-	-	-	-	-	-
	96	2.45	1.03	1.07	1.15	1.10	1.13	1.16	1.13	410	-	
	97	- 1.70	-	-	-	-	-	-	-	-	-	-
	98	1.70	-	-	-	-	-	-	-	-	-	-
	99	2.80	1.05	1.11	1.11	1.04	1.04	1.05	1.01	420	-	
	100	3.75	1.08	1.11	1.15	1.09	1.09	1.10	1.11	620	-	
	101	- 1.65	-	-	-	-	-	-	-	-	-	-
	102	- 1.25	-	-	-	-	-	-	-	-	-	-
	103	2.90	1.23	1.23	1.23	1.06	1.01	1.03	0.97	420	-	
	104	1.00	-	-	-	-	-	-	-	-	-	-
	105	1.00	-	-	-	-	-	-	-	-	-	-
	106	- 0.97	-	-	-	-	-	-	-	-	-	-
	107	- 0.35	-	-	-	-	-	-	-	-	-	-
Bending of Long'l 4½	115	- 0.50	-	-	-	-	-	-	-	-	-	-
	116	- 0.50	-	-	-	-	-	-	-	-	-	-
	117	0.60	-	-	-	-	-	-	-	-	-	-
	118	0.60	-	-	-	-	-	-	-	-	-	-
	119	0.45	-	-	-	-	-	-	-	-	-	-
	120	0.55	-	-	-	-	-	-	-	-	-	-
Bending of Transv. Beam Fr 174½	157	- 4.30	1.00	1.06	1.10	1.09	1.11	1.13	1.11	-710	-	
	158	- 5.75	1.00	1.04	1.09	1.11	1.17	1.18	1.15	980	-	
	159	5.80	1.00	1.08	1.15	1.15	1.18	1.20	1.16	1000	-	
	160	- 4.65	0.98	1.04	1.09	1.05	1.11	1.11	1.04	-720	-	
	161	4.60	1.02	1.08	1.13	1.10	1.13	1.17	1.13	770	-	
	Transv. Bent Fr 173	200	- 1.80	1.04	1.10	1.19	1.16	1.18	1.22	1.17	-310	-
201		- 0.05	-	-	-	-	-	-	-	-	-	
202		- 2.55	1.00	1.02	1.00	0.90	0.90	0.90	0.91	-	-	
203		- 2.55	0.93	0.98	1.08	1.13	1.20	1.25	1.27	-480	-	
204		0.00	-	-	-	-	-	-	-	-	-	
205		- 0.15	-	-	-	-	-	-	-	-	-	
206		- 0.55	-	-	-	-	-	-	-	-	-	
207		0.50	-	-	-	-	-	-	-	-	-	
208		1.00	-	-	-	-	-	-	-	-	-	
209		0.80	-	-	-	-	-	-	-	-	-	
210	0.60	-	-	-	-	-	-	-	-	-		
Long'l \bar{C} Girder	229	0.55	-	-	-	-	-	-	-	-	-	
	230	0.25	-	-	-	-	-	-	-	-	-	
	231	0.10	-	-	-	-	-	-	-	-	-	
		Static Deflection										
		Deflection-Sensitivity Coefficient Δ milli-in/kip										Dynamic Deflection at Maximum Deck Reaction inches
	180	2.06	0.87	0.93	1.03	1.08	1.16	1.19	1.21	0.37	-	
	184	2.30	0.91	0.94	0.97	1.04	1.13	1.16	1.15	0.40	-	
	185	2.60	0.97	1.02	1.17	1.14	1.14	1.16	1.07	0.41	-	
	186	1.07	-	-	-	-	-	-	-	-	-	
	189	1.87	1.12	1.15	1.19	1.23	1.28	1.32	1.34	0.37	-	
	190	0.78	-	-	-	-	-	-	-	-	-	
	199	0.85	-	-	-	-	-	-	-	-	-	

TABLE 6

Strains and Deflections at Test Position 3 for A3D-1

Gage Function	Test Position 3 (A3D-1)										Dynamic Strains at Maximum Deck Reaction $\mu\text{in/in/kip}$
	Gage	Static Strain Strain-Sensitivity Coefficient m $\mu\text{in/in/kip}$	Dynamic Response Factor								
			Drop	56	57	58	59	60	61	62	
			Height, in.	24	36	48	60	72	72	78	
		React., kip	67.2	83.3	99.0	122.0	138.2	138.2	147.8		
Shear on Web of Transv. Beam Fr. 175½	13	- 3.35		0.95	0.96	1.10	0.97	0.93	0.96	0.91	-450
	14	- 3.10		0.90	0.94	0.97	0.92	0.94	0.94	0.92	-420
	15	- 3.10		0.85	0.86	0.83	0.76	0.73	0.71	0.68	-310
	16	- 2.60		0.74	0.91	0.83	0.76	0.74	0.76	0.73	-280
	17	1.30		-	-	-	-	-	-	-	-
	18	1.65		-	-	-	-	-	-	-	-
Bending of Long'l 5½	68	- 4.65		0.84	0.97	1.06	1.18	1.57	1.92	1.62	-1110
	69	- 5.95		0.98	1.21	1.00	0.99	1.05	1.06	1.05	-920
	70	- 7.35		1.06	1.16	1.32	1.78	1.86	1.71	1.80	-1950
	71	6.05		0.82	0.79	0.76	0.86	0.60	0.49	0.45	402
	72	10.40		0.96	0.97	0.96	0.92	0.97	0.96	0.95	1460
	73	7.15		1.00	1.03	1.00	1.07	1.23	1.12	1.23	1300
	74	- 3.55		-	-	-	-	-	-	-	-
	75	- 3.45		-	-	-	-	-	-	-	-
	76	7.35		0.94	0.93	0.96	0.94	0.92	0.88	0.92	1000
	90	2.00		-	-	-	-	-	-	-	-
	91	2.15		-	-	-	-	-	-	-	-
	92	- 3.35		0.91	0.98	0.94	0.94	0.95	0.95	0.90	-450
	93	- 3.10		1.00	1.00	0.98	1.00	0.99	1.00	0.98	-450
Bending of Long'l 5	96	6.10		0.85	0.90	0.95	0.99	1.04	1.01	0.99	890
	99	2.30		-	-	-	-	-	-	-	-
	100	2.75		-	-	-	-	-	-	-	-
Bending of Transv. Beam Fr 175½	148	-12.20		1.00	1.04	1.05	1.17	1.22	1.14	1.20	-2160
	149	-12.20		0.98	0.99	1.02	1.09	1.15	1.09	1.21	-2180
	150	12.20		0.99	1.00	1.03	1.01	0.96	1.01	0.99	1780
	151	- 9.70		0.99	1.03	1.08	1.06	1.04	1.06	1.09	-1560
	152	10.20		1.00	1.04	1.05	1.06	1.07	1.06	1.07	1610
	153	- 8.20		1.03	1.08	1.12	1.16	1.12	1.16	1.17	-1420
	154	8.65		1.03	1.03	1.13	1.12	1.13	1.14	1.14	1460
	155	- 2.10		1.18	1.29	1.48	1.65	1.62	1.71	1.71	-530
	156	2.25		1.16	1.26	1.45	1.53	1.60	1.64	1.67	550
Bending of Transv. Beam Fr 174½	157	- 4.25		0.93	0.97	1.01	1.00	0.97	0.99	0.99	-620
	158	- 3.70		0.89	1.02	1.03	1.01	1.07	1.03	1.04	-570
	159	5.31		0.94	0.95	0.99	0.98	0.97	0.97	1.01	790
	160	- 4.33		0.98	1.00	1.06	1.05	1.08	1.08	1.06	-680
	161	4.35		0.97	1.01	1.03	1.05	1.05	1.05	1.04	670
Long'l 6	213	- 5.22		1.26	1.18	1.28	1.36	1.44	1.45	1.48	-1140
	214	- 5.07		1.16	1.25	1.34	1.43	1.46	1.49	1.48	-1110
	215	5.54		1.11	1.16	1.23	1.29	1.33	1.36	1.30	1060
		Static Deflection									Dynamic Deflection at Maximum Deck Reaction inches
		Deflection-Sensitivity Coefficient Δ milli-in/kip									
	178	4.25		1.09	1.13	1.19	1.21	1.28	1.30	1.27	0.80
	182	4.95		1.02	1.07	1.14	1.08	1.07	1.11	1.13	0.83
	183	4.60		1.07	1.10	1.14	1.09	1.13	-	1.09	0.74
	184	3.30		1.04	1.13	1.10	1.09	1.14	-	1.13	0.55
	187	4.50		0.92	1.07	1.12	1.07	1.09	-	1.13	0.75

TABLE 7

Strains and Deflections at Test Positions 4 and 6 for A3 D-1

Gage Function	Test Positions 4 and 6 (A3 D-1)										Dynamic Strains at Maximum Deck Reaction $\mu\text{in}/\text{in.}$
	Gage	Static Strain	Dynamic Response Factor								
			Drop	70	71	72	73	74	75	76	
				Height, in.	24	36	48	60	72	72	
		React., kip	67.2	83.3	99.0	122.0	138.2	138.2	147.8		
		Strain-Sensitivity Coefficient m $\mu\text{in}/\text{in}/\text{kip}$									
Shear on Web of Long'l 5½	7	-2.60		0.89	0.84	0.90	0.97	1.03	0.99	1.05	-410
	8	-1.10		1.00	1.04	1.10	1.11	1.29	1.26	0.82	-140
	9	3.50		0.70	0.83	0.81	0.78	0.76	0.76	0.82	430
	10	2.30		0.67	0.85	0.81	0.69	0.63	0.65	0.69	240
	11	0.40		0.63	0.81	0.94	1.05	1.20	1.00	1.05	60
	12	1.00		1.00	0.95	1.05	1.12	1.11	1.17	1.30	190
Bending of Long'l 5½	80	0.40		-	-	-	-	-	-	-	-
	81	0.25		-	-	-	-	-	-	-	-
	82	-0.15		-	-	-	-	-	-	-	-
	83	-0.15		-	-	-	-	-	-	-	-
	84	-1.55		0.71	0.85	0.90	0.92	0.95	0.95	1.00	-230
	85	-1.65		0.86	0.93	1.00	1.05	0.98	1.04	1.06	-260
	86	3.15		0.55	0.78	0.80	0.85	0.88	0.71	0.78	360
	87	-2.95		0.88	0.92	0.95	0.97	0.94	0.93	0.99	-430
	88	-6.45		1.00	0.55	0.60	0.66	0.64	0.67	0.71	-680
	89	4.70		0.95	0.96	1.03	1.04	-	-	-	-
	90	0.50		1.10	0.91	2.08	3.40	-	0.88	1.33	100
	91	-2.20		1.20	1.03	0.84	0.65	0.75	1.02	1.09	-360
	92	0.00		-	-	-	-	-	-	-	-
93	1.90		1.00	0.91	1.07	1.12	1.21	1.20	1.25	350	
Bending of Long'l 5	101	-0.75		-	-	-	-	-	-	-	-
	102	-0.65		-	-	-	-	-	-	-	-
	103	1.40		0.74	0.91	0.96	0.97	1.03	1.00	1.10	230
	104	0.25		-	-	-	-	-	-	-	-
	105	0.25		-	-	-	-	-	-	-	-
	106	0.10		-	-	-	-	-	-	-	-
	107	0.20		-	-	-	-	-	-	-	-
Transv. Bent Fr 173	200	-2.95		0.95	0.94	1.05	1.06	1.10	1.39	1.00	-440
	201	-1.10		0.87	1.00	0.91	0.96	0.97	0.87	0.82	-130
	202	-2.45		0.91	0.88	0.90	0.90	0.90	0.85	0.93	-340
	203	-5.15		0.94	1.00	1.21	1.27	1.45	1.47	1.58	-1200
	204	0.25		-	-	-	-	-	-	-	-
	205	0.00		-	-	-	-	-	-	-	-
	206	0.55		-	-	-	-	-	-	-	-
	207	0.50		1.14	1.38	1.30	1.42	1.50	1.36	1.40	10
	208	1.40		1.05	1.13	1.14	1.15	1.13	1.15	1.22	250
	209	-0.60		-	-	-	-	-	-	-	-
210	-0.60		-	-	-	-	-	-	-	-	
		Static Deflection									Dynamic Deflection at Maximum Deck Reaction inches
		Deflection-Sensitivity Coefficient Δ milli-in/kip									
	184	1.10		1.36	1.31	1.28	1.27	1.32	1.32	1.30	0.21
	186	1.00		0.74	0.60	0.80	0.73	0.65	0.72	0.88	0.13
	190	0.80		-	-	-	-	-	-	-	-
	199	0.75		-	-	-	-	-	-	-	-

Table 8 – Strains and Deflections at Test Position 5 for A3 D-1

Gage Function	Test Position 5 (A3 D-1)										Dynamic Strains at Maximum Deck Reaction $\mu\text{in/in.}$	
	Gage	Static Strain Strain-Sensitivity Coefficient m $\mu\text{in/in/kip}$	Dynamic Response Factor									
			Drop Height, in.	83	84	85	86	87	89	88		
				React., kip	67.2	83.3	99.0	122.0	138.2	138.2		147.8
Wood Planking See Figure 17	35			-	-	-	-	-	-	-	-	-
	36			-	-	-	-	-	-	-	-	-
	49			-	-	-	-	-	-	-	-	-
	53			-	-	-	-	-	-	-	-	-
Bending of Long'l 6	55	- 8.00		1.19	1.36	1.29	1.48	1.74	1.61	1.82	-2150	
	56	- 6.20		0.98	1.02	1.03	0.96	0.84	0.99	0.97	-890	
	57	13.00		1.11	1.21	1.24	1.25	1.28	1.28	1.31	2510	
	58	- 4.20		-	-	-	-	-	-	-	-	
	59	- 4.20		-	-	-	-	-	-	-	-	
	60	9.00		1.12	1.14	1.22	1.20	1.21	1.22	1.21	1610	
	61	- 1.70		-	-	-	-	-	-	-	-	
	62	- 1.70		-	-	-	-	-	-	-	-	
					-	-	-	-	-	-	-	-
		64	6.40		1.13	1.20	1.28	1.16	1.07	1.11	1.06	1000
		65	0.90		-	-	-	-	-	-	-	-
		66	0.50		-	-	-	-	-	-	-	-
		67	- 1.40		0.63	1.35	1.11	1.12	1.18	1.21	1.22	- 250
Bending of Long'l 5½	68	- 2.90		-	-	-	-	-	-	-	-	
	69	- 2.80		-	-	-	-	-	-	-	-	
	72	5.90		0.91	0.94	0.98	0.97	0.98	1.04	1.05	910	
	73	5.10		0.91	0.91	0.97	1.05	0.79	1.04	0.98	740	
	74	- 3.90		1.70	1.58	1.52	1.41	1.39	1.33	1.37	-790	
	75	- 5.90		1.26	1.20	1.23	1.11	1.34	1.32	1.55	-1350	
	76	11.40		0.99	1.00	1.00	0.96	0.94	0.96	0.93	1570	
	77	- 4.30		-	-	-	-	-	-	-	-	
	78	- 3.60		-	-	-	-	-	-	-	-	
	79	8.80		1.03	1.00	1.03	1.02	1.02	1.00	1.01	1310	
	80	- 2.60		-	-	-	-	-	-	-	-	
	81	- 2.30		-	-	-	-	-	-	-	-	
	82	3.50		1.04	1.05	1.13	1.12	1.13	1.18	1.17	640	
83	4.40		1.14	1.22	1.30	1.32	1.32	1.33	1.32	860		
84	0.70		-	-	-	-	-	-	-	-		
85	0.70		-	-	-	-	-	-	-	-		
86	0.90		-	-	-	-	-	-	-	-		
Bending of Long'l 5	94	- 2.60		-	-	-	-	-	-	-	-	
	95	- 2.60		-	-	-	-	-	-	-	-	
	96	5.30		0.97	0.97	0.95	0.96	0.98	1.18	1.17	920	
	97	- 2.20		-	-	-	-	-	-	-	-	
	98	- 2.20		-	-	-	-	-	-	-	-	
	99	3.40		0.89	0.91	0.88	0.87	0.86	0.86	0.85	430	
100	4.60		0.92	0.86	0.89	0.76	0.80	0.72	0.76	520		
Bending of Transv. Beam Fr 175½	148	- 7.70		-	-	-	-	-	-	-	-	
	149	- 7.60		-	-	-	-	-	-	-	-	
	150	7.90		0.93	0.96	0.99	0.94	0.95	0.94	0.93	1080	
	151	- 7.90		0.96	0.98	1.02	1.02	1.01	1.06	1.00	-1170	
	152	8.20		1.00	0.99	1.03	1.01	1.01	1.05	1.03	1250	
	153	8.20		1.00	1.01	1.07	1.04	1.07	1.07	1.07	1300	
	154	8.40		-	-	-	-	-	-	-	-	
	155	- 5.60		1.03	1.05	1.16	1.19	1.20	1.25	1.23	-1020	
	156	5.90		1.04	1.04	1.15	1.20	1.20	1.16	1.25	1090	
Bending of Transv. Beam Fr 174½	157	- 5.70		-	-	-	-	-	-	-	-	
	158	- 5.70		0.99	1.00	1.05	1.03	1.06	1.09	1.08	-910	
	159	7.00		1.01	1.01	1.00	0.98	1.01	0.97	0.99	1020	
	160	- 7.10		1.02	1.05	1.10	1.08	1.08	1.07	1.09	-1110	
	161	7.30		1.01	1.06	1.08	1.06	1.10	1.12	1.12	1210	
Static Deflection												
		Deflection-Sensitivity Coefficient Δ milli-in/kip									Dynamic Deflection at Maximum Deck Reaction inches	
	178	4.90		0.97	0.82	1.07	1.04	1.09	1.10	1.20	0.87	
	179	4.95		0.93	0.90	0.86	0.86	0.89	0.99	1.09	0.80	
	180	3.85		0.93	1.03	1.02	1.04	1.09	1.09	1.09	0.62	
	181	6.32		0.52	1.05	1.12	1.02	1.16	-	1.31	1.22	
	182	6.00		0.77	0.78	0.72	0.82	0.84	0.84	0.86	0.76	
	183	4.85		0.86	0.74	0.83	0.88	0.87	0.87	1.03	0.74	
	184	3.60		1.07	1.10	1.12	1.09	1.13	1.14	1.17	0.60	

Table 9 – Strains and Deflections at Test Position 7 for A 3 D-1

Gage Function	Test Position 7 (A 3 D-1)											Dynamic Strain at Maximum Deck Reaction μin/in.
	Gage	Static Strain Strain-Sensitivity Coefficient $\frac{m}{\mu\text{in/in/kip}}$	Drop Height, in. React., kip	Dynamic Response Factor								
				14	15	16	17	18	19	20	21	
				12	24	36	48	60	72	72	78	
				52.8	67.2	83.3	99.0	122.0	138.2	138.2	147.8	
Shear on Web of	19	-4.00		0.92	0.90	0.98	1.05	1.04	1.13	1.15	1.16	-690
	20	-3.25		1.00	0.93	1.02	1.06	1.01	1.00	1.00	0.95	-450
	21	-0.75		-	-	-	-	-	-	-	-	-
	22	-0.45		-	-	-	-	-	-	-	-	-
	23	1.90		1.00	0.96	0.97	1.08	1.07	1.06	1.08	1.05	300
	24	1.65		0.88	0.86	0.93	1.00	1.05	1.07	1.11	1.10	270
Transv. Beam Fr 175½	25	-0.90		-	-	-	-	-	-	-	-	-
	26	0.20		-	-	-	-	-	-	-	-	-
	27	5.30		0.88	0.83	0.91	0.95	0.96	1.00	1.02	0.99	770
	28	5.75		0.85	0.83	0.89	0.95	0.96	0.96	1.01	0.98	830
	29	0.60		-	-	-	-	-	-	-	-	-
	30	0.15		-	-	-	-	-	-	-	-	-
Bending of Long'l 5½	84	0.00		-	-	-	-	-	-	-	-	-
	85	-0.05		-	-	-	-	-	-	-	-	-
	86	0.00		-	-	-	-	-	-	-	-	-
	90	0.00		-	-	-	-	-	-	-	-	-
	91	0.00		-	-	-	-	-	-	-	-	-
	92	0.10		-	-	-	-	-	-	-	-	-
Bending of Long'l 5	104	0.00		-	-	-	-	-	-	-	-	-
	105	0.00		-	-	-	-	-	-	-	-	-
	106	0.00		-	-	-	-	-	-	-	-	-
	107	0.00		-	-	-	-	-	-	-	-	-
Bending of Long'l 1	122	-2.45		0.85	0.82	0.83	0.90	0.98	1.04	1.10	1.14	-410
	123	-2.20		1.05	0.93	0.97	1.02	0.98	1.00	1.05	1.06	-340
	124	3.60		0.84	0.81	0.85	0.93	0.92	0.97	1.00	0.95	500
	125	3.65		0.82	-	0.89	0.94	0.96	1.00	1.00	0.97	520
	126	-2.35		-	-	-	-	-	-	-	-	-
	127	-1.55		-	-	-	-	-	-	-	-	-
	128	3.80		0.71	0.69	0.74	0.77	0.79	0.82	0.86	0.84	470
	129	-1.40		-	-	-	-	-	-	-	-	-
Bending of Long'l ½	135	-3.85		1.37	1.41	1.15	1.05	0.85	0.75	0.74	0.72	-410
	136	-2.45		-	-	-	-	-	-	-	-	-
	137	3.90		1.03	1.02	1.04	1.07	1.06	1.09	1.24	1.39	800
	138	3.80		0.89	0.85	0.90	0.94	0.88	0.96	1.25	1.31	740
	139	-2.45		0.97	0.92	0.80	0.85	0.92	0.88	0.96	0.90	-320
	140	-5.60		0.59	0.75	0.86	0.95	0.85	0.83	0.90	0.83	-690
Bending of Long'l ½	141	5.50		0.98	0.92	0.95	1.02	0.99	1.05	1.10	1.05	850
	142	-1.60		-	-	-	-	-	-	-	-	-
	143	-1.55		-	-	-	-	-	-	-	-	-
	144	2.05		1.03	1.04	1.06	1.12	1.12	1.12	1.18	1.13	340
	145	0.25		-	-	-	-	-	-	-	-	-
	146	0.35		-	-	-	-	-	-	-	-	-
	147	-1.55		1.00	0.86	1.00	1.03	1.08	1.16	1.16	1.15	-260
	Bending of Transv. Beam Fr 175½	162	7.90		0.90	0.82	0.90	0.93	0.95	0.95	1.02	0.99
163		-6.05		0.84	0.94	0.90	0.95	0.93	0.99	1.00	1.00	-890
164		-7.10		0.62	0.71	0.71	0.90	0.96	1.14	0.98	1.05	-1100
165		-7.35		0.72	-	0.83	0.89	0.95	-	0.90	0.98	-1060
166		8.35		-	-	-	-	-	-	-	-	-
167		-6.95		1.15	0.84	-	-	-	1.07	1.06	-	-
Bending of Transv. Beam Fr 174½	168	7.95		0.95	0.88	0.98	0.98	0.98	1.05	1.09	1.05	1230
	169	-5.60		0.93	-	-	1.05	-	-	1.04	1.01	-830
	170	7.80		-	0.88	0.95	0.96	1.00	1.05	1.06	1.07	1230
	171	-3.45		-	-	-	-	-	-	-	-	-
	172	3.75		0.78	0.74	0.81	0.82	0.86	0.94	0.98	0.95	520
	Long'l Girder	226	1.40		-	1.06	1.10	1.12	1.13	1.70	1.78	1.64
227		-1.40		-	-	-	-	-	-	-	-	-
228		-2.20		-	-	-	-	-	-	-	1.15	-370
			Static Deflection									
			Deflection-Sensitivity Coefficient Δ mHI-in/kip									
Long'l Girder	192	1.85		1.12	1.05	1.10	0.93	1.10	1.17	1.21	1.24	0.34
	193	1.10		1.03	1.23	1.31	1.30	1.34	1.31	1.38	1.48	0.24
	194	1.70		1.01	1.05	1.12	1.19	1.22	1.27	1.32	1.35	0.34
	195	1.20		1.26	1.23	1.19	1.19	1.23	1.27	1.27	1.30	0.23
	197	0.90		-	-	-	-	-	-	-	-	-

TABLE 10 – Strains and Deflections at Test Position 8 for A3 D-1

Gage Function	Test Position 8 (A3 D-1)														Dynamic Strain at Maximum Deck Reaction $\mu\text{in/in.}$		
	Gage	Static Strain-Sensitivity Coefficient m $\mu\text{in/in/kip}$	Dynamic Response Factor														
			Drop	2	3	4	5	6	7	9	10	11	12	13			
			Height, in.	6	12	18	24	30	36	36	48	60	72	72			
React., kip	44.7	52.8	60.5	67.2	75.6	83.3	83.3	99.0	122.0	138.2	138.2						
Wood Planking See Figure 17	44 45 50 52 54																-7500 -7400 4300 3400 4000
Long'l 1	122	-1.25		0.91	0.85	0.87	1.00	1.00	1.00	0.90	1.00	1.06	1.23	1.06		-190	
	123	-1.05		1.00	1.00	1.00	1.07	1.13	1.06	1.06	1.14	1.19	1.41	1.28		-190	
	124	1.38		0.83	0.87	0.88	1.00	1.05	1.00	0.78	1.04	1.09	1.11	1.18		220	
	125	1.50		0.85	0.88	0.94	1.00	1.04	1.00	1.00	1.03	1.08	1.17	1.20		250	
	126	-1.40		0.85	0.86	0.89	0.89	0.90	0.91	0.91	0.93	1.00	1.18	1.03		-200	
	127	-1.50		1.00	0.94	1.00	1.05	1.00	0.96	1.36	0.97	0.92	1.02	0.95		-200	
	128	1.60		0.86	0.94	0.95	1.00	1.04	0.96	0.96	0.97	1.05	1.07	1.14		250	
	129	-1.20		0.82	0.85	0.87	1.00	0.94	0.95	0.90	1.00	1.07	1.27	1.12		-185	
	130	-1.30		1.00	0.93	1.00	1.00	0.90	0.91	0.86	0.67	0.94	1.06	0.92		-165	
	131	1.45		1.00	1.07	1.12	1.16	1.14	1.04	1.04	0.76	1.14	1.10	1.13		220	
Long'l 1/2	135	-0.25		-	-	-	-	-	-	-	-	-	-	-	-	-	
	136	-0.40		-	-	-	-	-	-	-	-	-	-	-	-	-	
	137			-	-	-	-	-	-	-	-	-	-	-	-	-	
	138	-0.80		-	-	-	-	-	-	-	-	-	-	-	-	-	
	139	-2.75		0.67	0.80	0.86	1.06	1.05	1.14	0.95	1.12	1.11	1.00	1.07		-410	
	140	-6.50		0.78	0.84	0.89	0.99	1.02	0.98	0.94	0.97	0.90	0.78	0.86		-770	
	141	5.20		0.68	0.82	0.86	0.94	0.97	0.93	0.89	0.99	1.01	1.00	1.09		780	
	142	-7.10		1.00	1.00	0.97	0.94	0.95	0.93	0.90	0.89	1.13	1.46	1.33		-1310	
	143	-7.10		1.05	1.03	1.03	1.05	1.01	0.93	0.91	0.89	1.03	0.69	0.54		-530	
	144	8.40		0.80	0.91	0.89	0.96	0.98	0.92	0.85	0.93	1.03	1.14	1.08		1260	
145	0.00		-	-	-	-	-	-	-	-	-	-	-		-		
146	0.20		-	-	-	-	-	-	-	-	-	-	-		-		
147	-1.60		0.93	1.00	1.11	1.10	1.00	1.00	0.96	1.03	1.05	1.09	1.14		-250		
Transv. Beam Fr 174 1/2	173	-1.25		1.00	1.00	1.00	1.06	1.00	1.10	1.00	1.16	1.10	1.21	1.17		-210	
	174	1.50		0.85	0.96	0.89	1.05	1.00	1.00	0.96	1.07	1.08	1.17	1.17		240	
	175	-2.85		0.85	0.97	0.97	1.03	1.05	1.04	1.00	1.09	1.13	1.19	1.22		-480	
	176	2.00		0.94	0.95	1.00	0.96	1.03	1.03	-	-	-	-	-		-	
	177	3.90		0.91	0.93	0.96	1.00	1.03	1.00	0.95	1.03	1.06	1.06	1.09		580	
Long'l G Girder	216	-4.00		1.28	1.40	1.27	1.26	1.22	1.13	1.12	1.06	1.16	1.25	-		-690	
	217	-2.00		0.46	0.88	0.89	0.91	0.88	0.89	1.14	1.17	1.23	1.28	1.17		-325	
	219	-2.60		1.13	1.19	-	1.03	0.95	0.98	0.98	1.04	0.92	0.86	0.90		-320	
	220	0.20		-	-	-	-	-	-	-	-	-	-	-		-	
	221	0.00		-	-	-	-	-	-	-	-	-	-	-		-	
	222	0.80		-	-	-	-	-	-	-	-	-	-	-		-	
	223	0.75		-	-	-	-	-	-	-	-	-	-	-		-	
	224	1.45		0.85	0.93	0.89	0.95	0.91	0.92	1.33	1.00	1.03	-	-		200	
	225	0.30		-	-	-	-	-	-	-	-	-	-	-		-	
	226	1.40		0.77	0.93	0.94	0.89	0.95	0.95	0.96	0.87	1.00	0.90	1.00		190	
227	-1.50		0.77	0.81	0.78	0.95	0.96	0.96	0.92	0.93	0.95	0.98	0.95		-200		
228	-1.45		-	-	-	-	-	-	-	-	-	-	-		-		
229	0.25		-	-	-	-	-	-	-	-	-	-	-		-		
230	1.25		-	-	-	-	-	-	-	-	-	-	-		-		
231	1.35		-	-	-	-	-	-	-	-	-	-	-		-		
		Static Deflection															Dynamic Deflection at Maximum Deck Reaction inches
		Deflection-Sensitivity Coefficient Δ milli-in/kip															
	194	1.20		-	1.41	-	1.37	-	1.00	1.11	1.27	1.37	1.39	-		0.23	
	195	1.20		-	1.41	-	1.12	-	0.90	1.20	1.19	1.43	1.40	-		0.23	
	196	2.20		-	1.03	-	1.14	-	0.92	0.98	1.10	1.23	1.77	1.84		0.56	
	197	0.75		-	-	-	-	-	-	-	-	-	-	-		-	
	198	0.85		-	1.36	-	1.00	-	0.85	1.42	1.31	1.52	1.36	1.36		0.16	

TABLE 11

Strains and Deflections at Test Position 9 for A 3 D-1

Gage Function	Test Position 9 (A 3 D-1)											Dynamic Strain at Maximum Deck Reaction $\mu\text{in/in.}$	
	Gage	Static Strain Strain-Sensitivity Coefficient m $\mu\text{in/in/kip}$	Dynamic Response Factor										
			Drop	22	23	24	25	26	27	28	29		30
			Height, in.	12	24	36	48	60	72	72	72		78
React., kip	52.8	67.2	83.3	99.0	122.0	138.2	138.2	138.2	147.8				
Long'l 5½	74	- 2.50		0.89	0.89	0.88	0.94	-	0.96	0.99	-	1.05	-390
	75	- 2.40		0.92	0.84	0.90	0.90	0.93	0.97	0.97	-	0.99	-350
	76	4.75		0.92	0.94	0.95	0.95	0.98	1.01	1.00	-	0.99	700
	80	- 2.15		0.96	0.86	0.89	0.93	0.98	1.02	1.02	-	1.00	-320
	81	- 2.40		0.96	0.88	0.88	0.88	0.93	0.95	0.98	-	0.99	-350
	82	3.80		0.93	0.96	0.94	0.96	1.02	1.05	1.05	1.05	1.04	580
	83	3.30		0.89	0.89	0.89	0.95	0.94	0.98	0.99	0.97	1.00	490
	84	0.05		-	-	-	-	-	-	-	-	-	-
	85	0.05		-	-	-	-	-	-	-	-	-	-
	86	0.35		-	-	-	-	-	-	-	-	-	-
Long'l 5	94	- 3.90		1.07	0.98	0.98	0.99	1.00	1.03	1.05	-	1.17	-670
	95	- 4.85		0.86	0.83	0.79	0.84	0.81	0.83	0.88	-	0.99	-700
	96	8.90		0.95	0.91	0.91	0.94	0.98	1.02	1.02	1.03	1.05	1380
	97	- 2.40		1.00	1.00	1.03	1.02	1.04	1.05	1.05	-	1.01	-360
	98	- 2.45		0.92	0.91	0.98	0.98	0.98	1.03	1.01	-	1.03	-370
	99	3.50		0.86	0.83	0.92	0.89	0.98	0.99	0.97	0.95	0.90	470
	100	5.25		0.91	0.92	0.95	0.95	0.99	1.03	1.04	1.03	1.03	800
	101	0.50		-	-	-	0.80	0.67	0.79	0.79	0.79	0.93	70
	102	0.50		-	-	-	-	0.92	-	1.07	1.07	1.00	70
103	- 0.30		-	-	-	-	-	-	-	-	-	-	
Long'l 4½	108	- 8.10		1.22	1.16	1.10	1.06	0.92	1.01	0.80	-	0.84	-1000
	109	- 7.70		0.91	0.90	0.95	0.97	1.05	1.40	1.42	-	2.41	-2740
	110	15.70		0.96	1.02	1.01	1.02	0.97	1.00	1.07	1.08	1.07	2480
	111	- 1.85		0.82	0.77	0.85	0.88	0.90	0.87	0.85	-	0.78	-210
	112	- 1.95		0.81	0.81	0.91	0.95	0.92	0.93	0.88	-	0.79	-230
	113	7.40		0.64	0.65	0.66	0.66	0.65	0.63	0.65	0.64	0.63	690
	114	9.05		0.94	0.97	1.01	1.01	1.04	0.99	1.05	1.04	1.01	1350
	115	0.70		1.00	1.00	1.00	1.14	1.12	1.16	1.26	1.32	1.33	140
	116	0.55		-	-	1.11	1.09	1.15	1.20	1.20	1.27	1.44	120
	117	-1.50		0.94	1.05	1.00	1.00	1.00	1.02	1.05	-	1.05	-230
		Static Deflection											Dynamic Deflection at Maximum Deck Reaction inches
		Deflection-Sensitivity Coefficient Δ milli-in/kip											
	183	4.30		0.70	0.76	0.78	0.75	0.80	0.91	0.84	0.91	0.88	0.56
	191	5.40		1.00	1.00	0.98	1.01	1.04	1.00	0.99	-	1.01	0.82
	188	-		-	-	-	-	-	-	-	-	-	0.70

TABLE 12

Peak Dynamic Strains and Deflections at Test Position 14 for A 3 D-1

Gage Function	Test Position 14 (A 3 D-1)							
	Gage	Drop	77	78	79	80	81	82
		Height, in.	24	48	60	72	78	78
		React., kip	67.2	99.0	122.0	138.2	147.8	147.8
		Dynamic Strain $\mu\text{in}/\text{in.}$	Dynamic Strain $\mu\text{in}/\text{in.}$	Dynamic Strain $\mu\text{in}/\text{in.}$	Dynamic Strain $\mu\text{in}/\text{in.}$	Dynamic Strain $\mu\text{in}/\text{in.}$	Dynamic Strain $\mu\text{in}/\text{in.}$	
Bending Long'l 6	55		- 785	-1020	-1030	-1630	-1660	-1840
	56		- 490	- 830	-1100	-1470	-1340	-1540
	57		1160	1640	2020	2290	2520	2530
	58		- 260	- 425	- 495	- 520	- 520	- 545
	59		- 285	- 475	- 535	- 595	- 580	- 605
	60		695	1110	1340	1520	1530	1570
	61		- 70	- 115	- 140	- 160	- 155	- 165
	62		- 75	- 130	- 145	- 160	- 205	- 170
	63		530	865	955	1020	1010	1030
	64		515	810	930	1020	1010	1020
	65		65	120	130	160	165	185
66		45	65	85	110	115	120	
67		- 130	- 195	- 240	- 265	- 270	- 280	
Bending Long'l 5½	72		370	575	670	770	810	850
	73		300	460	555	625	670	690
	74		- 210	- 345	- 430	- 500	- 540	- 570
	75		- 250	- 420	- 515	- 595	- 615	- 635
	76		435	730	880	1010	1070	1130
	79		430	710	855	765	1000	1050
	82		235	390	460	535	540	575
	83		325	515	675	730	735	760
Long'l 5	96		320	495	590	665	690	730
Long'l 4½	110		205	320	380	430	450	465
Transv. Beam Fr 175½	150		355	550	670	775	810	845
	151		- 425	- 665	- 785	- 595	- 615	- 635
	153		- 505	- 800	- 950	-1080	-1130	-1160
	154		520	845	985	1140	1180	1230
Transv. Beam Fr 174½	160		- 425	- 675	- 830	- 950	- 990	-1040
	161		450	720	835	975	1010	1040
Long'l 6	215		680	1060	1250	1440	1510	1510
			Dynamic Deflection in.	Dynamic Deflection in.	Dynamic Deflection in.	Dynamic Deflection in.	Dynamic Deflection in.	Dynamic Deflection in.
	178		0.32	0.47	0.57	0.66	0.71	0.71
	179		0.31	0.46	0.57	0.65	0.70	0.70
	180		0.23	0.34	0.42	0.48	0.51	0.51
	182		0.28	0.42	0.52	0.58	0.63	0.63
	183		0.27	0.40	0.49	0.55	0.60	0.60
	184		0.28	0.42	0.52	0.58	0.63	0.63

TABLE 13

Peak Dynamic Strains and Deflections at Test Position 15 for A3D-1

Test Position 15 (A3D-1) (Similar to 5 Except Load is 10-inches Aft)						
Gage Function	Gage	Drop	90	91	92	93
		Height, in.	48	60	72	78
		Reaction, kip	99.0	122.0	138.2	147.8
			Dynamic Strain $\mu\text{in/in.}$	Dynamic Strain $\mu\text{in/in.}$	Dynamic Strain $\mu\text{in/in.}$	Dynamic Strain $\mu\text{in/in.}$
Bending of Long'l 6	55		- 490	- 525	- 585	- 650
	56		- 475	- 570	- 625	- 625
	57		1000	1200	1350	1460
	60		500	590	740	765
	64		400	430	530	575
	67		- 205	- 250	- 275	- 290
Bending of Long'l 5½	68		- 475	- 620	- 640	- 665
	69		- 570	- 725	- 930	- 990
	70		- 480	- 495	- 860	- 885
	71		95	125	180	235
	72		800	985	1040	1160
	73		735	885	1100	1180
	74		- 370	- 445	- 475	- 500
	75		- 450	- 525	- 550	-
	76		800	1010	1190	1270
	79		530	650	730	780
82		205	265	280	325	
83		320	370	415	450	
Bending Long'l 5	96		480	585	685	730
	99		235	300	350	370
	100		325	415	425	435
Bending Transv. Beam at Fr 17½	150		1060	1040	1220	1260
	151		- 900	-1110	-1280	-1340
	152		800	1160	1360	1460
	153		- 945	-1240	-1400	-1480
	155		- 700	- 950	- 985	-1080
	156		730	975	1050	1220
Transv. Beam at Fr 17¼	158		- 440	- 535	- 650	- 685
	159		540	665	785	850
	160		- 575	- 710	- 800	- 845
	161		570	720	810	880

TABLE 14

Strains and Deflections at Test Position 10 for F 2 H-3

Gage Function	Test Position 10 (F 2 H-3)								Dynamic Strain at Maximum Deck Reaction $\mu\text{in/in.}$
	Gage	Static Strain	Dynamic Response Factor						
		Strain-Sensitivity Coefficient m $\mu\text{in/in/kip}$	Record	1090	1093	1095	1097	1101	
			Height, in.	24	48	60	72	78	
		React., kip	26.8	43.6	52.2	60.8	66.0		
Wood Planking See Figure 18	44 A	0.00	-	-	-	-	-	-	-
	45 B	3.20	0.71	0.68	0.67	0.62	0.65	140	
	50	5.60	-	-	-	-	-	-	
	52	30.80	1.08	-	0.93	0.95	0.90	1830	
	54	115.00	0.90	0.76	0.83	-	-	>5000	
Long'l 1	128	1.30	0.86	1.00	0.93	0.88	0.88	70	
	131	1.30	1.14	0.88	0.93	0.81	0.83	70	
Long'l 1/2	135	0.00	-	-	-	-	-	-	
	136	- 0.40	-	-	-	-	-	-	
	137	4.70	0.72	0.78	0.76	0.75	0.74	230	
	138	0.70	1.17	1.10	1.09	1.00	0.93	40	
	139	1.80	-	1.56	1.63	1.59	1.62	190	
	140	- 3.00	1.00	0.92	0.87	0.81	0.67	-130	
	141	4.10	0.73	0.75	0.79	0.78	0.76	200	
	142	9.30	0.64	0.73	0.80	0.88	0.87	530	
	143	- 6.30	0.74	0.84	0.80	0.79	0.77	-320	
	144	8.50	0.71	0.72	0.73	0.79	0.74	410	
	145	0.30	-	-	-	-	-	-	
	146	0.10	-	-	-	-	-	-	
	147	- 1.60	0.88	0.79	0.76	0.84	0.81	-85	
			Static Deflection						Dynamic Deflection at Maximum Deck Reaction inches
		Deflection-Sensitivity Coefficient Δ milli-in/kip							
	194	1.40	1.00	1.00	1.00	1.00	1.08	0.10	
	195	1.30	1.00	1.16	1.12	1.18	1.05	0.09	
	196	6.50	1.38	1.27	1.32	1.65	1.62	0.70	

TABLE 15

Strains and Deflections at Test Position 11 for F 2 H-3

Gage Function	Test Position 11 (F 2 H-3)										Dynamic Strain at Maximum Deck Reaction $\mu\text{in/in.}$
	Gage	Static Strain	Dynamic Response Factor								
		Strain-Sensitivity Coefficient m $\mu\text{in/in/kip}$	Record	1076 3301	1077 3302	1080 3304	1082 3306	1083 3307	1085 3309	1087 3310	
			Height, in.	24	48	60	66	72	80	80	
		React., kip	26.8	43.6	52.2	56.5	60.8	68.0	68.0		
Wood Planking See Figure 18	44 A	25.00		1.06	1.05	0.98	1.10	-	-	-	-
	45 B	-		-	-	-	-	-	-	-	-
	52	19.00		0.86	0.79	0.84	0.63	-	0.65	0.96	1250
	54	2.40		0.85	1.00	0.92	0.86	0.67	0.70	1.11	180
Long'l $\frac{1}{2}$	135	- 0.90		1.00	1.00	1.22	1.10	1.00	1.00	0.92	-60
	136	- 1.90		1.00	0.94	0.90	0.86	0.83	0.77	0.81	-100
	137	5.00		0.85	0.70	0.67	0.65	0.57	0.59	0.77	260
	138	1.50		0.88	0.77	0.69	0.71	-	0.65	0.72	70
	139	0.60		-	-	-	-	-	-	-	-
	140	- 8.40		0.89	0.64	0.73	0.67	0.63	0.66	0.54	-310
	141	3.40		0.82	0.74	0.68	0.66	0.60	0.60	0.81	200
	142	- 1.80		1.00	1.19	0.79	0.90	-	0.72	1.52	-180
	143	- 2.70		1.14	0.79	0.75	0.74	0.64	0.65	0.78	-140
	144	2.70		0.93	0.71	0.71	0.65	0.61	0.64	0.78	140
	145	0.00		-	-	-	-	-	-	-	-
146	0.00		-	-	-	-	-	-	-	-	
Long'l Girder	216	- 1.00		0.60	0.89	0.90	-	0.58	0.92	1.32	- 90
	217	- 1.90		0.80	0.94	0.95	0.95	-	0.85	0.81	-110
	218	- 1.20		0.50	0.88	1.00	1.00	0.92	1.21	1.56	-120
	224	1.30		1.00	1.00	1.00	1.07	1.00	1.00	1.00	90
	225	0.10		-	-	-	-	-	-	-	-
	226	1.40		1.00	1.00	0.93	1.00	1.00	0.90	0.90	-90
	227	- 2.90		0.88	0.84	0.83	0.79	0.74	0.74	0.74	-150
	228	- 0.80		-	-	-	-	-	-	-	-
		Static Deflection									Dynamic Deflection at Maximum Deck Reaction inches
		Deflection-Sensitivity Coefficient Δ milli-in/kip									
	194	1.60		1.42	0.56	0.54	0.55	0.52	-	0.55	0.06
	195	1.54		1.00	0.90	0.94	0.86	0.86	0.90	1.00	0.10
	196	2.00		-	0.63	0.43	0.49	0.49	0.60	0.69	0.10
	198	1.38		-	-	-	-	-	-	-	-

TABLE 16

Strains and Deflections at Test Position 12 for F 2 H-3

Gage Function	Test Position 12 (F 2 H-3)									Dynamic Strain at Maximum Deck Reaction $\mu\text{in/in.}$
	Gage	Static Strain	Dynamic Response Factor							
		Strain-Sensitivity Coefficient m $\mu\text{in/in/kip}$	Record	1102	1104	1108	1109	1111	1114	
			Height, in.	24	48	60	72	78	78	
	React., kip	26.8	43.6	52.2	60.8	66.0	66.0			
Shear Long'l 5½	1	3.50		1.00	1.00	1.00	1.00	0.97	0.97	220
	4	3.20		1.00	1.00	1.06	0.95	0.98	1.00	200
Wood Planking See Figure 19	35C	24.60		1.15	0.96	0.95	0.86	0.84	0.89	1430
	36D	54.50		1.03	0.87	0.88	0.87	1.01	1.01	3630
	49	47.00		0.87	0.90	1.02	0.97	0.71	0.69	2120
	51	28.60		0.93	0.86	0.79	0.76	0.74	0.75	1410
	53	6.00		1.18	0.96	0.94	0.90	0.87	0.85	345
Long'l 6	57	9.20		0.96	0.98	1.00	0.96	0.95	0.95	570
	60	6.00		0.94	0.94	0.98	0.92	0.94	0.92	365
	72	6.66		0.97	1.00	1.04	1.01	1.01	0.99	430
	73	6.50		0.74	0.89	0.93	0.92	0.95	0.96	410
	76	11.00		1.07	1.10	1.15	1.09	1.07	1.08	800
	77	- 2.40		0.77	0.95	1.00	0.97	0.94	0.94	-150
	78	- 2.60		0.88	0.92	1.00	0.94	0.90	0.90	-170
	79	7.00		0.95	0.95	0.99	0.94	0.95	0.92	430
	82	1.90		-	-	-	-	-	-	-
	83	2.64		1.07	1.04	1.00	1.09	1.06	1.00	170
Long'l 5	96	8.00		1.03	1.02	1.03	1.03	1.05	0.80	410
		Static Deflection								Dynamic Deflection at Maximum Deck Reaction inches
		Deflection-Sensitivity Coefficient Δ milli-in/kip								
	179	3.00		-	1.11	1.41	1.30	-	1.20	0.23
	181	4.90		-	0.86	0.86	0.94	-	0.74	0.24
	182	4.80		-	0.98	1.06	1.02	-	1.01	0.32
	183	4.90		-	0.85	0.94	0.92	-	0.84	0.27
	184	3.50		-	0.92	1.00	1.05	-	1.00	0.23

TABLE 17

Strains and Deflections at Test Position 13 for F 2 H-3

Gage Function	Test Position 13 (F 2 H-3)										Dynamic Strain at Maximum Deck Reaction $\mu\text{in/in.}$
	Gage	Static Strain	Dynamic Response Factor								
		Strain-Sensitivity Coefficient m $\mu\text{in/in/kip}$	Record	1117 3317	1119 3319	1120 3320	1123 3322	1125 3324	1129 3328	1130 3329	
			Height, in.	48	60	66	72	80	84	84	
		React., kip	43.6	52.7	56.5	60.8	68.0	72.0	72.0		
Wood Planking See Figure 19	35	4.00		1.17	1.73	1.18	1.11	1.06	1.06	1.06	-310
	36	11.00		-	-	-	-	-	-	-	-
	49	41.30		0.94	0.90	0.87	0.87	0.81	0.82	0.88	2640
	51	76.00		0.92	0.97	1.02	1.12	1.23	1.29	-	7050
	53	69.00		0.91	0.81	0.79	0.74	0.72	0.72	0.71	3550
Long'l 6	56	- 5.70		1.02	1.07	1.08	1.12	1.09	1.07	1.13	-460
	57	15.00		0.93	0.92	0.90	0.87	0.86	0.82	0.80	860
	58	- 2.70		1.00	1.07	-	1.06	0.97	-	1.00	-190
	61	- 1.20		1.00	0.92	0.93	1.13	1.19	1.05	1.06	-90
	63	6.80		0.91	0.90	0.87	0.88	0.85	0.83	0.83	400
	64	6.30		0.94	0.90	0.88	0.86	0.83	0.82	0.87	370
	65	1.10		0.67	0.62	0.57	0.67	0.75	0.72	0.72	55
	66	0.60		-	-	-	-	-	-	-	-
Long'l 5½	74	- 6.20		0.93	0.97	0.96	0.99	0.94	0.93	0.95	-430
	75	- 6.80		0.92	0.89	0.89	0.92	0.97	0.97	1.06	-510
	76	12.30		0.94	0.97	0.95	0.99	0.96	0.95	0.97	850
	80	- 2.10		0.94	0.91	0.83	0.85	0.86	0.87	0.87	-130
	81	- 1.60		0.93	0.88	0.83	0.95	0.82	0.87	0.82	-90
	82	3.10		0.96	0.97	0.91	1.00	0.95	0.93	0.91	200
	83	4.20		0.97	0.95	0.89	0.96	0.90	0.90	0.84	260
	84	1.00		0.64	0.67	0.77	0.86	0.81	0.89	0.83	60
	85	1.00		0.73	0.75	-	0.93	0.81	-	0.83	60
	86	- 1.20		0.86	0.76	0.83	0.95	1.00	1.00	1.00	-100
		Static Deflection									Dynamic Deflection at Maximum Deck Reaction inches
		Deflection-Sensitivity Coefficient Δ milli-in/kip									
	179	4.50		1.00	1.00	1.00	1.00	1.00	-	1.00	0.31
	181	8.70		0.71	0.72	0.70	0.70	0.75	-	0.75	0.48
	182	4.40		1.10	1.08	1.07	1.00	1.00	-	1.00	0.32
	183	4.80		0.62	0.76	0.74	0.72	0.80	-	0.80	0.27
	184	3.65		0.90	1.00	0.97	0.96	1.03	-	1.10	0.28

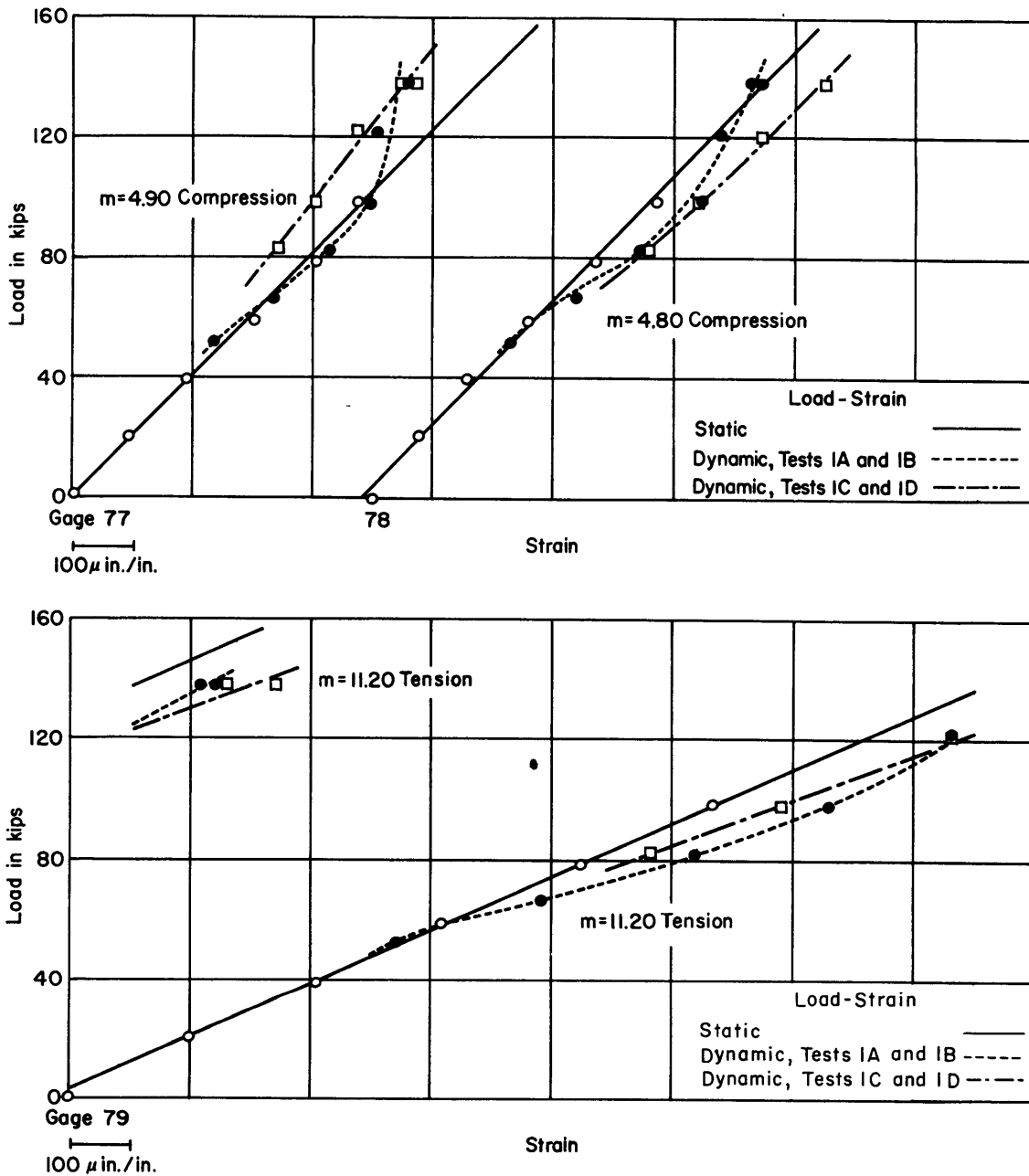


Figure 15 – Typical Plots of Load Versus Static Strain and Peak Dynamic Strain

the load-strain curves linearly; i.e., multiplying m times the applicable deck reaction. The last column in the tables gives the peak strain for each gage for the maximum dynamic load applied. This value is obtained by multiplying the strain-sensitivity factor by the maximum deck reaction and the corresponding dynamic response factor. At the bottom of each table, similar data are given for the deflections. Typical data from which Tables 3 through 17 are condensed are shown in Figures 15 and 16.

The strain data for wooden planking are given separately in the load-strain plots of Figures 17 through 19. They are not always a linear function of load, because of the air gaps between the wood and the steel plating.

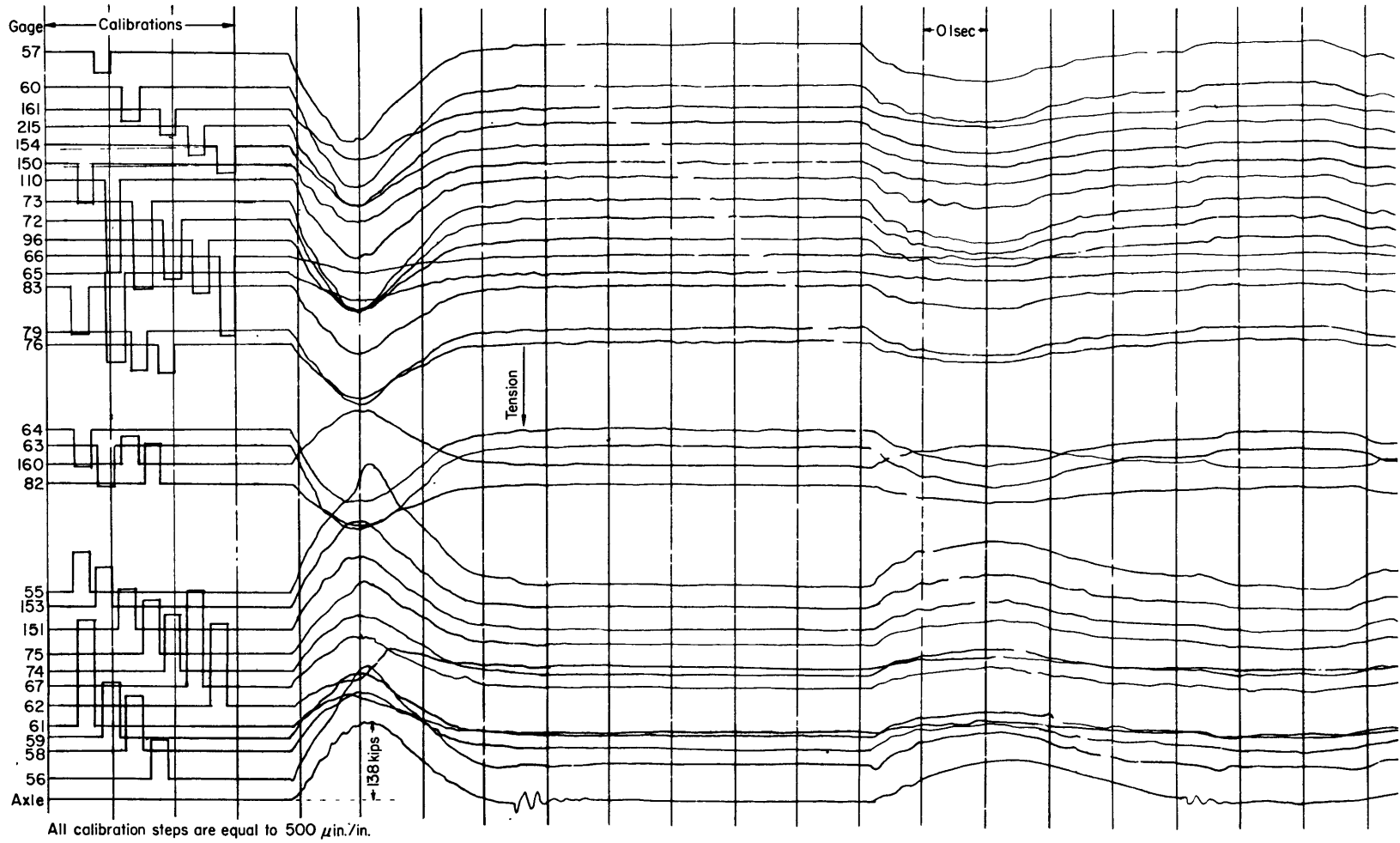


Figure 16 – Typical Oscillograph Record Obtained for an A3D-1 Deck Reaction of 138,200 Pounds at Position 14

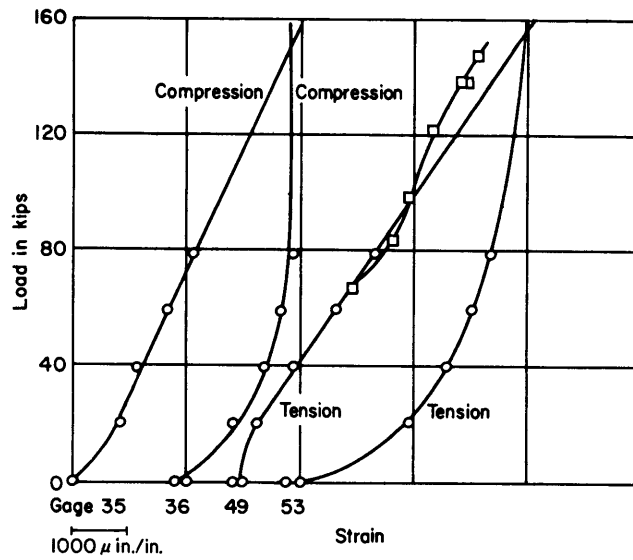


Figure 17a - Test Position 5

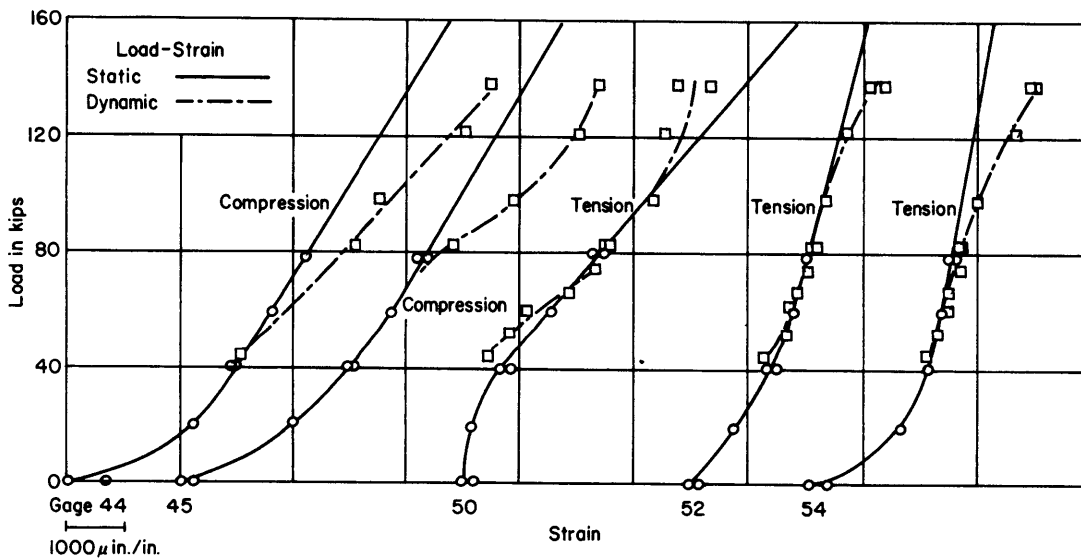


Figure 17b - Test Position 8

Figure 17 - Load-Strain Plots for Gages on Wooden Planking, Test Positions 5 and 8 (A 3 D-1)

With the exception of gages on the wood and those located so as to measure shear stresses in the steel members, bending stresses can be obtained by multiplying measured strains by the modulus of elasticity, $E = 30 \times 10^6$ psi. For the rosette gages on the steel web members, static shears and principal stresses are given in Table 18. In this Table dynamic stresses are omitted since the dynamic strain data are not as complete. For practical purposes the dynamic stresses can be considered approximately 10 percent higher.

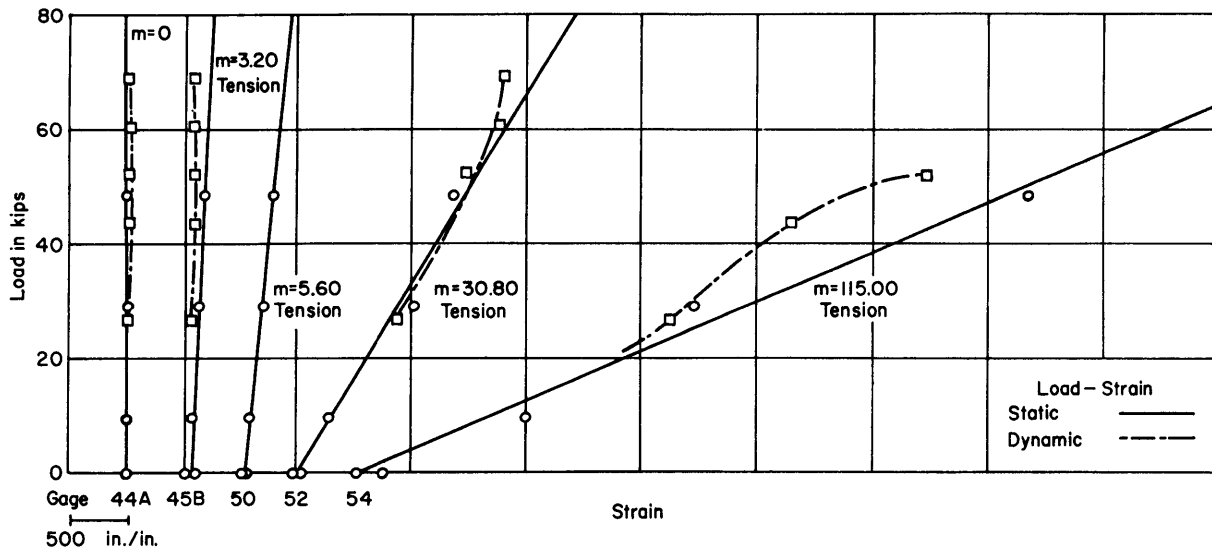


Figure 18a – Test Position 10

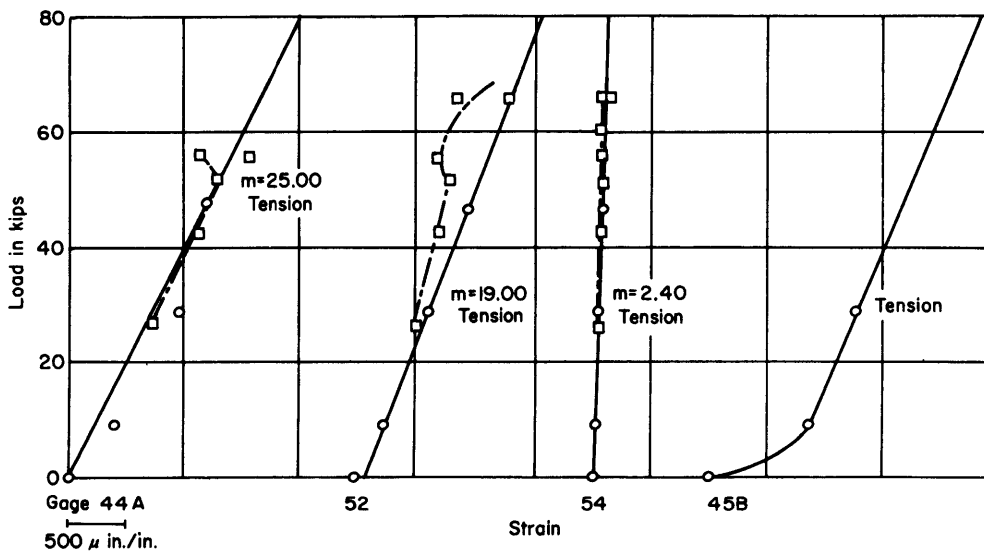


Figure 18b – Test Position 11

Figure 18 – Load-Strain Plots for Gages on Wooden Planking, Test Positions 10 and 11 (F 2 H-3)

Strain measurements on the wooden planking are not amenable to direct interpretation, because wood is an anisotropic structure with three Young's moduli, three shear moduli, and six Poisson's ratios. To obtain a correlation, laboratory tests were made on the planking with strain rosettes attached. These tests indicated that the directions of principal stress vary widely and that a single 45-deg diagonal strain (such as measured during the drop tests) varying anywhere from 4500 to 9000 $\mu\text{in./in.}$ can indicate a shear stress as high as 1000 psi, which is sufficient to cause failure of the wood.⁶ It is estimated that a maximum bending strain of 8000 $\mu\text{in./in.} \pm 20$ percent is required to cause failure of the planking in bending.

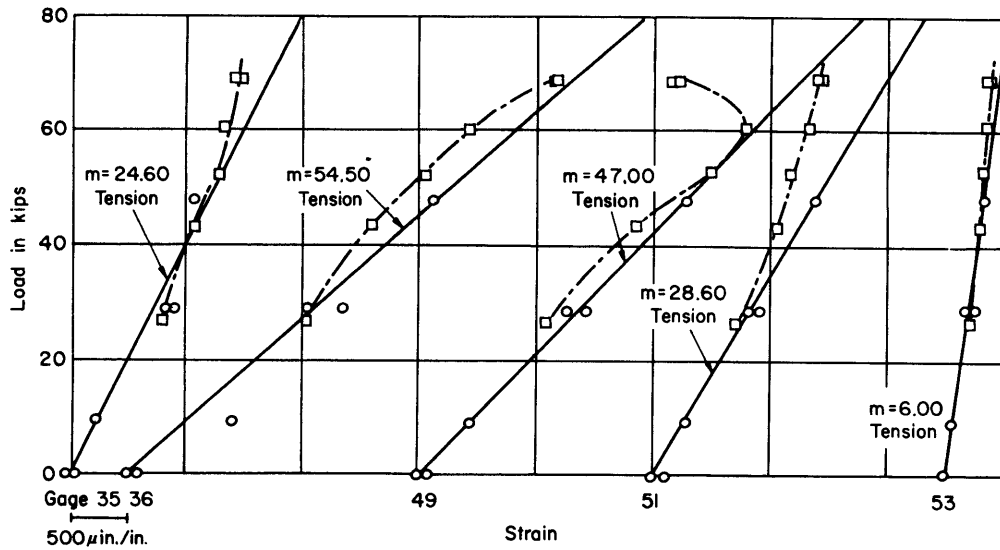


Figure 19a – Test Position 12

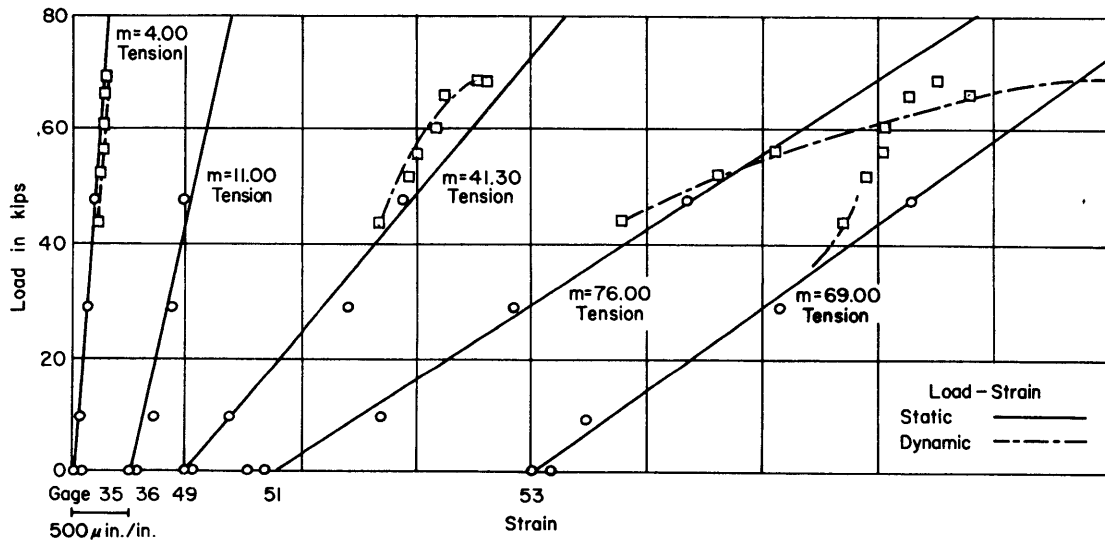


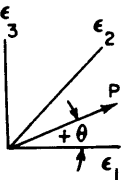
Figure 19b – Test Position 13

Figure 19 – Load-Strain Plots for Gages on Wooden Planking, Test Positions 12 and 13 (F 2 H-3)

Table 19 gives the permanent sets or zero shifts measured by the strain gages for all tests. Except where actual damage was noted, the permanent set or gage drift either is small or is associated with gages recording low total strains. This latter effect is probably due to residual welding and fabrication stresses in the structure. In this connection it should be noted that the structure was stress-relieved by the static loading to only 100,000 lb. Thus, for the higher loads of the drop tests, the structure was subject to a stress-relieving process,

TABLE 18

Shear Stresses Computed from Rosette Strains on Webs



Orientation	Gage	ε		Shear Stress τ_{max}	Major Principal Stress P	Minor Principal Stress Q	Angle θ	Gage	ε		Shear Stress τ_{max}	Major Principal Stress P	Minor Principal Stress Q	Angle θ
		$\mu\text{in/in/kip}$	psi/kip						$\mu\text{in/in/kip}$	psi/kip				
Test Position 1														
	5	$\epsilon_1 = 2.10$		145	+155	-140	+35	17	$\epsilon_1 = 1.30$		75	+30	-120	-20
	3	$\epsilon_2 = 5.55$						15	$\epsilon_2 = -3.10$					
	1	$\epsilon_3 = -2.50$						13	$\epsilon_3 = -3.35$					
	6	$\epsilon_1 = 1.80$		115	+160	-70	+35	18	$\epsilon_1 = 1.65$		75	+40	-105	-20
	4	$\epsilon_2 = 4.75$						16	$\epsilon_2 = -2.60$					
	2	$\epsilon_3 = -1.55$						14	$\epsilon_3 = -3.10$					
	5, 6	$\frac{\epsilon_5 + \epsilon_6}{2} = 1.95$		<u>130*</u>	<u>+135</u>	<u>-130</u>	<u>+35</u>	17, 18	$\frac{\epsilon_{17} + \epsilon_{18}}{2} = 1.47$		<u>75</u>	<u>+35</u>	<u>-110</u>	<u>-20</u>
	3, 4	$= 5.15$						15, 16	$= -2.85$					
	1, 2	$= 2.03$						13, 14	$= -3.23$					
Test Positions 4 and 6														
	11	$\epsilon_1 = -0.60$		80	+15	-145	+35	11	$\epsilon_1 = 0.40$		115	+70	-160	+35
	9	$\epsilon_2 = 1.70$						9	$\epsilon_2 = 3.50$					
	7	$\epsilon_3 = -2.50$						7	$\epsilon_3 = -2.60$					
	12	$\epsilon_1 = -0.45$		35	+30	-40	+50	12	$\epsilon_1 = 1.00$		60	+60	-65	+35
	10	$\epsilon_2 = 1.40$						10	$\epsilon_2 = 2.30$					
	8	$\epsilon_3 = 0.20$						8	$\epsilon_3 = -1.10$					
	11, 12	$\frac{\epsilon_{11} + \epsilon_{12}}{2} = -0.53$		<u>60</u>	<u>+20</u>	<u>-95</u>	<u>+40</u>	11, 12	$\frac{\epsilon_{11} + \epsilon_{12}}{2} = 0.70$		<u>85</u>	<u>+65</u>	<u>-110</u>	<u>+35</u>
	9, 10	$= 1.55$						9, 10	$= 2.90$					
	7, 8	$= -1.15$						7, 8	$= -1.85$					
Test Position 2														
	5	$\epsilon_1 = 1.30$		60	+45	-130	-5	23	$\epsilon_1 = 1.90$		70	+25	-115	+5
	3	$\epsilon_2 = -1.70$						21	$\epsilon_2 = -0.75$					
	1	$\epsilon_3 = -1.90$						19	$\epsilon_3 = -4.00$					
	6	$\epsilon_1 = 1.55$		35	+45	-25	-15	24	$\epsilon_1 = 1.65$		60	+25	-90	+5
	4	$\epsilon_2 = -0.55$						22	$\epsilon_2 = -0.45$					
	2	$\epsilon_3 = -1.05$						20	$\epsilon_3 = -3.25$					
	5, 6	$\frac{\epsilon_5 + \epsilon_6}{2} = 1.43$		<u>45</u>	<u>+45</u>	<u>-45</u>	<u>-20</u>	23, 24	$\frac{\epsilon_{23} + \epsilon_{24}}{2} = 1.78$		<u>65</u>	<u>+25</u>	<u>-100</u>	<u>+5</u>
	3, 4	$= -1.13$						21, 22	$= -0.60$					
	1, 2	$= -1.48$						19, 20	$= -3.63$					
	11	$\epsilon_1 = -0.80$		170	+160	-175	+50	29	$\epsilon_1 = 0.60$		130	+125	-135	+40
	9	$\epsilon_2 = 6.70$						27	$\epsilon_2 = 5.30$					
	7	$\epsilon_3 = 0.50$						25	$\epsilon_3 = -0.90$					
	12	$\epsilon_1 = 0$		130	+150	-115	+45	30	$\epsilon_1 = 0.15$		130	+140	-120	+45
	10	$\epsilon_2 = 5.95$						28	$\epsilon_2 = 5.75$					
	8	$\epsilon_3 = 0.80$						26	$\epsilon_3 = 0.20$					
	11, 12	$\frac{\epsilon_{11} + \epsilon_{12}}{2} = -0.40$		<u>145</u>	<u>+150</u>	<u>-140</u>	<u>+45</u>	29, 30	$\frac{\epsilon_{29} + \epsilon_{30}}{2} = 0.38$		<u>130</u>	<u>+135</u>	<u>-130</u>	<u>+45</u>
	9, 10	$= 6.33$						27, 28	$= 5.53$					
	7, 8	$= 0.65$						25, 26	$= -0.35$					

*The underlined stresses were obtained by averaging strains on directly opposite surfaces of the web in order to cancel stresses due to bending or twisting of the beam.

Table 19 – Measured Permanent Sets or Zero Shifts of Strain Gages

Test Position	Drop	Drop Height in.	Gage	Perm. Set or Zero Shift* $\mu\text{in/in.}$	Percent of Measured Strain	Test Position	Drop	Drop Height in.	Gage	Perm. Set or Zero Shift* $\mu\text{in/in.}$	Percent of Measured Strain
1A**	33	36	74	35	8	4 & 6	72	48	90	65	46
1A	34	48	74	- 70	11	4 & 6	73	60	91	40	21
			75	- 625	38				90	175	68
1A	35	60	1	60	8	4 & 6	74	72	91	55	33
			2	- 25	11	4 & 6	74	72	91	75	32
			3	- 25	7				202	- 25	8
			4	55	8	4 & 6	75	72	91	- 20	7
			5	80	23	4 & 6	76	78	90	- 40	50
			6	75	25				200	- 40	8
			68	40	16				202	- 55	15
			69	55	32						
			70	- 60	12	5	87	72	55	- 185	9
			72	- 60	9				56	195	28
			73	- 45	7				75	190	19
			75	-1680	55	5	88	78	55	- 255	12
			77	85	17				56	30	4
			78	80	14				75	- 180	14
			80	35	14				83	25	1
			82	- 60	14				96	40	4
			83	- 50	10	5	89	72	55	- 60	3
1A	36	72	86	- 20	9	7	18	60	137	- 85	13
			1	80	9				138	- 125	32
			4	65	8				164	- 85	11
			5	110	26				165	- 70	8
			6	290	29						
			68	55	22	7	19	72	137	- 110	13
			69	80	43				138	- 230	48
			70	- 95	16				164	- 260	24
			72	- 80	11				167	- 200	20
			73	- 80	11						
			74	- 780	41	7	20	72	138	- 55	8
			75	-1490	52				165	- 100	11
			77	110	8				171	- 265	36
			78	115	18	7	21	78	123	30	9
			80	70	27				135	125	30
			82	- 65	14				137	- 55	6
			83	- 75	13				138	- 120	15
1A	37	72							164	- 185	17
			6	45	14				165	- 185	17
			70	- 30	5						
			72	- 30	4	8	11	60	142	- 225	23
			73	- 40	5				143	- 300	34
			75	- 985	34	8	12	72	122	- 30	15
			77	65	12				123	- 30	13
			78	80	12				126	- 30	13
			80	45	17				127	- 25	13
			82	- 35	7				129	- 25	13
			83	- 30	5				130	- 20	11
2	67	72	67	40	6				140	30	5
2	68	72	84	115	18				142	- 485	34
			85	- 55	4				143	- 460	7
			87	15	9	8	13	72	142	- 210	16
2	69	78	84	80	10	9	26	60	108	- 115	10
			85	- 130	9				109	- 60	7
			87	25	15				110	- 100	7
			93	- 40	8						
3	58	48	70	- 125	13	9	27	72	108	- 215	19
			71	55	11				109	- 300	19
3	59	60	70	- 435	28				110	- 100	5
			71	255	37	9	28	72	111	15	12
			148	- 145	9				109	- 200	13
			149	- 80	5	9	30	78	111	20	7
3	60	72	15	- 55	6				95	- 50	3
			68	- 180	19				108	- 90	7
			70	- 500	27				109	- 115	4
			71	185	29				111	35	18
			73	100	8	14	78	48	55	35	7
			148	- 270	13	14	79	60	55	125	26
			149	- 220	11				56	- 85	8
			150	- 110	7				61	10	9
3	61	72	15	- 40	4	14	80	72	55	- 55	7
			68	- 290	25				56	- 180	14
			70	- 135	8				57	- 105	9
			73	70	6				61	35	16
			148	- 75	4				62	- 30	20
			149	- 80	4	14	81	78	55	- 135	14
3	62	78	68	- 125	12				56	- 160	10
			70	- 175	9				57	- 40	3
			73	165	13				61	25	15
			148	- 145	7				62	- 80	48
			149	- 290	13	14	82	72	55	- 30	4
			213	- 35	3				56	- 60	3
									62	- 25	23

*A plus value indicates tension; a minus value, compression. **Test 1A was conducted with an underinflated tire.

and for the second drop at a given height the strain gages showed either much smaller or no additional permanent set at all. The maximum permanent set indicated by the deflection gages was of the order of 0.02 in. However, the deflection gages could be read no closer than 0.01 in.

The dynamic response factors of the steel supporting members vary between 0.9 and 1.1 for A 3 D-1. The dynamic response factors are generally less than 1.0 for loads less than 70,000 lb and greater than 1.0 for higher loads. The dynamic response factors for F 2 H-3 vary principally between 0.8 and 1.0.

Experimental tire imprints for various static loads are shown in Figure 20. The imprint areas compare well with those computed by the BuShips design method.^{2,3} Similar experimental data obtained from the drop tests were unsatisfactory because the cloth wrinkled.

Detailed action of tires and struts is best seen in motion pictures of the test.* Frames showing the bottoming action of the A 3 D-1 and F 2 H-3 tires are shown in Figure 21. The A 3 D-1 tire bottomed between 80,000 and 100,000 lb. From visual inspection the F 2 H-3 tire appeared to bottom at approximately 50,000 lb. The tires were maintained at normal landing pressure at all times except on one occasion when, because of a tube failure with the A 3 D-1 landing gear, pressure dropped from 190 psi to 90 psi. When the landing gear was dropped in this condition, bottoming was very severe and the localized loading caused extensive crushing of the wood.

POSITIONS 1, 9, and 14 (A 3 D-1)

Loads applied at similar positions (Positions 1, 9, and 14 on longitudinals midway between transverse members) caused the highest strains in the steel supporting structure. These strains occurred on the longitudinal directly under the load midway between the transverse beam at midspan and an adjacent one. Maximum deck reactions were 138,200 lb at Position 1 and 147,800 lb at Positions 9 and 14.

On the centerline of the lower flange of the longitudinal directly under the load, maximum bending strains of +2500 $\mu\text{in}/\text{in.}$ were recorded at 147,800 lb. Permanent sets were small, -150 to -200 $\mu\text{in}/\text{in.}$, and were in the opposite direction. Repeated loading indicated no additional set. At 138,200 lb no permanent set was observed for a strain of +2400 $\mu\text{in}/\text{in.}$ The maximum deflection of the longitudinal was 0.82 in. with negligible permanent deflection.

These strains indicate that stresses as high as 72,000 to 75,000 psi at loads of 138,200 to 147,800 lb produced no significant permanent set at this location. However, the data indicate that the outer fiber of the longitudinal was beginning to yield at the higher load. Stresses as high as the minimum specified yield point of the material (47,000 psi) occur at a load of 97,000 lb. Subsequent standard tensile tests of material samples taken from the

*Copies of the film are available at the Bureau of Ships and the David Taylor Model Basin.

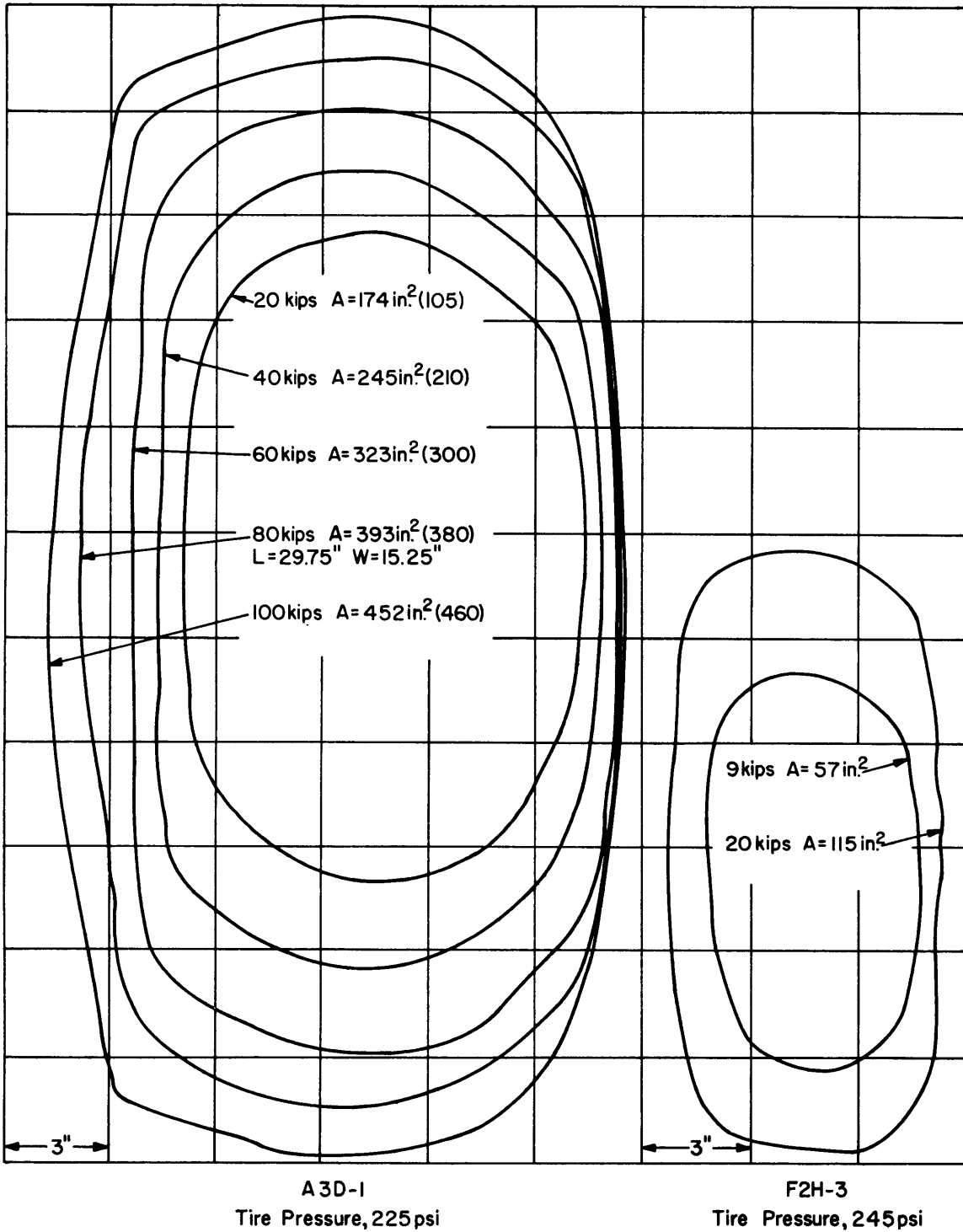


Figure 20 – Tire Imprints for Various Static Loads

A is the experimentally measured area of the tire imprint. Values in parentheses are areas obtained from BuShips design calculation.

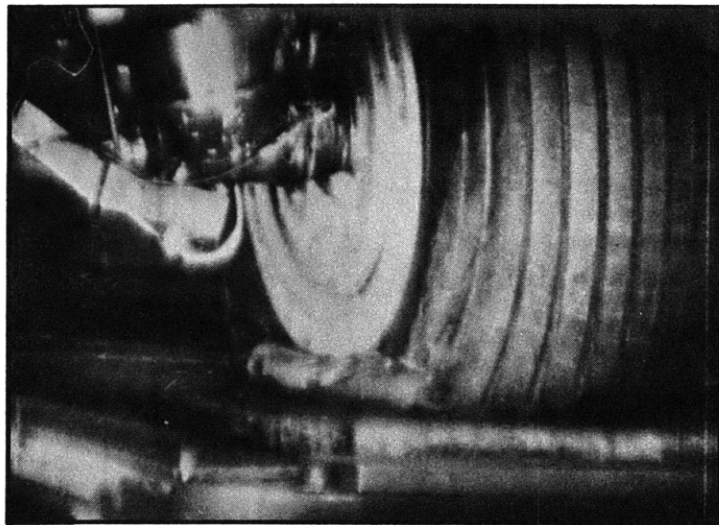


Figure 21a - A3D-1



Figure 21b - F2H-3

Figure 21 - Tire Bottoming during Drop Tests

longitudinal members in the test area showed that the actual yield point of the material was 58,000 psi. Material samples from the overstressed areas had the same yield point as those from lowly stressed areas. Thus, under the test loading, a stress at least 25 percent in excess of the actual static yield point of the material did not cause permanent set of the steel structure.

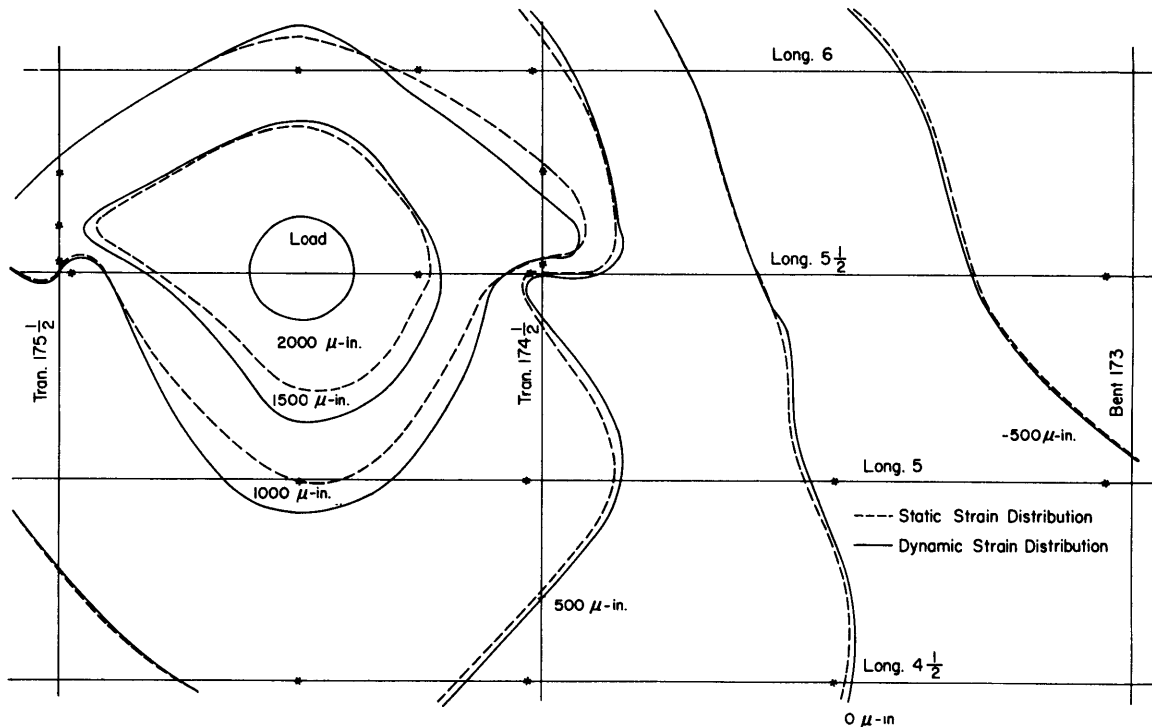


Figure 22 – Distribution of Static and Dynamic Strains in Lower Flanges of Grillage Members for an A 3 D-1 Loading of 138,200 Pounds at Test Position 1

Asterisks indicate gage locations. These curves were obtained from straight-line interpolation between points of known strain (gage locations).

The distributions of static and dynamic strain in the lower flanges of the transverse and longitudinal grillage members due to a 138,200-lb load at Position 1 are shown in Figure 22. Note their similarity.

Figure 23 shows how the distribution of deflections and corresponding bending stresses in the lower flange of the longitudinal vary for the different test positions (1, 2, 3, and 4) on the longitudinal. These distributions were obtained at a load of 99,000 lb, slightly higher than the certified deck reaction. At the higher loads strain gages on the upper flange of the longitudinal indicated bending or twisting, which probably resulted from loading by the wheel rim when the tire bottomed. Because of this, local permanent sets totaling -500 to -1000 $\mu\text{in}/\text{in.}$ were observed in the upper flange at maximum load (147,800 lb). This distortion of the upper flange is a local effect and is not considered detrimental to the load-carrying capacity of the structure. No permanent set was observed on the upper flange at loads of 90,000 lb or less. With an underinflated tire the upper flange yielded and was visibly distorted, as evidenced by a recorded set of -2300 $\mu\text{in}/\text{in.}$ for a load of 138,200 lb.

From Table 18 the maximum membrane shear stress in the web of the longitudinal was of the order of 19,500 psi for a 138,200-lb load at Position 1.

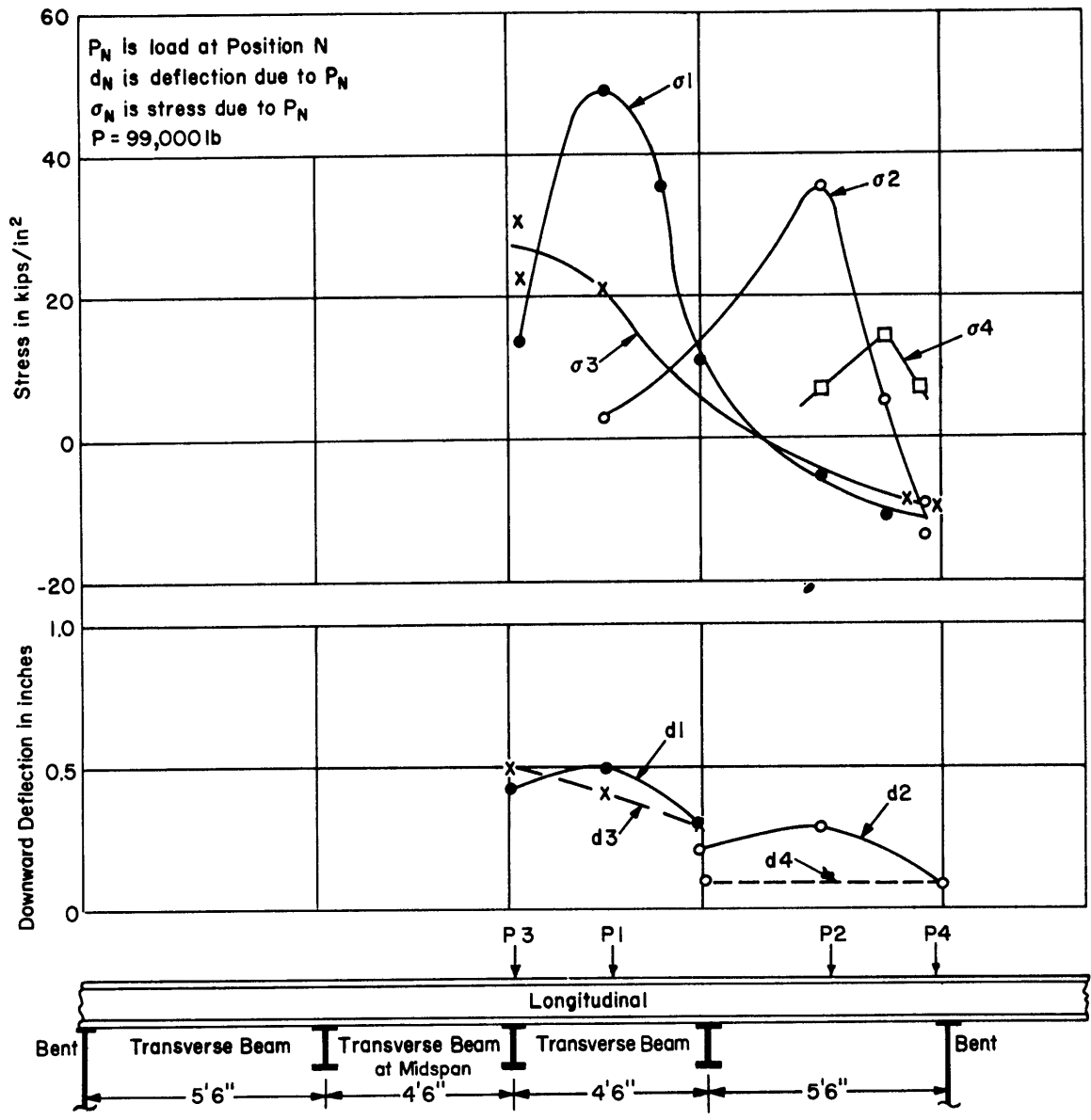


Figure 23 – Deflections and Corresponding Bending Stresses in Longitudinal Member for Deck Reaction of 99,000 Pounds for Various A 3 D-1 Test Positions

POSITION 2 (A 3 D-1)

At Position 2 the highest strains occurred under the load on Longitudinal $5\frac{1}{2}$ midway between Bent 173 and the transverse beam at Frame $174\frac{1}{2}$. At the maximum deck reaction of 147,800 lb, bending strains in the lower flange of the longitudinal measured $+1850 \mu\text{in/in.}$, corresponding to a stress of 55,500 psi, without any permanent set. Bending strains in the upper flange were as high as $-1510 \mu\text{in/in.}$ The shear stresses in the web of the longitudinal

are highest next to the heavy bent structure, the membrane value being approximately 24,000 psi for 147,800 lb.

The maximum deflection of the longitudinal directly under the load was 0.41 in.

POSITION 3 (A 3 D-1)

At Position 3 the highest strains occurred under the load on the transverse beam at Frame 175½ at the intersection with Longitudinal 5½. At the maximum deck reaction of 147,800 lb, bending strains of approximately +2200 $\mu\text{in/in.}$ (corresponding to a stress of 66,000 psi) were recorded in the top flange of the transverse beam, while the simultaneous strain in the lower flange of the beam was +1800 $\mu\text{in/in.}$ Shear stresses in the transverse beam were only about 12,000 psi.

The maximum deflection of the beam directly under the load was 0.83 in.

POSITIONS 4 AND 6 (A 3 D-1)

Because of the proximity of Positions 4 and 6, they were combined as one test position on the longitudinal 6 in. from the centerline of Bent 173. In general, the strains in Bent 173 and Longitudinal 5½ were small. Since Position 4 was slightly off the centerline of the bent, the highest strains (1200 $\mu\text{in/in.}$) resulted from local bending at the upper end of the web of the bent in line with the load at a maximum deck reaction of 147,800 lb. Shear stresses in the web of the longitudinal were not as high here as at Position 2 because the wheel was so close to the bent that the longitudinal did not carry the full load. The maximum deflection of the bent was 0.13 in.

POSITION 7 (A 3 D-1)

Position 7, directly over the intersection of a transverse beam and a longitudinal, is similar to Position 3. However, Position 7 is close to the heavy centerline girder. At a deck reaction of 147,800 lb, maximum bending strains of -1100 $\mu\text{in/in.}$ were recorded in the top flange of the transverse beam; the corresponding strain in the lower flange was +1230 $\mu\text{in/in.}$ At the intersection of the transverse beam with the heavy centerline girder, a maximum bending strain of +1150 $\mu\text{in/in.}$ was measured on the upper flange.

The maximum shear stress in the transverse beam at this location was approximately 20,000 psi. The maximum deflection of the beam directly under the load was 0.34 in.

POSITIONS 5, 8, AND 15 (A 3 D-1)

Although the most severe load condition on the wooden planking with the A 3 D-1 landing gear occurred at Positions 5, 8, and 15 at the center of panels midway between longitudinal and transverse members, the wooden planking consistently failed at *all* test positions for a deck reaction of 138,200 lb. An exception was noted at Position 1 with an underinflated

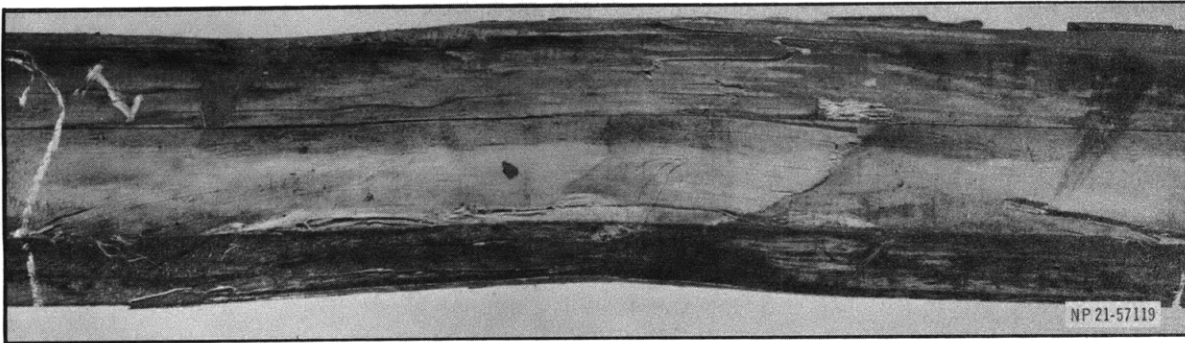


**Figure 24 – Portion of Flight-Deck Planking Removed from Test Position 1
after Tests with A 3 D-1 Landing Gear**

Tests were conducted with low tire pressure. Initial failure of planking occurred at a deck reaction of 122,000 lb; pictured damage is result of 138,200-lb loading.

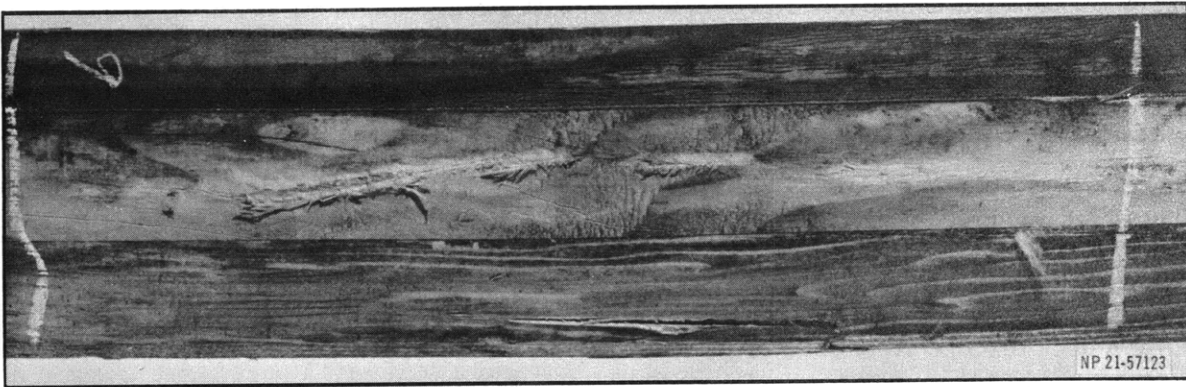


**Figure 25 – Portion of Flight-Deck Planking Removed from Test Position 9
after Deck Reaction of 138,200 Pounds with A 3 D-1 Landing Gear**

Failure occurred at a deck reaction of 138,200 lb.

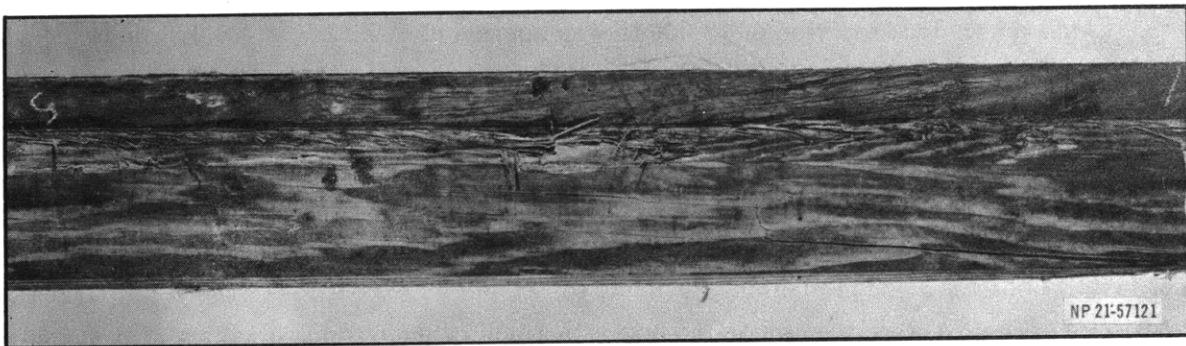


**Figure 26 – Portion of Flight-Deck Planking Removed from Test Position 5
after Deck Reaction of 138,200 Pounds with A 3 D-1 Landing Gear**

tire where initial damage to the wood occurred at 122,000 lb. Figure 24 shows the damage to this planking after an additional loading of 138,200 lb had been applied. Figure 25 shows failure of planking removed from similar Position 9 after a 138,200-lb loading with a properly inflated tire. Both failures were by horizontal shear but with the underinflated tire considerable crushing of the wood was noted.

Figure 26 shows the portion of the deck planking removed from Position 5 after loads up to 138,200 lb had been sustained. Failure is by horizontal shear. Although no reliable *dynamic* strain data were obtained from the 45-deg diagonal gages (Gages 35 and 36), *static* strains indicate that diagonal strains of the order of 4000 $\mu\text{in/in.}$ were present. Bending strains were approximately 5000 $\mu\text{in/in.}$ The maximum deflection at the center of the panel was 1.30 in. measured from the flight-deck planking. This is probably larger than normal because at this position the flight-deck planking was separated from the flight-deck plating by an air space of almost $\frac{1}{2}$ in. caused by prior tests at nearby Position 1 with an underinflated tire.

Tests at Position 15 (10 in. aft of Position 5) were conducted after initial failures of the wood had been induced by previous tests at both Longitudinals 5 $\frac{1}{2}$ and 6 and midway between the longitudinals at Position 5. In this case the planking was not repaired prior to test. Four drops were made, the maximum at a deck reaction of 147,800 lb. Even though the wooden planking was cracked slightly forward of this position, the planking under the load sustained one loading at 138,200 lb and one at 147,800 lb without causing visual damage any greater than that which occurred at a similar location with intact planking. The bowed 4.2-lb plating and adjacent undamaged planks must have carried some of the load.

Position 8 was close to the relatively rigid centerline girder. Wooden planking removed after a deck reaction of 138,200 lb had failed by horizontal shear. Figure 17 indicates that the diagonal gages (Gages 44 and 45) recorded dynamic strains of 7500 $\mu\text{in/in.}$ at this load, while the bending strains were approximately 4500 $\mu\text{in/in.}$ From the strain data, it appears that this is the most critical location for shear failure of the wooden planking.

POSITIONS 10, 11, 12, AND 13 (F 2 H-3)

A maximum deck reaction of 72,000 lb was applied at Position 13; 66,000 lb at Positions 10 and 12; and 68,000 lb at Position 11. Examination of the planking removed after each of these tests indicated that it had failed by horizontal shear, although the extent of damage was more moderate than for the failures observed after A 3 D-1 loadings. Stresses and deflections of the steel supporting members were moderate, generally less than 800 $\mu\text{in/in.}$ Because of the additional time which would have been required, diagonal strain gages were not installed on the wooden planking for these tests. As an expeditious substitute, Gages 35 C, 36 D, 44 A, and 45 A were located on the bottom surface of the wooden planking near supported ends of the planking.

Figure 27 shows the wooden planking removed from Position 10, similar to Position 8 for A 3 D-1, after it had sustained reactions up to 66,000 lb. It is noted that failure was by



Figure 27 – Portion of Flight-Deck Planking Removed from Test Position 10 after Deck Reaction of 66,000 Pounds with F 2 H-3 Landing Gear

horizontal shear. A maximum bending strain of approximately $+7500 \mu\text{in}/\text{in}$. (Gage 54) was measured.

At Position 11 adjacent to the horizontal centerline girder, Gage 45 B (located on wood under the load) indicated a maximum strain of $+4000 \mu\text{in}/\text{in}$. At Position 12, Gage 36 D (on the underside of the planking directly under the load) indicated a strain of $+3800 \mu\text{in}/\text{in}$. At Position 13, Gage 51 (under the load) indicated a maximum dynamic bending strain of $+7500 \mu\text{in}/\text{in}$.

COMPARISON OF EXPERIMENT WITH THEORY

BUREAU OF SHIPS DESIGN PROCEDURE

Table 20 gives experimental and maximum computed stresses at critical locations on the structure for the CVA 19 certified deck reaction of 90,000 lb for the A 3 D-1 aircraft. Computed values are obtained from the design method described in References 2 and 3. The experimental values are calculated from the tabulated data for the drop which caused a deck reaction closest to 90,000 lb. Shear stresses are obtained from Table 18. The maximum bending stress in the wooden planking is obtained from the strain data, using a value of Young's modulus of 1.6×10^6 psi.

For the most critically stressed location, i.e., the maximum bending stress in the longitudinal, the maximum stress obtained from experiment is only three percent less than that computed. Agreement for all locations is fairly good and on the conservative side. Agreement was poorest for the maximum shearing stress in the longitudinal, because Position 4 was too close to the transverse bent and Position 2 (midway between the bent and a transverse beam) was too far away from the support to cause maximum shear stresses to be developed. As mentioned previously, local deformation of the upper flange occurs first in this area at loads in excess of the design load. Although the design calculations in Table 20 indicate that the shear stress in the wooden planking at 90,000 lb is only 650 psi, it is noted that rim loads

TABLE 20

Comparison of Experimental and Calculated Stresses for
A 3 D-1 Deck Reaction of 90,000 Pounds

Location of Maximum Stress	Test Position	Stress σ , psi		Ratio $\frac{\sigma_{\text{Calc.}}}{\sigma_{\text{Exp.}}}$
		Experimental	Calculated	
Bending in Longitudinal	1	45,500	48,000	1.03
	9	46,600		
	14	44,900		
Shear in Longitudinal	2 4, 6*	13,100	29,500	2.25*
Bending in Transverse	3	31,000	45,000	1.45
Shear in Transverse	7	11,700	11,700	1.00
Bending in** Wooden Plank	5	5,600	5,400	0.97 1.12
	8	4,800		
Shear in Wooden Plank		-	650	-
<p style="text-align: center;">*Positions 4 and 6 were too close to the heavy transverse bent to give maximum shear, whereas Position 2 at midspan was too far away from support.</p> <p style="text-align: center;">**Modulus of elasticity of wood in bending is 1.6×10^6 psi.</p>				

resulting from bottoming at higher loads will cause these stresses to increase rapidly. On the basis of a tire-bottoming load of 95,000 lb, a shear stress of 1140 psi is calculated for a deck reaction of 122,000 lb. Although this stress is considered to be sufficient to cause failure of the wood, the only observed failure at this load was with an underinflated tire. However, the wood always failed at the next highest load increment; i.e., 138,200 lb.

A similar correlation of F 2 H-3 experimental results for the steel supporting structure is not attempted since the test positions were designed primarily to provide data on the wooden planking. However, it is noted that the F 2 H-3 design calculations indicate that tire bottoming occurs at a load of 31,000 lb. Since this value is based on the results of a more comprehensive test of tire action, it is believed that the visually observed F 2 H-3 tire bottoming load of 50,000 lb is in error. Calculations with 31,000 lb as the tire-bottoming load indicate that a shear stress of 1120 psi will be developed in the wood at a deck reaction of 47,000 psi. This value is considered sufficient to cause initial failure of the wood. Unfortunately, the lowest reaction at which wooden planking was removed for inspection during the F 2 H-3 tests was 66,000 lb, and at this reaction the wood had failed.

MAXWELL'S RECIPROCITY THEOREM

Strain and deflection data appropriate for checking Maxwell's reciprocity theorem are given in Table 21. Results are shown for adjacent longitudinals and for longitudinals two and three spacings apart. Dynamic strains and deflections observed at an A 3 D-1 deck reaction of 138,200 lb are used for the comparisons. In general, the results indicate that Maxwell's reciprocity theorem is valid. Poorest agreement occurs in the flange of the longitudinal at the intersection with a transverse, and is attributed to slight differences in the longitudinal or transverse positioning of the wheel between comparative tests.

DYNAMIC RESPONSE

In general, the dynamic response factor is a function of the shape, time of rise, and duration of loading, and of the natural frequency and damping of the structure. It was observed on HANCOCK that the strain distributions in the lower flanges of the longitudinals and transverse beams of the grillage were approximately the same for both static and dynamic loadings; see Figure 22. On this basis, it is reasonable to assume for a simplified analysis that the grillage structure can be considered to respond similarly to a single-degree-of-freedom system. Calculations of the dynamic amplification spectra for a single-degree-of-freedom system under impact loadings have been made by Fung.⁷

Figure 28 shows the amplification spectra for various degrees of structural damping for a sine-type pulse similar to the shape of the drop-test deck reaction. In this figure

t_1 = time of rise to 98 percent of peak load

$\frac{q_{\max}}{q_0}$ = positive dynamic response factor

$\frac{q_{\min}}{q_0}$ = negative dynamic response factor

$\frac{c}{c_c}$ = ratio of actual damping to critical damping

f = natural frequency of system

A realistic value for damping determined from vibration generator tests on the grillage with wooden planking is $c/c_c \approx 0.08$. It is noted that, for this value of damping, the maximum dynamic response factor for the worst possible condition is reduced to about 1.6.

TABLE 21

Experimental Verification of Maxwell's Reciprocity Theorem for Longitudinals
 Located One, Two, and Three Spacings Apart

Ratio	Static	Dynamic 138,200 lb	Ratio	Static	Dynamic 138,200 lb	Ratio	Static	Dynamic 138,200 lb
Test Position 1 versus 9 Static and Dynamic Spacings Two Longitudinal Spacings Apart			Test Position 1 versus 14 Dynamic Only Adjacent Longitudinals			Test Position 9 versus 14 Dynamic Only Three Longitudinal Spacings Apart		
$\frac{P_1 \epsilon_{76}}{P_9 \epsilon_{110}}$	0.97	1.03	$\frac{P_1 \epsilon_{76}}{P_{14} \epsilon_{57}}$	N.D.	1.04	$\frac{P_9 \epsilon_{110}}{P_{14} \epsilon_{57}}$	N.D.	0.95
$\frac{P_1 \epsilon_{96}}{P_9 \epsilon_{96}}$	0.81	0.93	$\frac{P_1 \epsilon_{79}}{P_{14} \epsilon_{60}}$	N.D.	1.14	$\frac{P_9 (\epsilon_{108} + \epsilon_{109})}{P_{14} (\epsilon_{55} + \epsilon_{56})}$	N.D.	1.17
$\frac{P_1 \epsilon_{110}}{P_9 \epsilon_{76}}$	0.93	1.01	$\frac{P_1 (\epsilon_{82} + \epsilon_{83})}{P_{14} (\epsilon_{63} + \epsilon_{64})}$	N.D.	0.57	$\frac{P_9 (\epsilon_{111} + \epsilon_{112})}{P_{14} (\epsilon_{61} + \epsilon_{62})}$	N.D.	1.47
$\frac{P_1 (\epsilon_{82} + \epsilon_{83})}{P_9 (\epsilon_{113} + \epsilon_{114})}$	0.44	0.58	$\frac{P_1 \epsilon_{86}}{P_{14} \epsilon_{67}}$	N.D.	0.83	$\frac{P_9 (\epsilon_{113} + \epsilon_{114})}{P_{14} (\epsilon_{63} + \epsilon_{64})}$	N.D.	0.93
$\frac{P_1 (\epsilon_{72} + \epsilon_{73})}{P_9 (\epsilon_{113} + \epsilon_{114})}$	0.64	0.75	$\frac{P_1 (\epsilon_{74} + \epsilon_{75})}{P_{14} (\epsilon_{55} + \epsilon_{56})}$	N.D.	0.83	$\frac{P_9 \epsilon_{117}}{P_{14} \epsilon_{67}}$	N.D.	0.79
$\frac{P_1 \epsilon_{86}}{P_9 \epsilon_{117}}$	1.07	1.02	$\frac{P_1 (\epsilon_{77} + \epsilon_{78})}{P_{14} (\epsilon_{58} + \epsilon_{59})}$	N.D.	1.18	$\frac{P_9 \epsilon_{115}}{P_{14} \epsilon_{65}}$	N.D.	0.69
$\frac{P_1 \epsilon_{103}}{P_9 \epsilon_{103}}$	0.84	N.D.	$\frac{P_1 \epsilon_{154}}{P_{14} \epsilon_{154}}$	N.D.	0.99	$\frac{P_9 \epsilon_{96}}{P_{14} \epsilon_{76}}$	N.D.	1.24
$\frac{P_1 (\epsilon_{14} + \epsilon_{75})}{P_9 (\epsilon_{108} + \epsilon_{109})}$	0.92	1.02	$\frac{P_1 \epsilon_{161}}{P_{14} \epsilon_{161}}$	N.D.	1.01	$\frac{P_9 (\epsilon_{94} + \epsilon_{95})}{P_{14} (\epsilon_{74} + \epsilon_{75})}$	N.D.	1.01
$\frac{P_1 (\epsilon_{94} + \epsilon_{95})}{P_9 (\epsilon_{94} + \epsilon_{95})}$	0.86	0.92	$\frac{P_1 \epsilon_{153}}{P_{14} \epsilon_{153}}$	N.D.	1.03	$\frac{P_9 \delta_{191}}{P_{14} \delta_{178}}$	N.D.	1.04
$\frac{P_1 (\epsilon_{80} + \epsilon_{81})}{P_9 (\epsilon_{111} + \epsilon_{112})}$	0.95	N.D.	$\frac{P_1 \delta_{183}}{P_{14} \delta_{179}}$	N.D.	1.14			
$\frac{P_1 (\epsilon_{97} + \epsilon_{98})}{P_9 (\epsilon_{97} + \epsilon_{98})}$	1.01	N.D.	$\frac{P_1 \delta_{182}}{P_{14} \delta_{178}}$	N.D.	1.03			
$\frac{P_1 (\epsilon_{84} + \epsilon_{85})}{P_9 (\epsilon_{115} + \epsilon_{116})}$	1.60	N.D.	$\frac{P_1 \delta_{184}}{P_{14} \delta_{180}}$	N.D.	1.14			
$\frac{P_1 (\epsilon_{101} + \epsilon_{102})}{P_9 (\epsilon_{101} + \epsilon_{102})}$	1.10	N.D.						
$\frac{P_1 \delta_{182}}{P_9 \delta_{191}}$	0.85	0.97						
<p>ϵ (strain) subscripts refer to gage number. δ (deflection) subscripts refer to gage number. P (load) subscripts refer to test position.</p>								

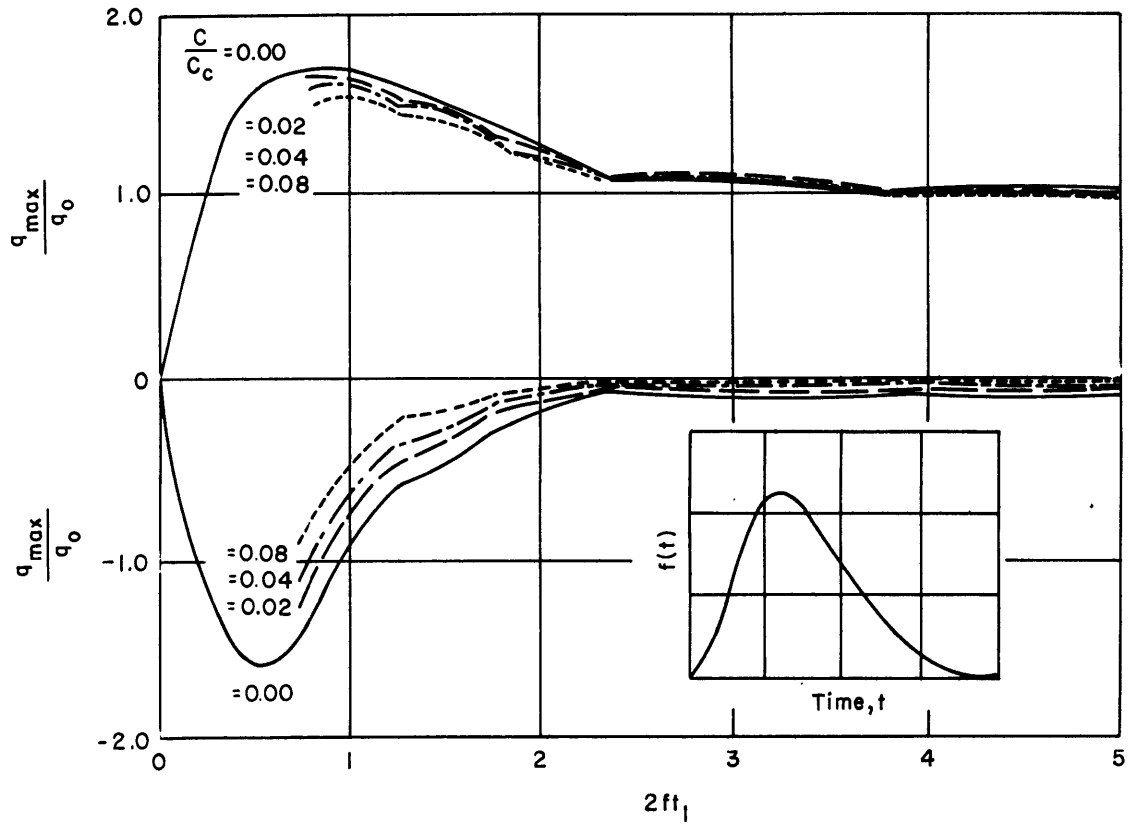


Figure 28 – Effect of Damping on Amplification Spectra

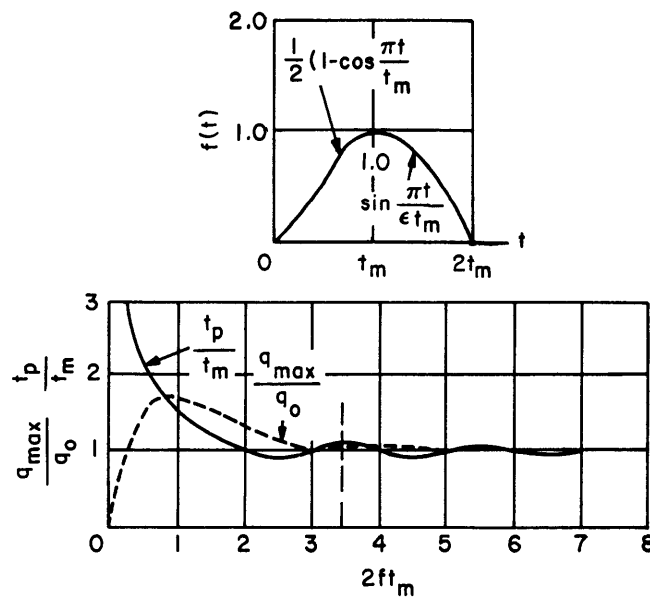


Figure 29 – Ratio of Peak Response Time t_p to Peak Pulse Time t_m

By applying the data obtained on HANCOCK, it can be shown that the time of rise of the deck reaction is slow compared with the critical frequency of the grillage. Figure 29 shows the ratio of time of rise of pulse t_p to time to peak response t_m plotted as a function of the dynamic response. The measured ratios of t_p/t_m and q_{\max}/q_0 on HANCOCK were approximately 1.0 and 1.1. The ratio of q_{\min}/q_{\max} was approximately zero. Therefore, the value of $2f t_m$ is ≥ 2.8 . Since t_m on HANCOCK is approximately equal to 0.1 sec, the natural frequency of the grillage should be equal to or greater than 14 cps.

An attempt was made to determine, by means of a vibration generator test, the critical frequency of a similar grillage with a wooden deck on USS TICONDEROGA (CVA 14). As nearly as could be determined, a frequency of 17.1 cps was believed to be the response of the longitudinals and transverse beams of the grillage in a mode closely related to the response of the grillage observed during drop tests.

On this basis, the dynamic response factor predicted by theory agrees well with the experimental results of the drop tests. A slightly more detailed discussion is given in Reference 4, where it is shown that the results of the drop tests on HANCOCK are applicable to subsequent A 3 D-1 landing tests on BON HOMME RICHARD.

EVALUATION OF STRENGTH

As noted previously, the calculated and experimental stresses agree very well for the most critically stressed location for A 3 D-1 landing reactions. However, it was noted that stresses higher than the actual yield point of the material occurred without significant permanent set. In Figure 30 experimental curves of stress versus load at this location are compared with calculated stresses. The experimental curve which gives the highest stress was obtained from the test where the wooden planks butted together directly over the loaded longitudinal, whereas the other experimental curve was obtained from a test where the wood was continuous over the loaded and adjacent longitudinals. The difference in stresses was caused by the distribution of a larger portion of the load to adjacent longitudinals where the wood was continuous. It is noted that at 138,200 lb, the failure of the wooden planking, with its attendant loss in carry-over strength, causes the stress in the loaded longitudinals to approach the same value for both test positions. This is particularly evident at the increased load of 147,800 lb.

From examination of Figure 30, it is possible to deduce or estimate the strength of the critically stressed longitudinals as follows:

1. The small difference between design and experimental stresses is due to assumptions in calculations, and provides a margin of safety equivalent to about a 7000-lb load.

2. Differences between the minimum specified yield point of the material and the actual yield point of the material in the beams installed on HANCOCK account for an additional increase in load of about 20,000 lb. Since this additional strength cannot be relied upon as characteristic of all such material, its effect must be discounted in a general strength evaluation.

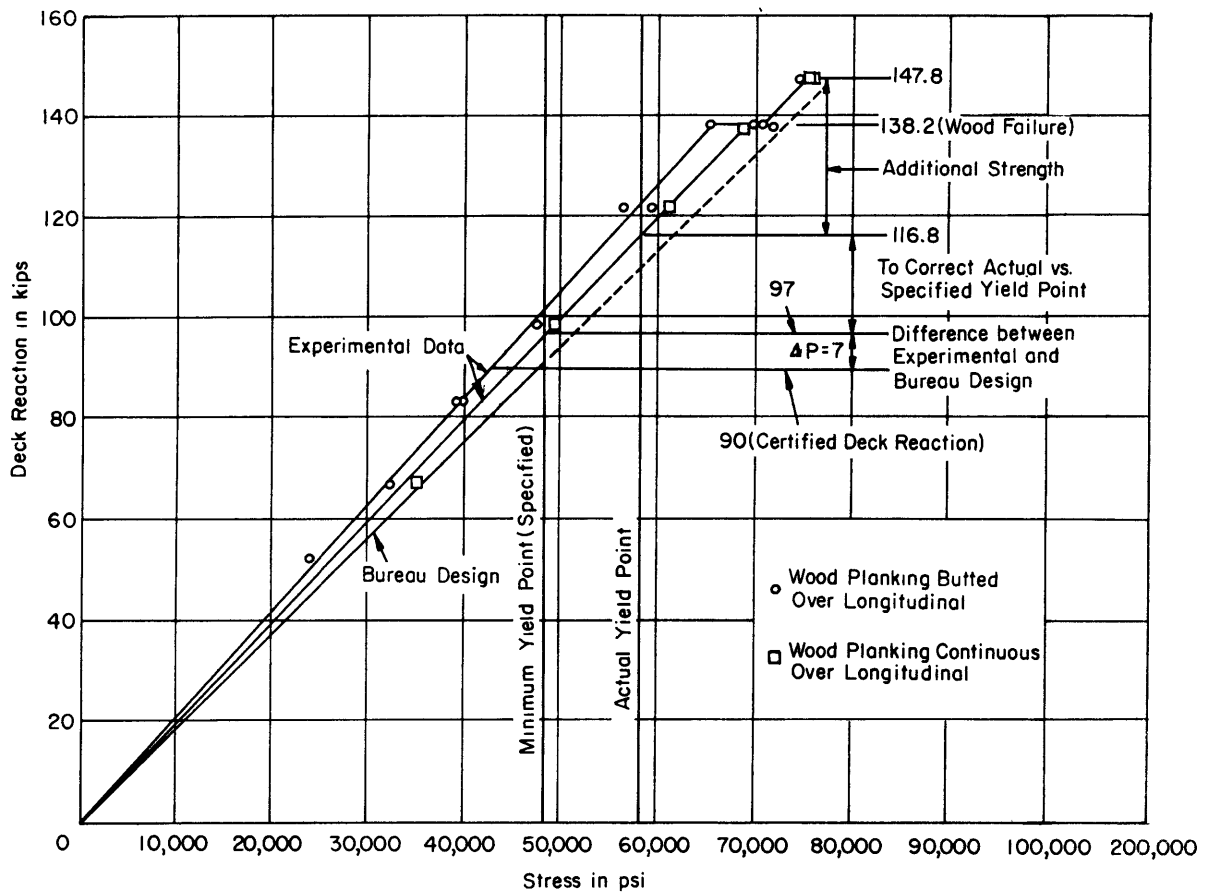


Figure 30 – Comparison of Drop-Test Results with BuShips Design Calculations of Maximum Bending Stress in Longitudinal Member versus Deck Reaction

3. The fact that the grillage sustained an additional 30,000-lb load with only small permanent set is attributed to two factors:

a. The difference noted between measurable initial yielding of I-beam material under static load in bending and the tensile yield point of a standard specimen of the material.

b. Possible dynamic loading effects.

To date these effects have not been thoroughly investigated at the Model Basin for beams, and comparable effects in a grillage have not been investigated at all. However, the results of this test clearly indicate that the grillage members supporting the wood-planked portion of the deck on CVA 19 (27 C conversion) are capable of withstanding an A 3 D-1 landing load of 120,000 lb without significant permanent set.

Results of A 3 D-1 and F 2 H-3 tests indicate that failure of the wooden planking will not occur at loads less than those assumed in design.

SUMMARY AND CONCLUSIONS

1. The present Bureau of Ships design procedure accurately predicts the stresses in the flight-deck structure under static and dynamic loading.
2. The strength of the flight-deck supporting structure is adequate for the A 3 D-1 certified deck reaction of 90,000 lb. Results of this test indicate that A 3 D-1 landing reactions of 120,000 lb, producing dynamic stresses about 30 percent beyond the nominal yield point of the material, will not cause significant permanent set of the structure.
3. Dynamic deck reactions up to 147,800 lb were applied to the deck with the A 3 D-1 landing gear. There was no visual damage in the steel structure *as long as proper tire pressure was maintained*. An underinflated tire damaged the upper flange only. Deflection gages indicated negligible permanent set in areas of high strain; strain records showed a small amount of permanent set. Some permanent sets were recorded by the strain gages in otherwise lowly stressed areas and may be considered largely the results of residual stress. Strains as high as +2500 $\mu\text{in/in.}$ were recorded in the longitudinals with no apparent effect on the mechanical properties of the material and with only small evidence of yielding.
4. The strength of the flight-deck structure is adequate for the F 2 H-3 certified deck reaction of 46,650 lb. Maximum dynamic load applied to the deck with the F 2 H-3 landing gear was 72,000 lb. Maximum dynamic strains in the steel structure were generally below 800 $\mu\text{in/in.}$
5. Failure of the flight-deck planking was by longitudinal shear and occurred consistently with a dynamic load of 138,200 lb applied with the A 3 D-1 landing gear and a dynamic load of between 66,000 and 72,000 lb with the F 2 H-3 landing gear. After initial failure of the wooden decking, additional tests at the same location showed no appreciable increase in strains in the steel supporting structure, and little additional damage to the wood itself.
6. The deck planking and not the steel supporting structure is the critical component of the flight-deck structure. Also, it should be noted that "spin-up" of the landing wheels might cause more severe effects on the wooden planking than those observed.
7. The dynamic response factor for A 3 D-1 loading varied generally between 0.90 and 1.10. The dynamic response factor tends to increase with load. For the F 2 H-3 landing gear the response factor was usually less than one.
8. Maxwell's reciprocity theorem is applicable.

ACKNOWLEDGMENTS

The tests were conducted by Mr. E.E. Johnson, CDR A.F. Hancock, USN, Messrs. L.A. Becker, R.L. Waterman, J.P. Hendrican, and the author.

The cooperation of personnel from Puget Sound Naval Shipyard and Douglas Aircraft Company aided materially in the successful completion of the work.

Much of the initial planning for the tests and the preparation of a preliminary report on the results of the tests were done by Mr. E.E. Johnson and CDR A.F. Hancock, USN.

REFERENCES

1. Bureau of Ships CONFIDENTIAL letter C-CVA 19 Class/S 83 (442) Serial 442-019 of 2 Sep 1953.
2. Fisher, A.W. and Park, Y., "Structural Design of Aircraft Handling Decks," Bureau of Ships Design Data Sheet DDS 1106-1 (1 Nov 1957) CONFIDENTIAL.
3. Newmark, N.M., "Design Study of Parameters of Aircraft Carrier Flight Deck Strength," Contract NObs 65546, NSM 731-040 (Apr 1956) CONFIDENTIAL Final Report.
4. Allnutt, R.B., "Strength Tests of Flight Deck on USS BON HOMME RICHARD (CVA 31) during Landings of an A 3 D Aircraft," David Taylor Model Basin Report C-809 (Sep 1957) CONFIDENTIAL.
5. Sabara, D.E., "Carrier Deck Drop Test Calibration Model XA 3 D-1 Airplane," Douglas Aircraft Company Report No. E.S. 17539 (Apr 1954) CONFIDENTIAL.
6. "Design of Wood Aircraft Structures," Subcommittee on Air Force-Navy-Civil Aircraft Design Criteria, Aircraft Committee, ANC-18 (Jun 1951).
7. Fung, Y.C., "On the Dynamic Amplification Spectra of Landing Impacts," Aercon, Inc. Final Report No. 1 on Bureau of Aeronautics Contract No. NOas 53-348-C (30 Dec 1953).

INITIAL DISTRIBUTION

Copies

- 15 CHBUSHIPS, Library (Code 312)
 - 5 Tech Library
 - 1 Tech Asst to Chief (Code 106)
 - 1 Prelim Design Br (Code 420)
 - 1 Hull Design Br (Code 440)
 - 2 Scientific & Research (Code 442)
 - 2 Structure (Code 443)
 - 2 Aircraft Carriers & Seaplane Tenders (Code 522)
 - 1 Hull Arrang, Structural, & Preser Br (Code 633)
- 2 CHBUAER
- 2 CNO
- 2 CHONR
 - 1 Code 438
 - 1 Code 530
- 2 DIR, USNRL
- 2 NAVSHIPYD NORVA
- 2 NAVSHIPYD PUG
- 2 NAVSHIPYD NYK
- 2 NAVSHIPYD SFRAN
- 2 NAVSHIPYD BSN
- 2 NAVSHIPYD LBEACH
- 2 NAVSHIPYD PEARL
- 2 NAVSHIPYD PHILA
- 1 CDR, NATC (ET)
- 1 CDR, NADC, Johnsville, Pa.
- 1 CDR, NAMC, Philadelphia, Pa.
- 1 Asst Sec of Defense (R & E)
- 1 COMOPDEVFORLANT
- 2 NRF, San Diego
- 2 SRF, Subic Bay
- 2 SRF, Yokosuka
- 1 Supt, USN Postgrad School, Monterey, Calif.

Copies

- 1 CO, NAVADMINUNIT, MIT, Cambridge, Mass.
- 1 OinC, Postgrad School, Webb Inst of Naval Arch, Glen Cove, N.Y.
- 1 SUPSHIPINSORD, NYSB Corp, Camden, N.J.
- 1 NYSB Corp, Camden, N.J.
- 1 SUPSHIPINSORD, NNSB & DD Co, Newport News, Va.
- 1 NNSB & DD Co., Newport News, Va.
- 1 SUPSHIPINSORD, Quincy, Mass.
- 1 Bethlehem Steel Corp, Quincy, Mass.

David Taylor Model Basin. Report 949.

STRUCTURAL TESTS OF FLIGHT DECK ON USS HANCOCK (CVA 19) UNDER SIMULATED A 3 D-1 AND F 2 H-3 AIRCRAFT LANDING LOADS, by Ralph B. Allnutt. April 1959. vi, 57p. photos., diagrs., graphs, tables, refs. UNCLASSIFIED

Static and dynamic strains and deflections were measured on the flight-deck structure of USS HANCOCK (CVA 19) after Project 27-C conversion. A specially designed loading apparatus was used for simulating wheel loadings of A 3 D-1 and F 2 H-3 aircraft. It is concluded that the present Bureau of Ships design method is accurate for calculating the stresses in the steel supporting structure for a wood-planked flight deck, and that failure of the planking will not occur at loads less than those determined by the design calculations. Also, the test results show that design based on initial yielding of the steel supporting structure is conservative.

1. Flight decks - Deflection - Measurement
 2. Flight decks - Structural analysis
 3. Aircraft (A 3 D-1) - Landing impact
 4. Aircraft (F 2 H-3) - Landing impact
 5. Attack aircraft carriers - Structural analysis
 6. HANCOCK (U.S. attack aircraft carrier CVA 19)
- I. Allnutt, Ralph B.
II. NS 731-040

David Taylor Model Basin. Report 949.

STRUCTURAL TESTS OF FLIGHT DECK ON USS HANCOCK (CVA 19) UNDER SIMULATED A 3 D-1 AND F 2 H-3 AIRCRAFT LANDING LOADS, by Ralph B. Allnutt. April 1959. vi, 57p. photos., diagrs., graphs, tables, refs. UNCLASSIFIED

Static and dynamic strains and deflections were measured on the flight-deck structure of USS HANCOCK (CVA 19) after Project 27-C conversion. A specially designed loading apparatus was used for simulating wheel loadings of A 3 D-1 and F 2 H-3 aircraft. It is concluded that the present Bureau of Ships design method is accurate for calculating the stresses in the steel supporting structure for a wood-planked flight deck, and that failure of the planking will not occur at loads less than those determined by the design calculations. Also, the test results show that design based on initial yielding of the steel supporting structure is conservative.

1. Flight decks - Deflection - Measurement
 2. Flight decks - Structural analysis
 3. Aircraft (A 3 D-1) - Landing impact
 4. Aircraft (F 2 H-3) - Landing impact
 5. Attack aircraft carriers - Structural analysis
 6. HANCOCK (U.S. attack aircraft carrier CVA 19)
- I. Allnutt, Ralph B.
II. NS 731-040

David Taylor Model Basin. Report 949.

STRUCTURAL TESTS OF FLIGHT DECK ON USS HANCOCK (CVA 19) UNDER SIMULATED A 3 D-1 AND F 2 H-3 AIRCRAFT LANDING LOADS, by Ralph B. Allnutt. April 1959. vi, 57p. photos., diagrs., graphs, tables, refs. UNCLASSIFIED

Static and dynamic strains and deflections were measured on the flight-deck structure of USS HANCOCK (CVA 19) after Project 27-C conversion. A specially designed loading apparatus was used for simulating wheel loadings of A 3 D-1 and F 2 H-3 aircraft. It is concluded that the present Bureau of Ships design method is accurate for calculating the stresses in the steel supporting structure for a wood-planked flight deck, and that failure of the planking will not occur at loads less than those determined by the design calculations. Also, the test results show that design based on initial yielding of the steel supporting structure is conservative.

1. Flight decks - Deflection - Measurement
 2. Flight decks - Structural analysis
 3. Aircraft (A 3 D-1) - Landing impact
 4. Aircraft (F 2 H-3) - Landing impact
 5. Attack aircraft carriers - Structural analysis
 6. HANCOCK (U.S. attack aircraft carrier CVA 19)
- I. Allnutt, Ralph B.
II. NS 731-040

David Taylor Model Basin. Report 949.

STRUCTURAL TESTS OF FLIGHT DECK ON USS HANCOCK (CVA 19) UNDER SIMULATED A 3 D-1 AND F 2 H-3 AIRCRAFT LANDING LOADS, by Ralph B. Allnutt. April 1959. vi, 57p. photos., diagrs., graphs, tables, refs. UNCLASSIFIED

Static and dynamic strains and deflections were measured on the flight-deck structure of USS HANCOCK (CVA 19) after Project 27-C conversion. A specially designed loading apparatus was used for simulating wheel loadings of A 3 D-1 and F 2 H-3 aircraft. It is concluded that the present Bureau of Ships design method is accurate for calculating the stresses in the steel supporting structure for a wood-planked flight deck, and that failure of the planking will not occur at loads less than those determined by the design calculations. Also, the test results show that design based on initial yielding of the steel supporting structure is conservative.

1. Flight decks - Deflection - Measurement
 2. Flight decks - Structural analysis
 3. Aircraft (A 3 D-1) - Landing impact
 4. Aircraft (F 2 H-3) - Landing impact
 5. Attack aircraft carriers - Structural analysis
 6. HANCOCK (U.S. attack aircraft carrier CVA 19)
- I. Allnutt, Ralph B.
II. NS 731-040

David Taylor Model Basin. Report 949.

STRUCTURAL TESTS OF FLIGHT DECK ON USS HANCOCK (CVA 19) UNDER SIMULATED A 3 D-1 AND F 2 H-3 AIRCRAFT LANDING LOADS, by Ralph B. Allnutt. April 1959. vi, 57p. photos., diagrs., graphs, tables, refs. UNCLASSIFIED

Static and dynamic strains and deflections were measured on the flight-deck structure of USS HANCOCK (CVA 19) after Project 27-C conversion. A specially designed loading apparatus was used for simulating wheel loadings of A 3 D-1 and F 2 H-3 aircraft. It is concluded that the present Bureau of Ships design method is accurate for calculating the stresses in the steel supporting structure for a wood-planked flight deck, and that failure of the planking will not occur at loads less than those determined by the design calculations. Also, the test results show that design based on initial yielding of the steel supporting structure is conservative.

1. Flight decks - Deflection - Measurement
 2. Flight decks - Structural analysis
 3. Aircraft (A 3 D-1) - Landing impact
 4. Aircraft (F 2 H-3) - Landing impact
 5. Attack aircraft carriers - Structural analysis
 6. HANCOCK (U.S. attack aircraft carrier CVA 19)
- I. Allnutt, Ralph B.
II. NS 731-040

David Taylor Model Basin. Report 949.

STRUCTURAL TESTS OF FLIGHT DECK ON USS HANCOCK (CVA 19) UNDER SIMULATED A 3 D-1 AND F 2 H-3 AIRCRAFT LANDING LOADS, by Ralph B. Allnutt. April 1959. vi, 57p. photos., diagrs., graphs, tables, refs. UNCLASSIFIED

Static and dynamic strains and deflections were measured on the flight-deck structure of USS HANCOCK (CVA 19) after Project 27-C conversion. A specially designed loading apparatus was used for simulating wheel loadings of A 3 D-1 and F 2 H-3 aircraft. It is concluded that the present Bureau of Ships design method is accurate for calculating the stresses in the steel supporting structure for a wood-planked flight deck, and that failure of the planking will not occur at loads less than those determined by the design calculations. Also, the test results show that design based on initial yielding of the steel supporting structure is conservative.

1. Flight decks - Deflection - Measurement
 2. Flight decks - Structural analysis
 3. Aircraft (A 3 D-1) - Landing impact
 4. Aircraft (F 2 H-3) - Landing impact
 5. Attack aircraft carriers - Structural analysis
 6. HANCOCK (U.S. attack aircraft carrier CVA 19)
- I. Allnutt, Ralph B.
II. NS 731-040

David Taylor Model Basin. Report 949.

STRUCTURAL TESTS OF FLIGHT DECK ON USS HANCOCK (CVA 19) UNDER SIMULATED A 3 D-1 AND F 2 H-3 AIRCRAFT LANDING LOADS, by Ralph B. Allnutt. April 1959. vi, 57p. photos., diagrs., graphs, tables, refs. UNCLASSIFIED

Static and dynamic strains and deflections were measured on the flight-deck structure of USS HANCOCK (CVA 19) after Project 27-C conversion. A specially designed loading apparatus was used for simulating wheel loadings of A 3 D-1 and F 2 H-3 aircraft. It is concluded that the present Bureau of Ships design method is accurate for calculating the stresses in the steel supporting structure for a wood-planked flight deck, and that failure of the planking will not occur at loads less than those determined by the design calculations. Also, the test results show that design based on initial yielding of the steel supporting structure is conservative.

1. Flight decks - Deflection - Measurement
 2. Flight decks - Structural analysis
 3. Aircraft (A 3 D-1) - Landing impact
 4. Aircraft (F 2 H-3) - Landing impact
 5. Attack aircraft carriers - Structural analysis
 6. HANCOCK (U.S. attack aircraft carrier CVA 19)
- I. Allnutt, Ralph B.
II. NS 731-040

David Taylor Model Basin. Report 949.

STRUCTURAL TESTS OF FLIGHT DECK ON USS HANCOCK (CVA 19) UNDER SIMULATED A 3 D-1 AND F 2 H-3 AIRCRAFT LANDING LOADS, by Ralph B. Allnutt. April 1959. vi, 57p. photos., diagrs., graphs, tables, refs. UNCLASSIFIED

Static and dynamic strains and deflections were measured on the flight-deck structure of USS HANCOCK (CVA 19) after Project 27-C conversion. A specially designed loading apparatus was used for simulating wheel loadings of A 3 D-1 and F 2 H-3 aircraft. It is concluded that the present Bureau of Ships design method is accurate for calculating the stresses in the steel supporting structure for a wood-planked flight deck, and that failure of the planking will not occur at loads less than those determined by the design calculations. Also, the test results show that design based on initial yielding of the steel supporting structure is conservative.

1. Flight decks - Deflection - Measurement
 2. Flight decks - Structural analysis
 3. Aircraft (A 3 D-1) - Landing impact
 4. Aircraft (F 2 H-3) - Landing impact
 5. Attack aircraft carriers - Structural analysis
 6. HANCOCK (U.S. attack aircraft carrier CVA 19)
- I. Allnutt, Ralph B.
II. NS 731-040

MIT LIBRARIES

DUPL



3 9080 02754 1918

